Effect of vegetation cover and transitions on regional wind erosion in drylands

Feras Youssef

Effect of vegetation cover and transitions on regional wind erosion in drylands

Feras Youssef

Acknowledgement

I would like to thank my co-supervisor Dr. Saskia Visser for her support and guidance to complete this research. Saskia, your support started from the first hour of my arrival at Schiphol Airport in 2008 and continued until the time of writing these lines. I learned a lot from you; thank you for all your help in both the research and life. My endless great thank words go to my promoter em. prof. Leo Stroosnijder; you were extremely sympathetic and supportive during all steps of this research. Your door was continuously open for all kind of support, help and encouragement which gave me the feeling of safe, peace, and confidence; thank so much for all your great support. Big thanks also go to my co-supervisor Dr. Derek Karssenberg who was all time extremely supportive and helpful. Derek, your great guidance was the key process in all challenges achieved in this research. I learned a lot from you; thank you so much for the countless support in my in writing and modelling steps. Further, I want to thank my supervisor at Ankara University prof. Gunay Erpul who was continuously positive and supportive to ensure the successes of this research. Gunay, your great contacts in Gent and in Wageningen was very useful for my PhD, thank you for all your support during my time in Ankara and in Gent.

I want to thank Dr. Adriana Bruggeman who gave all kind of support during my time in ICARDA, Aleppo, and provided me with all data I requested about Khanasser valley. Adriana I am sure without your great help and supervision my field measurement would never have be completed. Also, I want to thank Dr. Feras Ziadat who was all time supportive, positive and encouraging during field measurements, thanks for your guidance and ideas. At ICARDA, further thanks to Pierre Hayek, Goerge Estefan, Muhammed Ali and the farmers in Khanasser who supported our experiments for all of their time and help. Moreover, thank words go to the Branch of the General Commission of Badia and Development and Management in Aleppo, Syria (Mr. Bader and his team).

In Gent, great thanks for prof. Donald Gabriels and prof. Wim Cornelis for their ideas and logistical support during my wind-tunnel experiments and their assistance with the papers related to this experiments. Both of them were supportive and helpful to garantee the success of these experiments. Thanks also for Pieter Bogman, Maarten De Boever, Jan Vermang and Muhammed Khlosi for their support, help and sharing life (and beer) in Gent.

In Wageningen, big thanks words go to Marnella van der Tol for her incredible support and willingness to help. Your immediate solutions for all logistical and organizational problems are highly appreciated. Huge thank you goes to Demie Moore for her kind help in editing English writing. I would like to thank Dirk Meindertsma for his help upon my arrival to Wageningen and during my staying in 2008. Thanks for Anita Kok and Esther Van den Brug for their kind help in financial issues. Specific thanks words go to both Erik Slingerland and Ate Poortinga for their help in data collecting and sharing life in Wageningen.

I want to thank all staff members in the Land Degradation and Development Group, I do enjoyed sharing the life in Wageningen with all of you; in names; Jantiene Baartman, Saskia Keesstra, Jan de Graaff, Michel Riksen, Aad Kessler, Manuel Seeger, Joep Keijsers, Coen Ritsema, Alma de Groot and Piet Peters. Thanks for all PhD colleagues who I share with them the tough but very nice days in Wageningen in names: Nadia, Jeanelle, Ali, Javier, Desire, Araya, Mohammadreza Mounique, Cathelijne, Anna, Abraham, Zenebe, Isaurinda, Birhanu, Ryan, Akalu, Anna, Edmond, Innocent and Birhane. Also I would like to thank Erik van den Elsen, Simone Verzandvoort and Rudi Hessel from the Desire project team for their kind helpful. Furthermore I want to thank all friends who I shared with them nice days during my time in Wageningen, Ankara, and Gent.

Finally the biggest thanks is for all my family members in Syria; my father, my mother my brothers, and my sisters. Their voices from thousands kilometres provided me with a great feeling that was very helpful to deal with all obstacles in my life.

Table of Contents

Chapter 1

Introduction

Introduction

1.1 Wind erosion, land degradation and vegetation cover

Land degradation is a serious environmental problem (Sivakumar et al., 2005; Stroosnijder, 2007). It is defined as the decrease in ecosystem services to a point at which land yields become insufficient as an essential subsistence (MEA, 2005). The areas most sensitive to land degradation can be found in the arid, semi-arid and dry sub-humid regions (Stroosnijder, 2005), where wind erosion is one of the dominant degrading processes (Lal, 1990; Leenders et al., 2011; Maurer et al., 2010; Shao, 2008; Stroosnijder, 2005).

Wind erosion occurs when the soil is dry, bare and loose (Sterk and Spaan, 1997). It causes the loss of fertile topsoil, and has a negative effect on agricultural production (Visser and Sterk, 2007) and on human health (Breshears et al., 2009; Copeland et al., 2009). When conditions favourable for wind erosion are present, the process may result in large-scale environmental disasters like the Dust Bowl in the USA in the 1930s. This event is considered one of the worst environmental disasters in the 20th century. Researchers who studied the Dust Bowl concluded that the main cause for this disaster was the change in land use combined with the increased drought in the region (Cook et al., 2008).

Wind erosion involves the detachment, transport, and deposition of soil particles. Depending on their size, soil particles can move in three different types of transport: creep, saltation and suspension (Fig 1.1) (Chepil, 1942; Chepil, 1954; Lyles, 1988). The wind erosion process starts with saltation in which sediment particles jump, through the lift force of the wind, in the airflow and hit the soil surface while falling down. These saltating particles (63-500 µm) bounce over the soil surface, and may reach heights of up to 2 m. Saltating particles can be transported over a horizontal distance between several meters and a few hundred meters (Visser and Sterk, 2007).

Particles moving through creep (500-1000 µm) are mainly set in motion by the bombardment of saltating grains, but are sufficiently large to remain in contact with the soil surface. Transport distances of sediment moving in creep mode range from several centimetres up to several meters (Sivakumar et al., 2005). Through the bombardment of the saltating grains, sufficient energy is released to put also the fine particles (2-63 µm) in transport (Shao, 2001;). These particles are held high in the air by the wind as suspended dust creating dust clouds which may travel up to thousands of kilometres (Herrmann et al., 1996; Sterk, 1997).
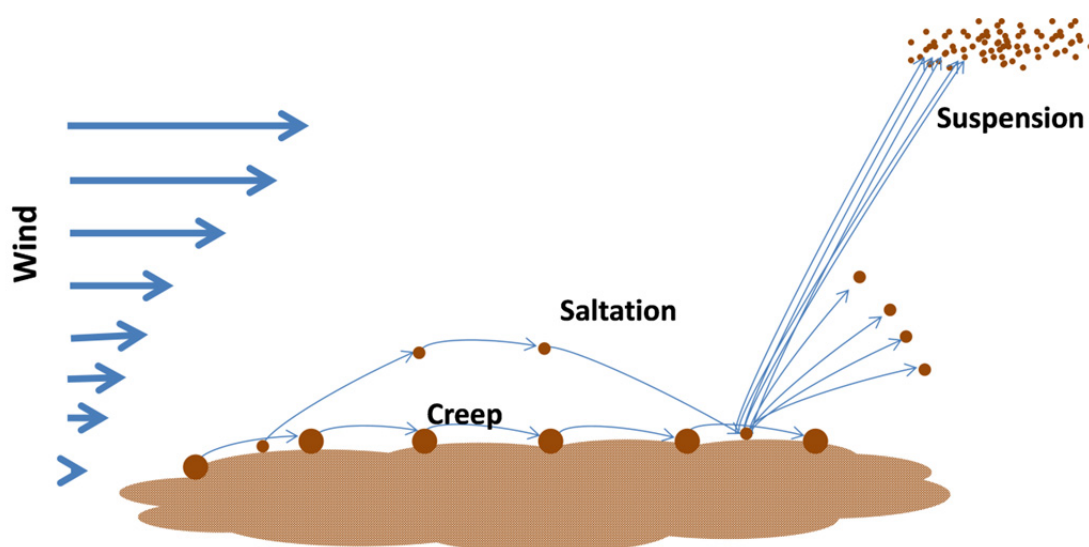

Figure 1.1. Wind erosion transport types

In soil erosion research generally and in wind erosion specifically the scale of the research carries specific importance. The scale determines the preferred method of research and has effect on the validity of the findings of the research (Zobeck et al., 2000; Bierkens et al., 2000). For wind and water erosion, Stroosnijder (2005) identified the scales of point (1-10 m^2), field (10-10^4 m^2), village (10^4-10^8 m^2), and region (>10 km^2). In this research, we identify the size of 20-25 km^2 as a minimum size for the regional scale.

As dust clouds are transported over large distances and because they can be observed by remote sensing technology (satellites), suspension is most often considered in large-scale wind erosion research (Shao and Leslie, 1997; Webb et al., 2006). However, particles can hardly come into suspension without saltation (Zhang and Lee, 2009; Nishimura and Hunt, 2000). Sterk (1993) studies the relationship between the saltation flux (measured by a saltiphone) and the mass flux measured by sediment samplers in a wind-tunnel experiment, and he reported that the saltation flux is linearly related to the measured mass flux at the same height. Depending on wind speed and soil texture approximately 50-80 % of total transported sediment moves through saltation (Sterk, 1997; Visser and Sterk, 2007; White, 1997; Humberto and Rattan, 2010). According to Zhang and Lee, (2009) the use of high-speed photography in observing sediment flux proved that 75 % of the total transported sediment during wind events occurs throughout saltation. Thus saltation is the transport mode in which the main mass of sediment is transported. As saltating particles often consist of aggregated particles, which are rich in plant nutrients, the removal of soil mass by saltation seriously affects soil fertility. In addition, abrasion due to the saltation process may damage the plant by the scouring effect of saltating soil particles (Sterk, 1997; Baker 2006; Baker et al.,2009). For land use planning at a regional scale (20-25 km^2) saltation is a transport process that should be avoided, on the one hand to avoid damage to agricultural fields through abrasion and fertility loss and on the other hand to prevent the starting of suspension that may result in dust clouds that can be transported over a large distance (>10,000 km). So, saltation is an important process at the regional scale and is thus chosen as the subject of study in this thesis.

Vegetation is an important factor in the protection of the soil surface against erosive wind. Therefore, a change in vegetation cover in an area that is vulnerable to wind erosion has direct impact on wind erosion and thus on the rate of land degradation. The effect of vegetation cover on the wind erosion process, with an emphasis on saltation, has been studied by a large number of researchers (i.e. Van De Ven et al., 1989; Hagen, 1996; Sterk and Spaan, 1997; Leenders et al., 2005; Visser et al., 2005a). In general, these studies concluded that vegetation has the potential to decrease the soil loss due to wind erosion through the protection of the soil surface, the reduction of the wind speed and the trapping of saltating particles. Sterk and Spaan (1997) showed that covering the soil surface with millet stalks in a Sahelian agricultural field reduced the sediment transport during five wind storms. However, they also showed that a minimum level of surface cover should be applied to avoid the increase in sediment transport due to increased turbulence.

Leenders (2006) studied the effect of dispersed shrubs and trees on wind erosion in an agricultural field in Sahelian Africa. The results indicated that whereas shrubs affect the mass transport process by catching saltating soil particles, trees affect the process by decreasing the wind speed. Therefore, both shrubs and trees should be present in agricultural fields for optimal protection of the soil surface from the wind (Leenders et al., 2007). According to Leenders (2006), scattered natural vegetation can be effective in reducing large-scale wind-blown sediment transport, but insight on the optimal spatial distribution (pattern) of the vegetation elements is still limited.

In wind erosion regions, land use at one land unit may have a significant effect on the quantity and intensity of the wind erosion process at its neighbouring land units (Hupy, 2004; Leenders, 2006; Visser and Sterk, 2007). Thus, the amount of incoming and outgoing sediment into or from a field is interrelated with the surrounding area. Since a region (20-25 km^2) may include several land units associated with different land uses and land covers, the interrelation between one land unit and its neighbouring units from the

perspective of sediment transportation is required for better understanding of wind erosion at the regional scale. Therefore this thesis addresses the effect of vegetation and vegetation transitions on regional scale wind erosion.

1.2   Modelling and upscaling wind erosion models

Nicholson (2000) showed that at the regional scale, reduction of the vegetation cover caused an increase in the degradation process. Insight into wind erosion at a regional scale is necessary for policy makers and land managers to draw policies for future land use, because wind erosion has direct negative effects on economy, agriculture, health and environment of the inhabitants in the vulnerable regions (Bunn, 1997; Nordstrom and Hotta, 2004; Andrew, 2007; Warren, 2010; Almansa et al., 2012). However, sizable knowledge on the effect of wind erosion on regional scale land degradation is not available (Sterk et al., 1998; Visser and Palma, 2004). This is most probably due to the absence of measurement and modelling methods of wind erosion at the regional scale. Although research on land degradation and wind erosion in particular has been carried out on the point scale (Hoogmoed et al., 2000) on the field scale (Mazzucato and Niemeijer, 2000) and recently on the village scale (Niemeijer and Mazzucato, 2002; Okoba and Sterk, 2006; Tenge et al., 2005), research on wind erosion at the regional scale is still limited (Visser and Palma, 2004). In the current research we aim at observing wind-blown sediment transport over a region with a size of 20-25 Km^2. There are only a few models that were developed to predict wind erosion at regional scale (McTainsh and Lynch, 1996; McTainsh and Pitblado, 1987; Nickling et al., 1999; Shao and Leslie, 1997; Sterk, 1997). Most of these studies integrate field measurements, wind erosion modelling, remote sensing techniques and geographical information system techniques to predict wind erosion at a regional scale. These attempts have a relatively high degree of uncertainty in their predictions. This is partially because these models often consider only mass transport by suspension, neglecting other transport processes (Leys et al., 2001; Shao, 2008). The physically based Wind Erosion Assessment Model (WEMA) was used to predict erosion and mass movement across the continent of Australia (Zealand, 2001). The WEMA model can be applied both at the village scale and at the regional scale (Leys et al., 2001). The disadvantages of the WEMA model are the uncertainty in using data derived from low-resolution satellite images. Also the model neglects a number of factors that affect the wind erosion process such as soil crusting and the roughness of the soil surface (Leys et al., 2001).

Zobeck et al. (2000) applied a field scale model of the Revised Wind Erosion Equation (RWEQ) at the regional scale using input data that were derived from remote sensing and soil maps in a Geographic Information System (GIS). They concluded that some of the major challenges in applying field-scale wind erosion models to a non-homogeneous region is finding a correct upscaling method (Zobeck et al., 2000). In this research, we assume that up-scaling a field scale model (150 x 150 m), calibrated and validated for a large range of land uses, to the regional scale (20-25 km^2) could provide a model that takes into account the essential processes and parameters of wind erosion, and provides a reliable output.

Processes in natural environmental catchments show high variability in both space and time on a large range of scales (Blöschl and Sivapalan, 1995). Also, there is often a discrepancy between the scale of the observations and the scale at which predictions are required (Blöschl and Sivapalan, 1999). For policy makers, information on wind erosion at the regional scale is required for resource management decisions and for future planning of the land use in the vulnerable regions (Visser and Palma, 2004; Jason, 2009; Cai and Barry, 1996; Riksen et al., 2003). In wind erosion, processes at the larger scale are different from those at a smaller scale. Therefore, a small scale model is not directly applicable at a larger scale (Seyfried and Wilcox, 1995). Problems in scale transfer are mainly due to heterogeneity at all scales (Bierkens et al., 2000). If the parameters modelled and measured were similar to each other at different scales they could

be scaled up without any changes (Bierkens et al., 2000). However, representative parameter values change with scale and new parameters. Parameters that do not exist at the small scale may arise at the larger scale (Blöschl, 1999).

When scaling up a model it is essential to know which processes will have the largest impact at the new coarse scale and which ones can be ignored (Visser and Palma, 2004). For wind erosion, parameters that are important at the regional scale include mainly vegetation cover, surface roughness and certain soil properties (Zobeck et al., 2000). The behaviour of wind over a vegetated surface is a good example of a process that should be taken into account when moving from a high- to a low-resolution scale. Thus, in a field scale model, each individual vegetation patch should be represented in the model and the effects of these patches on sediment transport should be represented in a distributed manner. On the contrary, at a larger scale, these patches and their effect on wind erosion driving processes are aggregated over one grid cell and a different representation of processes is required.

1.3   Measuring wind erosion

In the last decade, many measurements have been carried out on wind erosion, which increased our understanding of the wind erosion processes at the point (e.g., Burri. et al., 2011; Udo. et al., 2007), field (i.e. Leenders 2006; Visser et al., 2005b; Sterk 1997), village (Rajot, 2001), and limitedly at the regional scale (Shao, 2008; Webb et al., 2006). Furthermore, there are few studies that have been carried out to improve the knowledge on the effect of land uses on the quantity and intensity of wind erosion (i.e. Sharratt et al., 2012; Young and Schillinger, 2012; Zhang et al., 2012). Though this research has provided insight in the wind erosion process it did not provide decision support data that is required for land managers and policy makers who need comprehensive knowledge about the possible causes and solutions to this problem. Furthermore these studies did not provide data that can be used for calibration and validation of regional scale wind erosion models (Zobeck et al., 2003). Therefore, a new measurement method for regional scale wind erosion is needed. The new method should provide accurate knowledge on the saltation process taking place within different land units in the region, should provide knowledge on the interrelation among neighbouring land units (Breshears et al., 2003; Breshears et al., 2009), and should provide data that can be used for calibration and validation of regional scale models.

Measuring saltation is possible by direct sampling of windblown sediment, using sediment samplers (Zobeck et al., 2003). There are several sediment catchers developed for field use, and those developed by Bagnold (1954), Leatherman (1978), De Ploey (1980) and Wilson and Cooke (1980) are among the most widely used sediment catchers. These samplers are developed to trap the wind-blown sediment at a specific height at a specific point in a field. And the calculation of the mass flux in a specific field is based upon the amount of sediment trapped and the duration of the erosive event. Therefore, the trapping efficiency of a sampler plays an essential role in the calculation of the actual mass flux (Goossens and Offer, 2000). In most (small scale) wind erosion studies, a fixed efficiency for the sediment catcher is used for the catcher in the calculation of the total wind-blown mass flux. Since the trapping efficiency of most catchers varies with both the texture (size of the particles), and the wind speed, in larger scale studies, it is important to determine the efficiency of the catcher for different texture classes and for different wind speeds.

1.4   Research questions and hypothesis

Considering the increasing number of regional scale disasters over the world in the last decades, it is not enough to study environmental phenomena at field or village scale (Blöschl and Sivapalan, 1995). There is an imperative necessity to understand these phenomena and to predict their impact on a regional or even at a global scale to improve governance that may help in avoiding regional environmental disasters.

Although wind erosion is a serious environmental problem, a validated regional-scale model that takes into account the saltation mode of the transport process does not exist. The complexity of the wind erosion process makes the prediction of wind erosion at the large scale difficult (Zobeck et al., 2003). As the vegetation cover is one of the most important parameters in protecting the soil surface from the forces of the wind; a calibrated and validated model taking into account the transitions in vegetation cover which is capable of predicting the effect of vegetation cover on wind erosion will be a useful tool for policy makers. Therefore the central research question of this thesis is: ***is it possible to improve our insight into the effect of vegetation on wind erosion at a regional scale with the help of a regional scale wind erosion model?***

Consequently, the following research questions were defined:
1. How efficient is the currently available equipment for measuring saltation?
2. What is the best method to measure wind erosion at the regional scale?
3. How can a field scale model be adapted for use at the regional scale?
4. What is the effect of spatial vegetation transitions on saltation transport?

Figure 1.2 shows how answers to these research questions will help to evaluate the central research question.
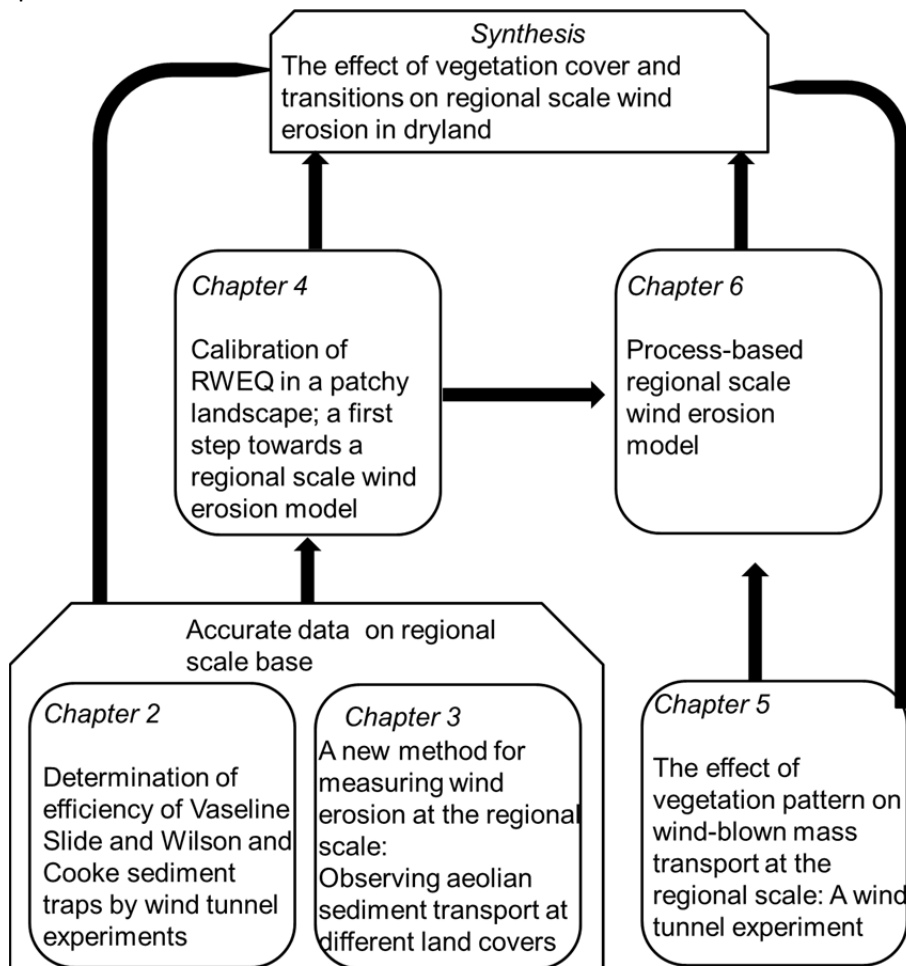

Figure 1.2. The research objectives and the relationships among them.

1.5 Overview of methodology

1.5.1 Study area

The Khanasser valley, Syria was chosen as the study area for this research. The valley is situated between the Al Hass and Shbeith mountains, southeast of Aleppo city (Figure 1.3). At an altitude of 350 m above sea level, the valley is rather flat. Annual rainfall ranges from 150 to 250 mm, which relates to stability zones 4 and 5 (Figure 1.3). The rainy season starts in October and ends in May (Masri et al., 2003). Wind in the dry season (from June to September) blows from south to west with exceptional high wind speed events from other directions. During the dry season, the daily average wind speed (at 2 m height) is high and may exceed 10 m s^{-1} (Masri et al., 2003). The intensive agricultural and livestock activities and poor management of the natural resources are dominant problems in the valley, and have resulted in a significant increase in the land degradation in the valley (ICARDA, 2005). Wind erosion is one of the most dominant land degradation problems here threatening not only the agricultural and livestock activities but also the settlements in the valley (Thomas and Turkelboom, 2008).
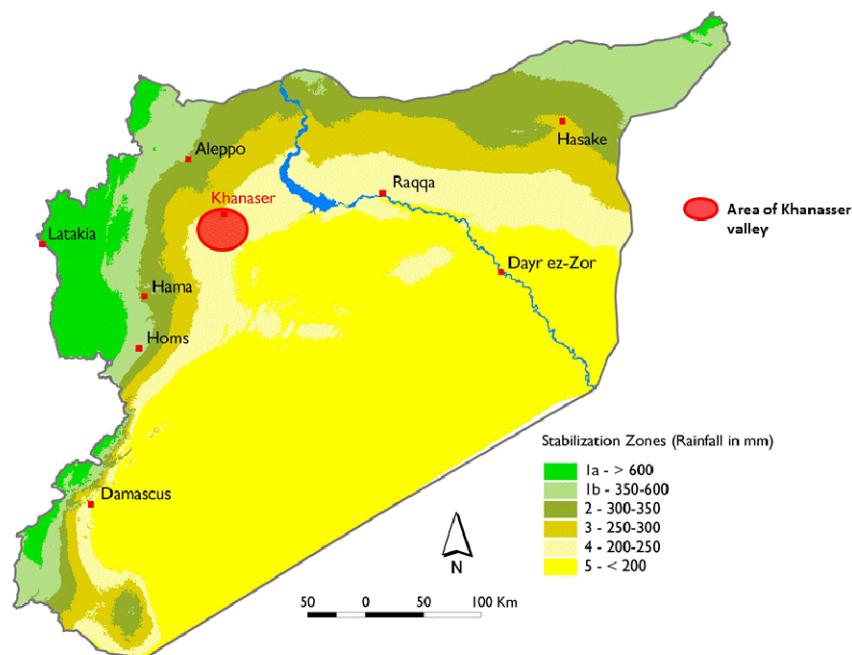
Figure 1.3. The location of Khanasser valley, and the stability zones in Syria (ICARDA, 2005b).

1.5.2 Wind tunnel measurements

Wind tunnel experiments were conducted in the wind tunnel of the International Centre for Eremology (ICE), Ghent University, Belgium. This tunnel is 12 m long, 1.2 m wide and has an adjustable roof height up to 3.2 m (Cornelis and Gabriels, 2004; Gabriels et al., 1997). Wooden spires and roughness cubes were used to create a boundary layer of 0.60 m at the upwind border of the experimental section which is 6 m from the entrance of the wind tunnel (Cornelis and Gabriels, 2004). Wind speed was measured with vane probe type and associated recording equipment (Gabriels et al., 1997) placed at X = 5.85 m (measured from the entrance), Y = 0.60 m (measured from the wall of the working section) positioned at several heights starting from 2 cm from the surface of the test tray up to 70 cm (with the efficiency test, Chapter 2) or up to 110 cm (with the vegetation simulation test, Chapter 4) characterized by the Prandtl–von Karman logarithmic law (Figure 1.4).
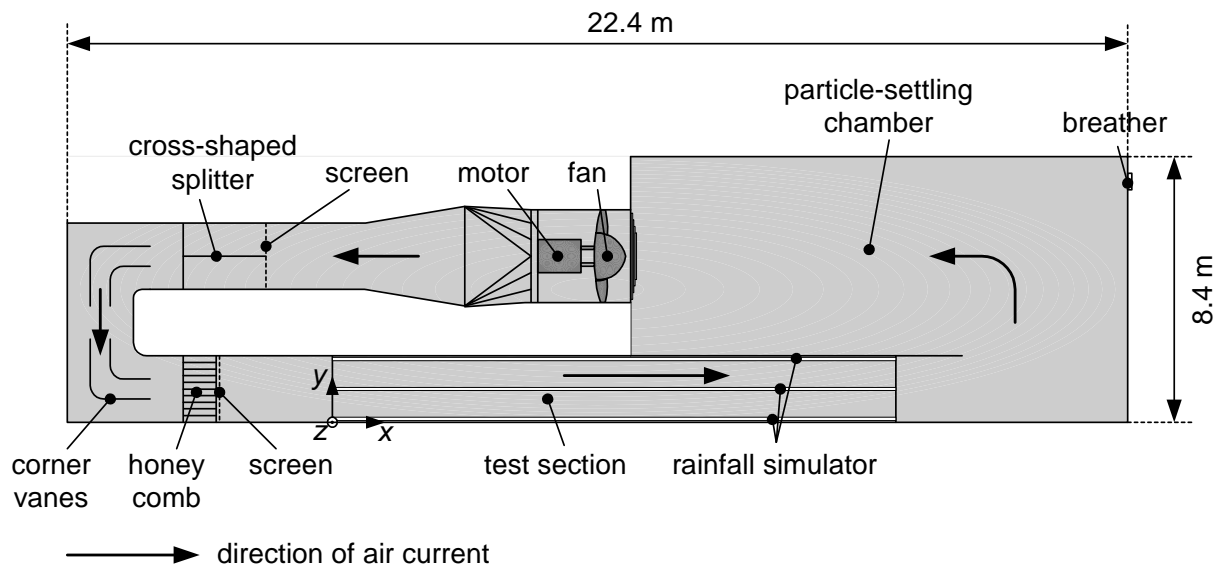
Figure 1.4. Top view of the closed-circuit low-speed blowing-type wind tunnel of the International Centre for Eremology, Ghent University, Belgium (on scale), (after Gabriels et al. 1997).

1.5.3 Field measurements

In this research, a new measurement method with a portable equipped plot was developed. In this method, measurement locations should represent the major land uses in the region. For each land use, measurements at a minimum of two plots are executed. The interaction between neighbouring land units in the region is measured by measuring aeolian mass fluxes at the transition between two neighbouring land units. The duration of measurement in the portable plot method was 21 days during the wind erosion season in our research region. This period was enough to draw conclusions on the sensitivity of the land units for wind erosion. At each plot, 16 MWAC catchers (Wilson and Cooke, 1980) were installed on a regular grid to retrieve information on the spatial variability of the mass flux over the plot area. To measure border effects, the edge of some plots was chosen close to or just over the edge of the land units. This, allowed us to observe the effect of neighbouring land units. The average of the observed mass fluxes at the 16 catchers provides information about the mass flux for the land use on the plot. Consequently the differences in averages of aeolian mass flux from one plot to another show the effect of land use on wind erosion process.

1.5.4 Modelling wind erosion

The RWEQ model was calibrated and validated against ground data collected for several land uses in the region of Khanasser valley. Thus, the model has the potential to be used at a regional scale. However, the model was developed for the application for a single field and not for series of fields. In this study, an extension to RWEQ is developed resulting in a simple model that is applicable to series of neighbouring fields. In this simple model, the effect of land use transition is taken into account. Therefore, the behaviour (erosion or deposition) of aeolian sediment transport within one single field is not only related to the land use of the field itself but also related to the neighbouring fields.

The model was tested for a number of land uses, field lengths and wind speed scenarios. The land use scenarios (bare, wheat and Atriplex) were prepared based on real observations in the Khanasser valley region. The tested wind speeds (10.0, 12.5, 15.0 m s^{-1}) were chosen to represent the wind speeds at which saltation process of sediment occurs. The field lengths (50.0, 150.0, 450.0 m) were chosen to represent the widely used field length in the arid regions in general and in Khanasser valley, Syria in particular.

1.6   Outline of this thesis

The thesis has 7 chapters of which 5 are or will be published in international refereed journals as independent papers. Chapter 1 is an introduction to the study. Chapter 2 and 3 focus on the measurement of wind erosion. In Chapter 2 the effect of aggregate size and wind speed on the efficiency of two types of sediment traps is discussed and in Chapter 3 the "moving plot" measurement method is described. The method is applied in the Khanasser valley in Syria and the obtained data are used to calibrate and validate the adapted field scale model RWEQ (Chapter 4). To be able to scale up a field scale model to regional scale more insight in the regional scale saltation process is required, specifically on the effects of transitions in vegetation cover on the saltation process. Chapter 5 discusses the results of a wind tunnel study on this issue and in Chapter 6 the approach for up-scaling a field scale model to the regional scale is presented. The last chapter (7) is the synthesis, a presentation of the major conclusions, the newly generated knowledge, limitations and recommendations from the study.

Chapter 2

Determination of Efficiency of Vaseline Slide and Wilson and Cooke Sediment Traps by Wind Tunnel Experiments

Determination of Efficiency of Vaseline Slide and Wilson and Cooke Sediment Traps by Wind Tunnel Experiments

Abstract

The trap efficiency of a catcher in wind erosion measurements plays an important role, and in many cases suspension trap efficiencies at high wind velocities are still unknown. The sediment trap efficiency generally changes with particle size and with wind speed. In this study, the efficiency of Vaseline Slide (VS) and Modified Wilson and Cooke (MWAC) catchers were determined with specific soil particle sizes (<50, <75, 50–75, 200–400, and 400-500 μm) at a fixed wind speed (13.3 m s^{-1}) and with different soil textures at different wind velocities (10.3, 12.3, and 14.3 m s^{-1}) in the wind tunnel of the International Center for Eremology (ICE), Ghent University, Belgium. The traps were placed at different heights (4, 6.5, 13, 20, 120, and 192 cm for VS and 1.5, 3,5, 8, 11, and 30 cm for MWAC) to catch saltating and suspended sediments in a 12-m long, 1.2-m wide and 3.2-m high working section of the wind tunnel. In the specific soil particle experiments, the efficiency of the VS catcher was 92% for particles smaller than 50 μm and decreased with increasing particles size, falling to 2% for 400–500 μm particle size at 13.4 m s^{-1}. However, the MWAC's efficiency was 0% for particles smaller than 50 μm and increased with increasing particle size to 70% at 400–500 μm. In the experiments with different soil textures, the efficiency of each catcher importantly changed with soil and with wind speed. It also considerably varied with the catchers: for instance, for sand (S), the MWAC efficiency was very high (67, 113, and 91% at 10.3, 12.3, and 14.4 m s^{-1}, respectively) while the efficiency of VS was relatively very low (5, 4, and 2% at 10.3, 12.3, and 14.4 m s^{-1}, respectively). Results indicated that the efficiency depends critically on the particle size, type of catcher, and wind speed, and these could be helpful to increase the robustness of wind erosion measurements.

Keywords: Trap efficiency, Vaseline slide catcher, Wilson and Cooke catcher, Wind erosion

2.1 Introduction

Wind erosion is a serious problem in many parts of the world; eroded soil moves nutrients out, severely affecting soil productivity, and wind erosion destroys land and crops (Wassif, 1998). The eroded dust can carry harmful chemicals many miles from the source of sediment causing serious off-site environmental problems (Middleton et al., 1986).

The processes that explain the sediment transport by wind were documented very well by the World Meteorological Organization (WMO) in 1983. Zobeck et al. (2003) showed that saltation did not seem to be a major factor to cause suspended dust, which might occur as a direct response to wind as well as to saltation activities (Kjelgaard et al., 2004) although, in many cases, vertical dust flux is accepted as a result of saltation flux (Alfaro and Gomes, 2001; Shao and Leslie, 1997).

Due to its potential effects on human health, researchers have paid a great attention to the measurement and modelling of dust emission (McKie, 2001; Pietersma et al., 1996). Kind (1992) and Loosmore and Hunt (2000) showed that large quantities of PM$_{10}$ and PM$_{2.5}$ might be released from the top soil and transported over long distances downwind as an element of the suspension component of eroded soil, and they explained how aerosols were detached from the soil surface by abrasion of saltating aggregates and by direct entrainment of mineral grains by turbulent eddies in surface winds. There are many factors affecting the quantity and quality of airborne sediment (Chepil and Woodruff, 1963) and according to Gillette (1977), the proportion of fine particles to total soil moved was related to soil texture,

wind speed, mineralogy and physical weathering. The calculations of Tegen and Fung (1995) showed that about 50% of the total atmospheric dust would originate from destroyed soils by cultivations, deforestation, erosion, and frequent loss in vegetation due to droughts and rains.

The literature describes a lot of models for vertical distributions of the horizontal mass flux (Sterk and Raats, 1996; Vories and Fryrear, 1991; Zobeck and Fryrear, 1986). In order to measure total mass transport by wind, there are two methods: the first is directly by samplers that collect the transported material, and the second is indirectly by devices such as the saltiphone (Spaan and van den Abeele, 1991) or the sensit. Again, accurate and direct measurements of the sediment flux are necessary for two purposes, which are: to confirm and assess theoretically derived flux equations (Nickling and Neuman, 1997) and to determine the intensity of aeolian processes in an environment (Goossens and Offer, 2000). Drew and Lippmann (1978) reported that it was not necessary for sediment traps to have 100% efficiency, and sediment traps might also be useful even if they have a low efficiency. There are several sediment traps for field use, those of which developed by Bagnold (1954), Leatherman (1978) , De Ploey (1980) and Wilson and Cooke (1980) are very well known. Collectors have ranged from open pits or trench traps dug in sand (Jackson, 1996) to vertical cylindrical traps oriented into the flow (Leatherman, 1978).

Zobeck et al. (2003) stated that the type of sediment to be measured would determine the kind of traps to be used. He also made a distinction between passive and active sampling processes such that the former depended on wind conditions during sample collection and the latter relied on some type of suction provided by a vacuum pump to draw a known volume of air and particles into traps. Gillette (1977) informed that active samples were often used to trap suspended dust particles (smaller than 70 µm, Bagnold, 1941)). Thus, most sediment traps have a range of efficiencies changing with wind speed and particle diameter or aggregate size. On a mass basis, Zobeck (2002) showed that the dry aggregate size distribution (DASD) refers to the relative amounts of air-dry aggregates or clods present on the soil surface by size class. Wind-erodible soil was described by Chepil (1942) as the amount of dry soil aggregates smaller than 0.84 mm in diameter, and therefore, sensitive soils are those, which have a low percentage of aggregates larger than 0.84 mm, whereas resistant ones are those, which have high percentages of these aggregates. Usually, the gradation of aggregates is measured by sieving methods.

In sediment trapping, generally, it is more difficult to catch particles that move by suspension than particles that move by saltation because finer suspended particles are easy to be carried by a wind stream and may not enter into traps if it is not iso-kinetic, and they are not easily trapped by a screen or other physical barrier as well (Zobeck et al., 2003). The efficiencies of Big Spring Number Eight (BSNE) and Modified by Wilson and Cooke (MWAC) traps were determined at low wind velocities (1–5 m s^{-1}) using silty loess that consisted of 95% silt (2–63 µm), and results showed that the efficiencies of BSNE and MWAC traps were 40 and 80%, respectively (Goossens and Offer, 2000). It is possible to study a lot of wind erosion aspects in wind tunnels. Hagen (1999) demonstrated that the applicability of wind tunnel results to field applications could improve if attention was given to non-dimensional scaling and proper selection of instrumentation. The aim of this study was to determine the efficiencies of VS and MWAC sediment traps by wind tunnel experiments, using different soil textures at different wind velocities.

2.2   Materials and Methods

The experiments were conducted in the wind tunnel of the International Center for Eremology (ICE), Ghent University, Belgium. The wind tunnel is a closed blowing-type tunnel with a 12 m long, 1.2 m wide and 3.2 m high working section (Cornelis and Gabriels, 2004; Gabriels et al., 1997). Wind speed profiles over the test area were measured from 2 cm from the test tray surface up to 70 cm with a vane-type anemometer and associated recording equipment and were characterized by the Prandtl–von Kármán logarithmic equation (2.1).

$$u(z) = (\frac{u_*}{k})\ln(\frac{z}{z_0}) \qquad \text{For } z \gg z_0 \qquad\qquad [2.1]$$

Where:

$u(z)$ is the wind speed (m s^{-1}), at height z(m),

z_0 is the aerodynamic roughness height (m),

u_* is the wind shear velocity, and

k is the von Kármán's constant.

The boundary layer was set at 0.6 m above the soil tray (Figure 2.1). The aerodynamic roughness height was 0.0006 m. Efficiencies of the catchers were tested with different specific soil particle sizes (<50, <70, 50–70, 70–200, 200– 400, and 400–500 μm) at a fixed wind speed of 13.4 m s^{-1}, and with different soil textures (seven soils taken from different parts of Belgium) at different wind velocities (10.3, 12.3, and 14.3 m s^{-1}).
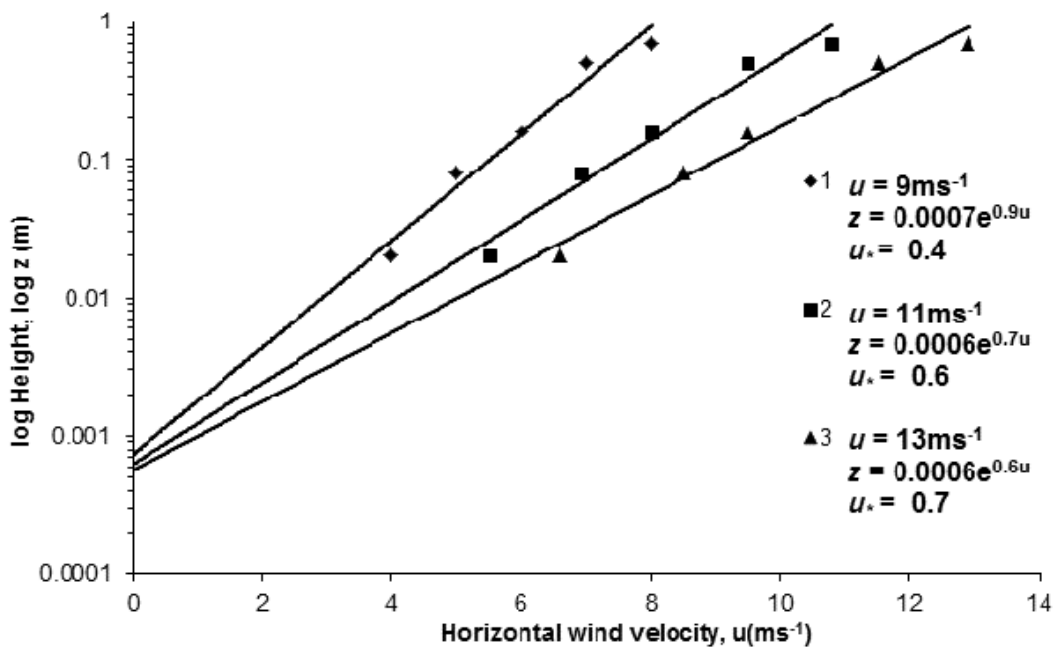
Figure 2.1. Wind speed profiles for free stream wind velocities of 9, 11 and 13 m s^{-1}

Texture of soils was determined by the pipette method (Table 2.1) (Gee and Bauder, 1986), and aggregate-size distributions were determined by the dry sieving method using a nest of flat sieves ranging in size from 75 to 2,000 μm and shaken with a sieve shaker (Table 2.2).

    A test tray, which was 0.95 m long, 0.40 m wide and 0.02 m deep, was placed at x = 6 m horizontal distance from the entrance of the test section. It was packed with 5 kg air-dried soil after the soils were sieved on a 3-mm sieve (Figure 2.2). Similarly, in case of using specific soil particle sizes , the soil was sieved from the different sieves to obtain the required particle sizes.

Table 2.1. Particle size distribution (%), organic matter (OM) (%) and CaCO₃ content (%) of the soils used in the determination of the catch efficiency of VS and MWAC catchers.

Name (texture)	Ø (µm)								%	
	0–2	2–10	10–20	20–50	50–100	100–200	200–500	>500	OM	CaCO3
Zdc (sand)	7	0	1	4	22	46	17	2	4.2	0.1
Sdm (clay sand)	9	0	3	12	31	35	9	1	2.6	0.0
Lda (sandy loam)	9	3	10	33	31	10	3	1	2.7	0.0
Aba (loam)	11	3	12	42	21	7	3	1	2.0	0.0
Pdc (high sandy loam)	8	0	6	12	28	33	11	2	2.8	0.0
Efp (clay)	19	1	6	19	22	22	10	0	3.5	0.0
Ugp (heavy clay)	39	7	9	14	11	14	5	1	10.2	0.3

Ø Particle size. The regions are Zdc Grembergen; Sdm Dendermone; Lda Lebke; Aba Asse; Pdc Dendermone; Efp Denderbelle; Ugp Denderbelle

Table 2.2. The aggregate distributions of test soils (%).

Soils	Ø						
	<75 (µm)	75–100 (µm)	100–200 (µm)	200–500 (µm)	500–1,000 (µm)	1,000–2,000 (µm)	>2 (mm)
Zdc	7	5	44	31	7	5	1
Sdm	20	6	34	19	9	11	1
Lda	42	3	16	13	11	12	2
Aba	39	4	12	15	13	14	3
Pdc	22	5	31	21	8	11	2
Efp	11	3	14	18	14	28	12
Ugp	6	2	10	15	15	32	19

Ø Particle size
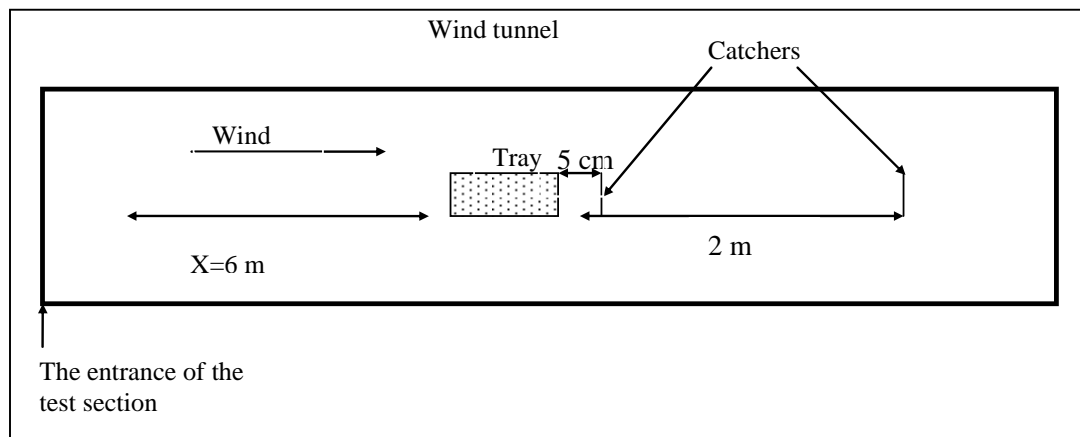
Figure 2.2. The top view of experimental set-up with a tray and catchers in the wind tunnel.

2.3   Description of the vaseline slide catcher

The vaseline slide (VS) catcher consisted of a small transparent glass slide with 7.5 cm length and 2.6 cm width, and one surface of this plate was rugged with vaseline in order to catch soil particles (Figure 2.3). The catcher was positioned perpendicularly to the wind flux at different heights (4.0, 6.5, 13.0, 20.0, 120.0, and 192 cm) during each run. The duration of each run was 126 s.
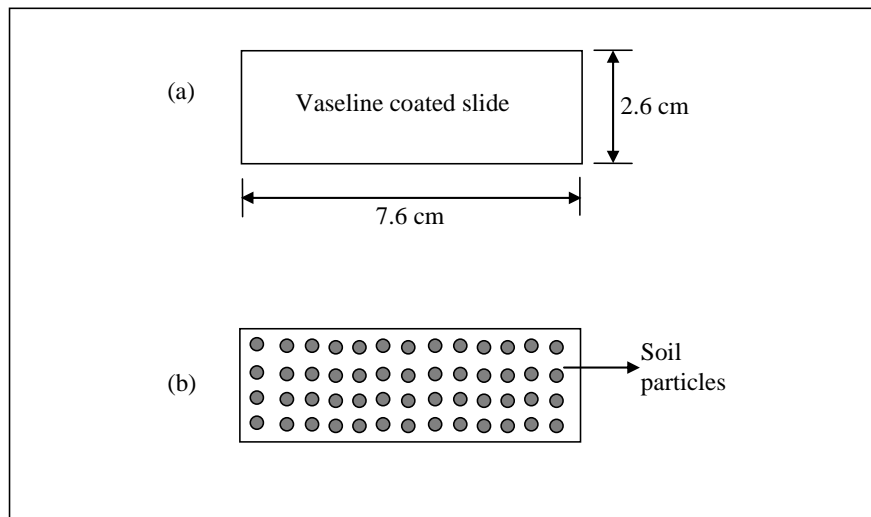
Figure 2.3. Vaseline slide catcher before the test (a) and after the test (b).

The catchers were located at horizontal distances of 0.05 and 2.0 m from the leeward side of the test tray. Locating the catchers at 2.0 m distance and at the different heights allowed to mainly trap suspended small particles passing horizontally (Figure 2.4). The ones located at 0.05 m caught the particles, which moved by saltation.
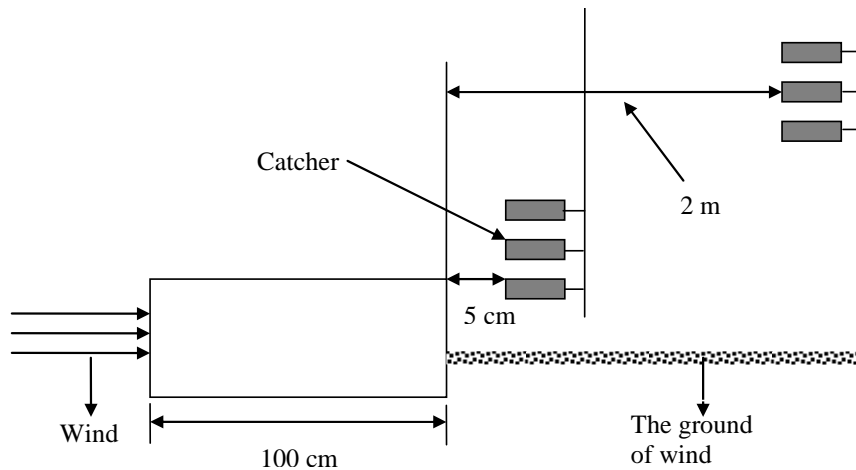
Figure 2.4. The set-up of catchers inside the wind tunnel.

The efficiency of VS was evaluated by the number (#) of particles counted on the slide surface placed at the six different heights as # cm^{-2} s^{-1} after each run, using a Leitz polarizing microscope with graduated ocular. Ten field areas per slide are observed with a 10:1 object-lens, representing an area of 2.545 mm^2 per field area. To obtain the amount of soil in milligrams from the number of particles caught by the slide, equation 2.2 was used (adjusted from Cornelis et al. 1998).

$$I = \rho . \frac{1}{n.A} . \frac{1}{D_u} . 10^{-12} \sum_{i=1}^{n} \sum_{j=1}^{m} X_{ij} V_j \hspace{2cm} [2.2]$$

Where:
I = the eroded sediment (kg m^{-2}s^{-1})
q = particle density (kg m^{-3}),

17

A = field area marked out on the slide surface ($2.545 \cdot 10^{-6}$ m^2),
D_u = duration of the experiment (seconds)
n = number of analysed fields (normally 10, Cornelis et al. 1998),
m = number of diameter classes (normally 10, Cornelis et al. 1998),
X_{ij} = number of particles in diameter class j (=1,2, ..., m) in field i (=1,2, ..., n), and
V_j = volume of particles in diameter class j (m^3).

The parameter V_j depends on the shape of the particles. In case of e.g. spherical particles V_j becomes:

$$V_j = \frac{4}{3}\pi\left(\frac{d_j}{2}\right)^3$$
[2.3]

Where:
d_j = mean diameter in diameter class j (m) = 10 + 20 $(j-1)$.

Similarly, the efficiency of MWAC was evaluated by the amount of soils trapped in the bottles placed at six different heights as kg m^{-2} s^{-1} (1.5, 3.0, 5.0, 8.0, 11.0, and 30.0 cm). Experiments lasted for 126 s (2.1 min) as they were conducted simultaneously with the VS measurements. Finally, the dimensionless efficiencies (η) of VS and MWAC were calculated by equation 2.4.

$$\eta = \frac{Q}{Q_t}$$
[2.4]

Where:
Q is the trapped sediment weight by either slides or bottles (kg) and
Q_t is the total sediment weight (kg) lost from the soil tray during every run, which was determined by weighing the soil in the tray before and after the experiments (*Wb* and *Wa*, respectively):

$$Q_t = W_b - W_a$$
[2.5]

Q was calculated based on measurements of the mass flux $q(z)$ (g m^{-2} s^{-1}) (as the amount of sediment trapped was slight the unit of kg m^{-2} s^{-1} was converted to g m^{-2} s^{-1}) at different heights. The mass transport Q_z (g m^{-1} s^{-1}) was then analytically estimated by integrating $q(z)$ over the saltation height by equation 2.6.

$$Q_z = \int_0^h q(z)\partial z$$
[2.6]

Where:
h is the maximum transport height (m).
With an invariable width of the soil tray (L, m) and runtime (T, s) (40 cm and 126 s, respectively), the amount of the trapped sediment (Q, g) was computed by equation 2.7.

$$Q = Q_z L T$$
[2.7]

The mass flux, $q(z)$, was described by both the models proposed by Williams (1964; Figure 2.5) and by Sterk and Raats (1996; Figure 2.6), respectively, expressed according to equation 2.8.

$$q(z) = q_0 e^{-\alpha z}$$
[2.8]

Where:
q_0 is the extrapolated mass flux at height z = 0 (g m^{-2} s^{-1}) and
α is the slope factor (cm^{-1}); and

$$q(z) = a(z+1)^{-b} + ce^{\left(\frac{-z}{d}\right)}$$

[2.9]

Where *a, b, c*, and *d* are the regression coefficients of the model.

Yet, the four-parameter model of Sterk and Raats (1996) could only be used with the data of the VS catcher, but not with those of MWAC catcher since it needed at least four data points for getting the curve fitted. In other words, there were insufficient data points to fit the model in most of the runs with MWAC catcher.
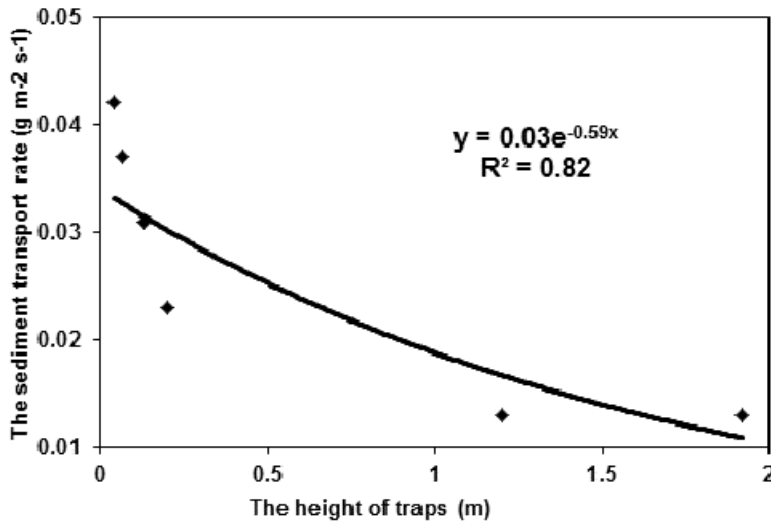
Figure 2.5. Example of the sediment transport rate (g m^{-2} s^{-1}) against the height (m). The solid line is the fitted equation of Williams (1964) and dots are observations.
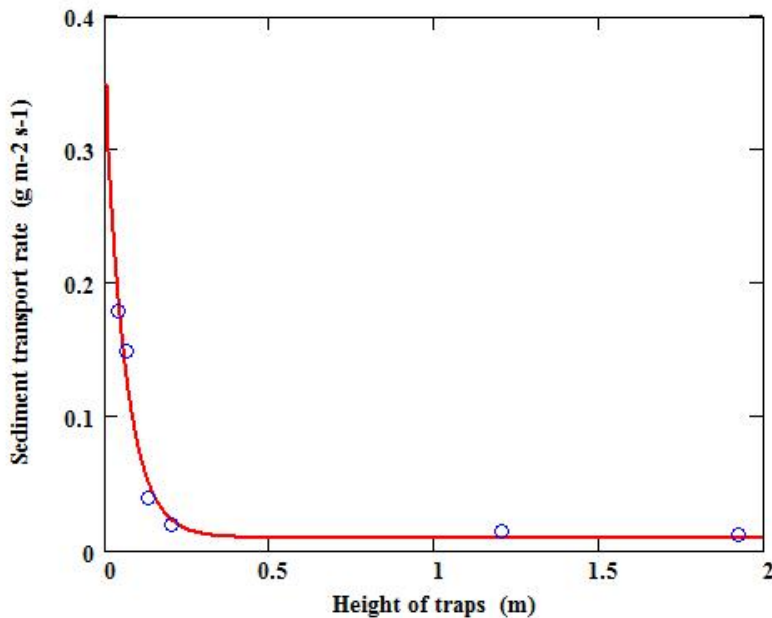
Figure 2.6. Example of the sediment transport rate (by VS catcher) (g m^{-2}s^{-1}) against the height (m). The solid line is the fitted equation of Sterk and Raats (1996) and dots are observations.

2.4   Results and discussion

2.4.1 The efficiency of the catchers with specific soil particle sizes

The efficiencies of VS and MWAC catchers are given in Tables 2.3, 2.4, and Figures 2.7, 2.8, respectively. Table 2.3 shows a considerable decrease in VS catcher's efficiency with increasing particle size. This was due to the limited capacity of the slide in catching sediments: it stopped catching when the surface became completely saturated by sediments. Therefore, with big particles (200–400 and 400–500 μm) the VS catcher was saturated in a short time after starting the experiment, and the slide could only catch a low number out of the total eroded amount before it was blocked. But, when VS catcher was used to catch small particles (<50, <75, and 50–75 μm), it took a longer time before the slide was saturated, and the number of sticking particles was relatively high compared with the total eroded amount.

Table 2.3. The efficiencies of the VS catcher with specific soil particle sizes.

(∅ μm)	u (m s^{-1})	η (%) (Eq. 2.8)	η (%) (Eq. 2.9)
<50	13.4	59	92
<75	13.4	36	26
50–75	13.4	26	25
200–400	13.4	2	2
400–500	13.4	3	2

u Wind velocity; ∅ particle size; η efficiency (Equation 2.4)

Table 2.4. The efficiencies of Wilson and Cooke catcher with specific soil particle sizes.

∅ (μm)	u (m s^{-1})	η (%) (Eq. 2.8)
<50	13.4	0.0
<75	13.4	0.5
50–75	13.4	14.5
200–400	13.4	37.8
400–500	13.4	24.8

u Wind velocity; ∅ particle size; η efficiency (Equation 2.4)

Figure 2.7 shows comparisons of the results obtained by Equations 2.8 and 2.9 for the efficiency of VS catcher. The efficiencies of the particles sizes of 50–75, 200–400, and 400–500 μm by Equations 2.8 and 2.9 were similar and had values of 26 and 25%, 2 and 2%, and 3 and 2 %, respectively (Table 2.3).
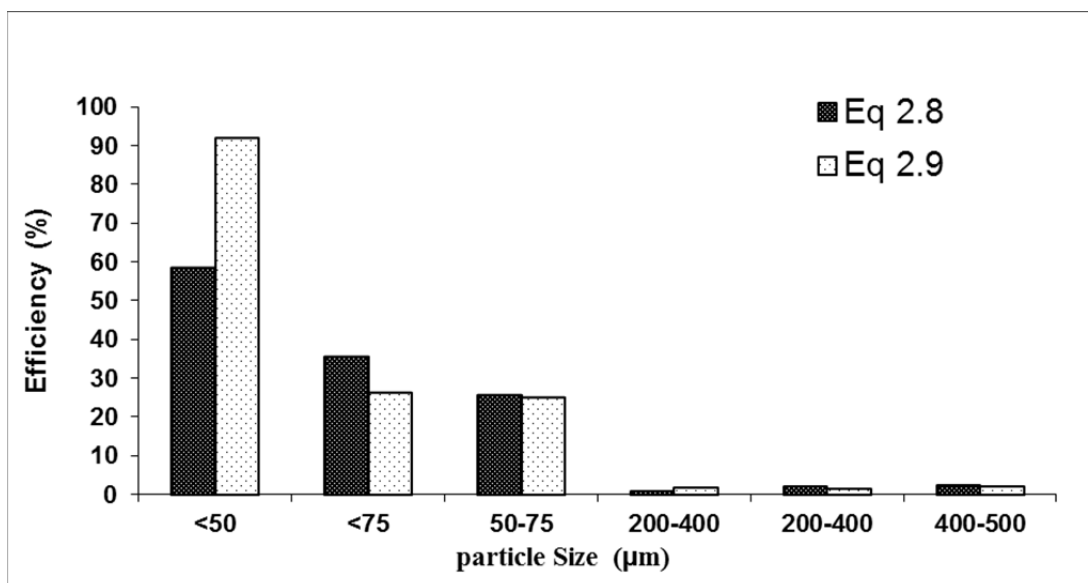
Figure 2.7. The efficiency of the VS catcher with the specific soil particle sizes, black bar (Equation 2.8) and grey bar (Equation 2.9).
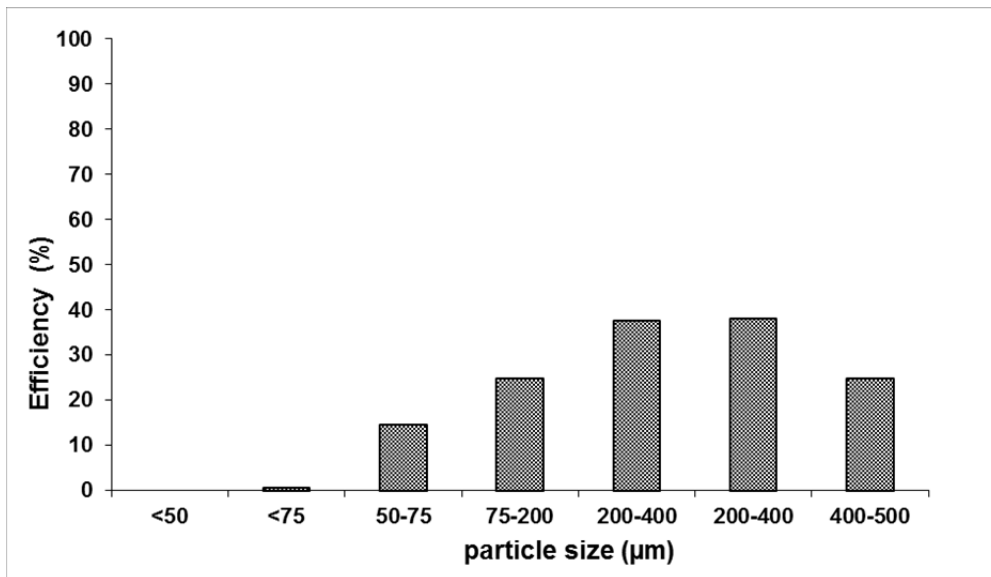
Figure 2.8. The efficiency of MWAC catcher with the specific soil particle sizes, Equation 2.8.

On the other hand, important differences occurred in the VS efficiency when using Equation 2.8 or 2.9 with the particles sizes of <50 μm and <75 μm, and values were 59 and 92% and 38 and 26%, respectively. To a particularly a large degree, the efficiency when using Equation 2.8 was smaller than when using Equation 2.9 for the particle sizes of <50 μm. This was because Equation 2.9 had a better fitting performance than Equation 2.8 to account for catching smaller particles sizes at the lower heights of the VS trap. A better fit of Equation 2.9 than that of Equation 2.8 in this region is shown in Figures 2.6, 2.5, respectively. Regardless of the goodness of the curve fitting, the wind tunnel experiments with VS catcher indicated that the efficiency decreased as the particle sizes increased.

On the other hand, it was clear from Table 2.4 that there was an important increase in the efficiency of MWAC catcher with increasing particle size (Figure 2.8). η values were 15, 25, 38, and 25% for 50–75, 75–200, 200–400, and 400–500 μm, respectively. With the particles smaller than 50 and 75 μm, the efficiency of MWAC was 0 and 1%, respectively. These results suggested that MWAC could not catch any particles smaller than 50 μm and hardly trapped those smaller than 75 μm. This could be attributed to the pressure that happened at the entrance of the bottle's inlet, which prevented small particles to enter into the bottle. However, the behaviour of big particles was different and they could more easily enter into the bottle.

2.4.2 The efficiency of VS and MWAC catchers for the soils with different texture

2.4.2.1The efficiency of vaseline slide catcher
The efficiency of VS was also determined using seven different soils at the different wind velocities of 10.3, 12.3, and 14.3 m s^{-1} (Table 2.5; Figure 2.9). η values calculated by Equation 2.8 and Equation 2.9 were mostly similar except for a few cases. For example, the efficiency of VS calculated by Equation 2.8 was importantly greater than that by Equation 2.9 for Lda sandy loam at the wind speed of 10.3 m s^{-1} and for Efp loam at the wind speed of 14.3 m s^{-1}.

Table 2.5 The efficiency of VS with different soil

u (m s^{-1})	Soils	η (%) (Eq. 2.8)	η (%) (Eq. 2.9)	Q_t (g) (Eq. 2.5)
	Zdc (sand)	6	5	45.0
	Efp (loam)	20	18	14.0
	Lda (sandy loam)	16	2	18.0
10.3	Aba (loam)	8	7	15.0
	Sdm (clay sand)	4	4	43.4
	Ugp (heavy clay)	2	2	40.0
	Pdc (high sandy loam)	3	3	55.0
	Zdc (sand)	5	4	182.0
	Efp (loam)	24	22	21.0
	Lda (sandy loam)	17	15	34.0
12.3	Aba (loam)	12	9	41.6
	Sdm (clay sand)	8	5	48.0
	Ugp (heavy clay)	10	9	45.0
	Pdc (high sandy loam)	12	7	67.0
	Zdc (sand)	4	2	335.0
	Efp (loam)	61	14	43.8
	Lda (sandy loam)	34	30	34.4
14.3	Aba (loam)	10	9	86.0
	Sdm (clay sand)	6	5	95.7
	Ugp (heavy clay)	14	12	50.0
	Pdc (high sandy loam)	6	5	160.0

As previously discussed, this could be due to the performance of the model in fitting the sediment transport rate (g m^{-2} s^{-1}) with the height of traps (m) (Figures. 2.5, 2.6). In terms of different wind speeds, there was no clear trend in the efficiency of VS; it either increased or decreased as the wind speed (u, m s^{-1}) increased. For example, given Equation 2.8, as u increased, the efficiency of VS also increased for Efp loam, Lda sandy loam and Ugp heavy clay but it decreased for Zdc sand. On the other hand, for Aba loam, Sdm clay sand and Pdc high sandy loam, there was an increase in the efficiency of VS when u increased from 10.3 to 12.3 m s^{-1} values were 8, 4 and 3% and 12,8 and 12%, respectively, and this increasing trend was not continuous and overturned when u increased from 12.3 to 14.3 m s^{-1} values were 12,8 and 12% and 10, 6 and 6%, respectively. When Equation 2.9 was considered, these three cases suggested themselves again, but, there was an inconsistency between Equation 2.8 and Equation 2.9 only for the soil of Efp loam regarding variation of the efficiency of VS with u. In the latter, for Efp loam, the efficiency of VS increased when u increased from 10.3 to 12.3 m s^{-1} values were 18 and 22%, respectively and this reversed and started to decrease η values were 22 and 14%, respectively. Again, apart from the goodness of the curve fitting, the results indicated that the efficiency of VS importantly changed with the soils because of the different aggregate distributions of the soils or because of the erodibility of the soils to the wind erosion, which is measured by the percentage of aggregates smaller than 0.84 mm.
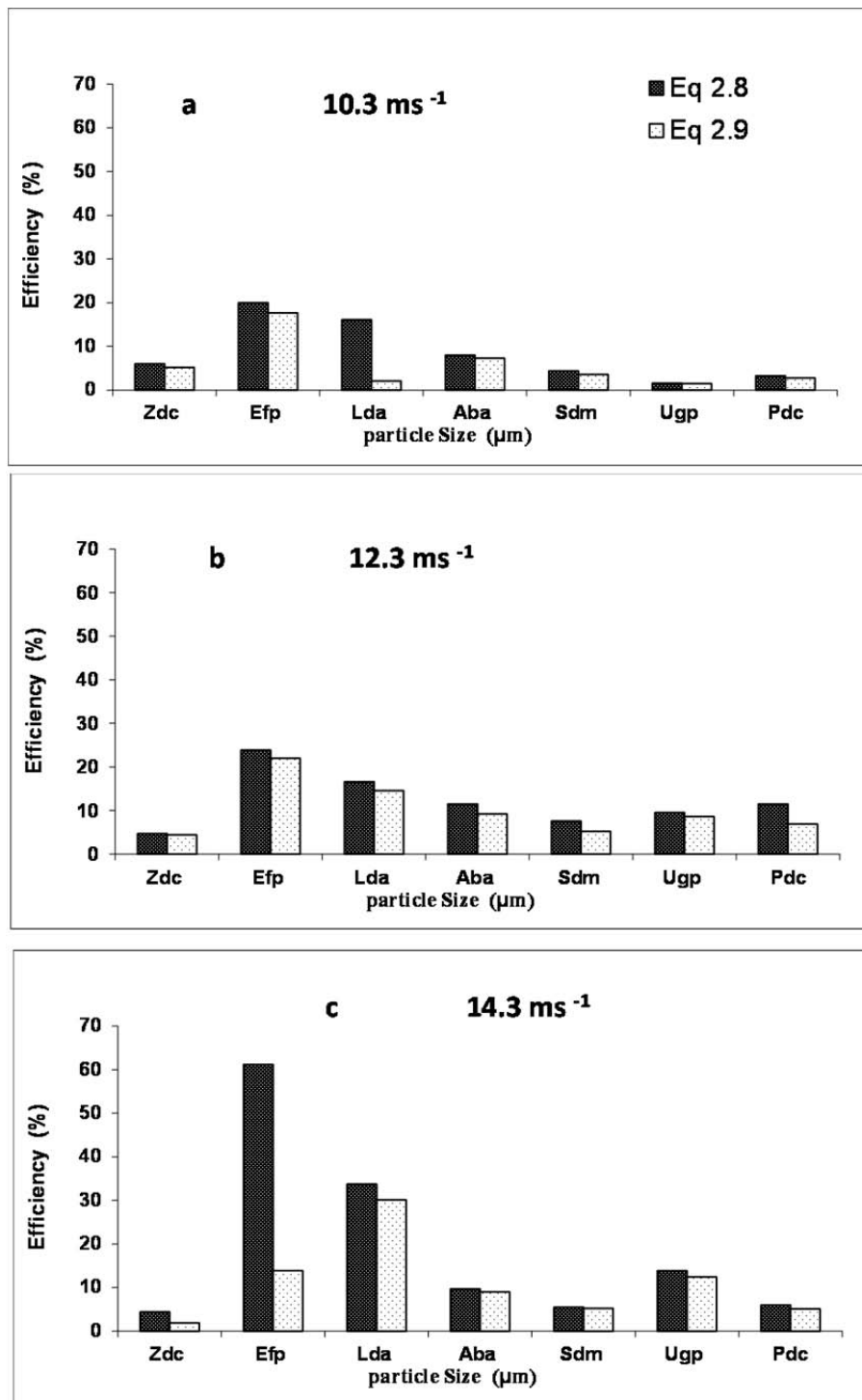
Figure 2.9 The efficiency of VS with different soils, (black bar (Eq. 2.8) and grey bar (Eq. 2.9)), a: at 10.3 m s^{-1}, b: at 12.3 m s^{-1}, and c: at 14.3 m s^{-1}.

The mass of total eroded sediment (Q_t) calculated by Equation 2.5 for every soil is given in Table 2.5 and the variation of Q_t among soils can be explained by the erodibility of soils, measured by the percentage of aggregates larger than 0.84 mm, to the wind erosion. Since the efficiency of VS depends strongly upon the aggregate distribution, it implies that the sensitivity of the sandy soil (Zdc) was the highest although the most resistant soil was loam (Efp) in terms of the aggregate distribution (Table 2.2). Generally, the efficiency decreased when Q_t increased and importantly changed with wind speed. For instance, the results for sandy soil Zdc indicated that the efficiencies were 5, 4, and 2% at 10.3, 12.3, and 14.3 m s^{-1}, respectively. Since the slide had a known surface and its capacity was reasonably limited, its efficiency was low when it

was used to catch the particles of the sensitive soils. On the other hand, it seemed to be different with resistant soils, and the efficiency increased with increasing wind speed. For the sandy loam soil Lda the efficiencies were 2, 15, and 30% at 10.3, 12.3, and 14.3 m s^{-1}, respectively. Similarly, for heavy clay soil Ugp the efficiencies were 2, 9 and 12% at 10.3, 12.3, and 14.3 m s^{-1}, respectively, and this was because the slide surface was still able to stick more particles at 10.3 m s^{-1} speed but there were not enough particles to reach it. Also, the same happened at 12.3 m s^{-1}, and therefore, the highest efficiency was at 14.3 m s^{-1}. With some soils the highest efficiency was at 12.3 m s^{-1}, for instance with Efp, Aba, and Pdc (Table 2.5), and η values were 22, 9, and 7%, respectively. This was ascribed to the fact that the catcher reached its limit at 12.3 m s^{-1} wind speed.

2.4.2.2 The efficiency of Wilson and Cooke catcher
The efficiency of MWAC trap was also determined using different soils (seven different soils) and different wind speeds of 10.3, 12.3, and 14.3 m s^{-1} (Table 2.6; Figure 2.10). The efficiency of MWAC changed with the soil and wind speed. Generally, the efficiency of MWAC increased with increasing wind speed. At the wind speed of 10.3 m s^{-1} η values were 67 and 70%, respectively, for Zdc sand and Lda sandy loam, but for Efp loam, Aba clay, Sdm clay sand, Ugp heavy clay, and Pdc high sandy loam, it was 0%. Unlike VS, MWAC could not trap any particle of these soils, and, it was shown by the sand experiments that MWAC could not catch any particles smaller than 50 µm and hardly trapped those smaller than 75 µm. These results indicated that Zdc sand and Lda sandy loam had rather high percentage of aggregates transportable by saltation at the wind speed of 10.3 m s^{-1} than the others. As a result, the aggregates of Efp loam, Aba clay, Sdm clay sand, Ugp heavy clay, and Pdc high sandy loam were either transported by the suspension or too strong to be dislodged for saltation at this wind speed. Although the aggregate distributions of the soils are given in Table 2.2 and some explanations could be made about these values, this might be very ambiguous since we could not know aggregate distributions of the soils after the wind shear stress on the soils; important variations are expected to take place in the distributions, and this was explicit from the fact that the rises in the wind speed caused increases in the efficiency of MWAC. At the wind speed of 12.3 m s^{-1}, while Efp loam, Sdm clay sand, and Ugp heavy clay had η values of 0, Aba clay and Pdc high sandy loam reached satisfactory η values, 51 and 46%, respectively. For Zdc sand there was an overestimation in the efficiency of MWAC owing to the curve fitting and for Lda sandy loam there was an inconvenient condition in the wind tunnel to complete the experiment at this wind speed. Therefore, the efficiency of MWAC was not estimated for this soil. On the other hand, at the wind speed of 14.3 m s^{-1} η values of MWAC were more than 40% for all soils except Ugp heavy clay, the values of which were 0. The efficiency values of MWAC were 99, 41, 120, 47, 74, and 74% for Zdc sand, Efp loam, Lda sandy loam, Aba clay, Sdm clay sand, and Pdc high sandy loam. Those different results consequently emphasized the fact that the efficiency of MWAC changed with particle size and wind speed and indicated that there was selectivity in trapped materials because the soils had different aggregate distributions depending on the applied wind shear stress. This selectivity could be related to the sizes and shapes of the soil particles.

Table 2.6. The efficiency of Wilson and Cooke catcher with different soils.

u (m s^{-1})	Soils	η (%) (Eq. 2.8)	Q_t (g) (Eq. 2.5)
	Zdc (sand)	67.4	45.0
	Efp (loam)	0.0	14.0
	Lda (sandy loam)	69.8	18.0
10.3	Aba (clay)	0.0	15.0
	Sdm (clay sand)	0.0	43.4
	Ugp (heavy clay)	0.0	40.0
	Pdc (high sandy loam)	0.0	55.0
	Zdc (sand)	113.4	182.0
	Efp (loam)	0.0	21.0
	Lda (sandy loam)[a]	–	34.0
12.3	Aba (clay)	50.7	41.6
	Sdm (clay sand)	0.0	48.0
	Ugp (heavy clay)	0.0	45.0
	Pdc (high sandy loam)	45.9	67.0
	Zdc (sand)	99.3	335.0
	Efp (loam)	41.0	43.8
	Lda (sandy loam)	120.2	34.4
14.3	Aba (clay)	47.2	86.0
	Sdm (clay sand)	73.8	95.7
	Ugp (heavy clay)	0.0	50.0
	Pdc (high sandy loam)	73.8	160.0

u Wind velocity; $\varnothing$ efficiency (Equation 2.4); Q_t total eroded soil (Equation 2.5).

[a] The test with Lda sandy loam at the wind speed of 12.3 m s^{-1} could not be completed because of an inconvenient condition emerged during the experiment.

Goosens et al. (2004) investigated the efficiency of the MWAC catcher. Opposing to what we found, they reported that the efficiency of MWAC increased with a decrease in particle sizes and they showed that the efficiency of MWAC ranged from 90-120% for wind speed in the range of 6.5-14.4 m s^{-1}. The difference between the two studies can be linked to the dissimilarities in the range of particle sizes used in the two studies and the wind speed applied. In the current study the efficiency was tested for a wide range of particle sizes (from <50 µm to 400 µm), compared to the study of Goosens et al. (2004); from 132 µm to 287 µm. Given the sensitivity of the traps for variation in wind speed particle size, we conclude that the comparison between the two studies is quite difficult due to the different class range of particle sizes and wind speed.

This current study highlighted the recommendation of Zobeck et al (2003) who mentioned that the type of sediment catcher to be used should be chosen upon the sediment to be trapped.

2.5 Conclusion

By wind tunnel experiments, MWAC and VS sediment traps were tested for different soil particle sizes at a fixed wind speed and for different soil textures at different wind speeds. Both catchers worked well with specific soil particle sizes at a fixed wind speed (13.4 m s^{-1}). Generally, with fine soil particles, VS had a high efficiency while MWAC had a low efficiency. Particularly, the efficiencies of VS and MWAC with the specific soil particles smaller than 50 µm were 92 and 0% respectively. However, the reverse happened with bigger soil particles: VS had a low efficiency while MWAC had a high efficiency. Especially, the efficiencies of VS and MWAC were2 and 2% and 37.8 and 24.8% with the particles of 200–400 µm and 400–500 µm,

respectively. These results obviously indicated that VS could be used with the sediments moved by the suspension (<75 μm) and MWAC could be used with the sediments moved by saltation (<500 μm).
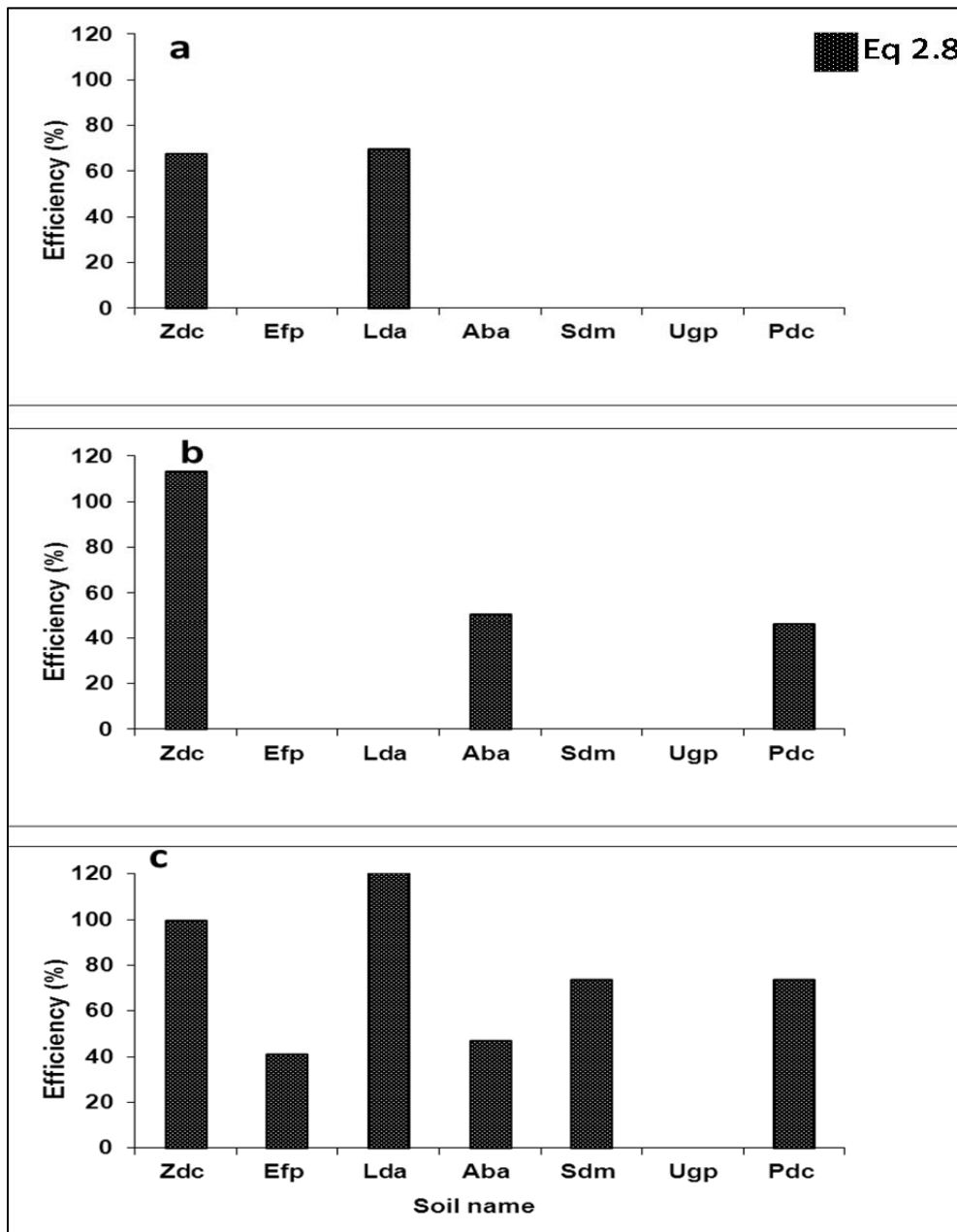
Figure 2.10. The efficiency of MWAC with different soils a at 10.3 m s^{-1}, b at 12.3 m s^{-1}, and c at 14.3 m s^{-1}. The empty bars for some soils indicated that the values efficiency with these soil were around 0

Soil experiments with increasing with speeds also showed that the efficiency of VS and MWAC changed with soil and wind speed. Depending upon the variations in the aggregate distributions of the soils, which were greatly affected by the wind shear stress, the efficiency of VS and MWAC varied accordingly. Although more soil aggregates or particles were available for suspension with a rise in the wind shear stress, the efficiency of VS was determined by its limited trap capacity. However, when there were more aggregates moveable by the saltation with increases in wind speed, the efficiency of MWAC increased. Results consequently affirmed that MWAC catcher was not useful to catch the suspended materials, and VS trap had a very low efficiency when it used to catch the saltating materials. During the series of experiments, the ability of MWAC catcher was low at greater heights while that of VS was reasonably better with height.

Chapter 3

A new method for measuring wind erosion at the regional scale: Observing aeolian sediment transport at different land covers

A new method for measuring wind erosion at the regional scale: Observing aeolian sediment transport at different land covers

Abstract

Wind erosion is a serious environmental problem in the arid and semi-arid regions of the Earth. In spite of this fact, to date, the majority of measurements on wind erosion, with a focus on saltation, were undertaken on the scale of plots, fields, and recently paddocks. Consequently, regional scale data for wind erosion, in general, and for the saltation process, in particular, are not available. The objective of this research is to develop a method for measuring regional scale wind erosion with a specific focus on the saltation process. So far, equipment that directly measures regional scale wind erosion and more specifically provides insights at the saltation process at the scale of a region is not available. A possible solution for this to measure of the transport at the various land use areas found in a region and at borders between them. In this research, aeolian mass transport was measured using a portable plot method at 16 plots in the Khanasser Valley, Syria in 2009 and 2010. During the measurement period, a full climate station was installed at each plot together with a saltiphone in addition to Modified Wilson and Cooke (MWAC) sediment catchers. The results of this research showed that, with this method, information on the effect of wind regime and land use on the aeolian mass transport for different land uses a region can be obtained. Also, the technique provides insights into the interrelation between neighbouring land units. It was concluded that data collected with this method are suitable for calibration and validation of regional scale wind erosion models.

Key words: Measuring wind erosion, regional scale, aeolian mass transport, Khanasser Valley, Syria

3.1   Introduction

Wind erosion causes major agricultural and environmental problems, especially in the arid and semi-arid regions of the world (Sivakumar et al., 2005; Stroosnijder, 2005; Maurer et al., 2010). The wind erosion process comprises encroachment, transport and deposition of sediment by the force of the wind (Shao, 2008). Once the wind speed exceeds the threshold velocity for transport, particles are pulled from the surface by the airflow (Bagnold, 1954). Research on wind erosion identifies this problem at different spatial scales including point (i.e. Hoogmoed et al., 2000), field (i.e. Sterk, 1997; Visser and Sterk, 2007), village (i.e. Rajot, 2001), region, and continental to global scales (i.e. Leys et al., 2001, Shao, 2008).

The occurrence of wind erosion is a function of weather factors interacting with soil properties and vegetation cover (Sivakumar et al., 2005). Land use in regions vulnerable to wind erosion has a critical effect on the vegetation cover and soil properties (Sharratt et al., 2012; Young and Schillinger, 2012; Sivakumar et al., 2005). Insight into the wind erosion process at different land use types in a region and an understanding of the interrelation between neighbouring land units is required for a better understanding of the problem at the regional scale (Hupy, 2004; Leenders, 2006). Wind erosion models are useful tools that provide insights into the process and predict the effect of different land management practices on the quantity and intensity of wind erosion in vulnerable regions (Hagen, 1991; Fryrear et al., 2000; Webb et al., 2006).

Based on the spatial scale, the available wind erosion models can be divided into field and regional scale models. Field scale models – such as the revised wind erosion equation (RWEQ) (Fryear et al., 1998), the wind erosion prediction system (WEPS) (Hagen, 1991), and the Texas Tech University wind erosion

analysis model (TEAM) (Gregory et al., 2004) – can be calibrated and validated against ground data and thus, their predictions are relatively reliable (Zobeck et al., 2003). The majority of field scale models are applicable for a single land use in a region and they do not provide insights into the interactions between neighbouring land units. Therefore, field scale wind erosion models do not provide the information required by policy developers and land managers who need knowledge that covers the entire region to better plan the future land use for sustainable resources managements.

Regional scale wind erosion models include primarily the Wind Erosion Assessment Model (WEAM) (Shao et al., 1996), the Australian land erodibility model (AUSLEM) (Webb et al., 2006), the land type erodibility index model (LEI) (McTainsh et al., 1999) and the dust transport model (DUSTRAN) (Butler et al., 1996). These models require inputs for climate, soil and vegetation at relatively large scale (Zobeck et al., 2003). To obtain these inputs a long time of preparation and analyses is required and sometimes the use of Remote sensing (RS) technology is required to collect the required to collect the inputs to run these models (i.e. DUSTRAN). Some inputs derived through RS for a large-scale area will have a relatively high level of uncertainty when using low resolution RS images. Furthermore, the use of high-resolution images will result in a large cost and will need a long time for processing. Moreover, the calibration and validation of current regional scale models depends mainly on the RS technology because ground data on wind erosion for the large scale areas are not available (Zobeck et al., 2003). Hence, the application of the current regional scale models is limited due to the high cost to collect the inputs and the absence of ground data needed for the calibration and validation of these models.

Developing a measurement method that provides data on wind erosion at the regional scale would be a large step towards the understanding of wind erosion at the regional scale and to provide data required for developing regional scale models. This measurement should cover the wind erosion process within different land use areas in the region and the interactions between neighbouring land units (Breshears et al., 2003; Breshears et al., 2009).

Current wind erosion measurements can be divided into two main groups: the saltation-based group and the suspension-based group. In the saltation-based measurements, the sampling of wind-blown sediment is widely applied (Sterk, 1997; Visser et al., 2005b; Leenders, 2006). These measurements provide precise information on the wind erosion process at the point, field, and village scales and, thus, this approach is suitable for calibration and validation of field scale models. While these measurements are expensive and require a long preparation time (Stroosnijder, 2005; Chappell et al., 2006), the spatial coverage is mostly small and, thus, their value for understanding the wind erosion process at the large scale is limited. Furthermore, data collected by these measurements cannot be used sufficiently for the calibration and validation of regional scale models.

The suspension-based group depends on RS technology, such as multi-temporal SPOT high resolution visible imagery and RADARSAT-1 imagery, to derive data on suspended dust and uses these data for calibration and validation of regional scale models. The suspension-based group mainly considers the suspended materials as constituting the main matter transported and relatively underestimates the saltation process that is the main reason for suspension (Zhang and Lee, 2009). Furthermore, saltation causes nutrient lose and thusly reduction in soil productivity (Sterk, 1997). Also saltation has a direct negative effect on crops causing a decrease in production (Sivakumar et al., 2005, Baker, 2007; Baker et al., 2009). Moreover, recent studies showed that approximately 50 to 80% of the total eroded sediment is transported through saltation (Sterk, 1997; Visser and Sterk, 2007; Zhang and Lee, 2009).

To develop a measurement method for obtaining information on regional scale wind erosion, it is important first to define the data requirements. The key requirements are that the data should provide insights into:

- The effect of wind on aeolian sediment transport for different land uses in a particular taking into account the saltation process.

- The effect of land use and vegetation cover on the wind erosion process in a region
- The interactions among neighbouring land units when sediment is transported across different land units.
- Data should provide an overview of the temporal variation in aeolian mass transport in the region.

The objective of this research is to develop a measurement method that will provide data on wind erosion at the regional scale, given the above mentioned requirements. The main research questions are the following.

1. What is the effect of the wind regime on aeolian mass transport in a region?
2. How does land use affect aeolian mass transport in a region?
3. How does land use at one land unit affect aeolian mass transport at a neighbouring land unit?
4. How data can be collected using our new measurement method progress the modelling of wind erosion at the regional scale?

3.2 Materials and methods

3.2.1 Wind erosion measurement techniques

A large body of existing work, which uses a wide range of different sampling methods and equipment, can be identified for saltation-based measurements. Table 3.1 summarizes recent work and provides details of the scale, the sampler, a land unit description, and the objective for sampling the mass transport.

Table 3.1 shows that field measurements of aeolian mass transport have been carried out at different scales ranging from 300 m^2 to 1.600.000 m^2 (160 ha). They were carried out on bare surfaces, agricultural fields with residues, and on fields with scattered shrubs and they used different sediment samplers. The objectives of these studies included calibration and validation of wind erosion models, determination of the efficiencies of sediment samplers, and providing information on wind erosion at a large scale such as the Sahel region.

The results obtained from these measurements improved our understanding of wind erosion processes at the point, field, and village scales. However, most of these studies discussed the wind erosion problem by focusing on a single land use and not a single study provided data for several land uses in a region. The present study was undertaken to fill this gap. While past sampling schemes focused on dense sampling at a limited number of locations, we propose an approach using a portable plot method in which measurement equipment is moved to a large number of plots to enable the sampling at a large number of locations and at a wide range of different vegetation covers and soil types.

The measurement locations represented the major land uses in the region. For each land use, measurements were taken at a minimum of two plots. The interaction between neighbouring land units in the region is determined by measuring the aeolian mass transports at the boundary between two neighbouring land units. Measurements for the portable plot method were taken for 21 days during the wind erosion season. In the study region of this research, this time period was long enough to obtain a good impression of the sensitivity for the land units to wind erosion. Usually, however, the period of measurement should be determined from an analysis of the wind data of the region over an extended period. In addition to the aeolian mass transport, the parameters of climate, soil, roughness, and vegetation cover were recorded (Table 3.2).

Table 3.1. A summary of current wind erosion measurements at the field and plot scales (adapted from Zobek et al., 2003).

Citation	Scale (m^2)	* Sampler for saltating material	Land unit Land use	Focus
Basaran et al., 2011	Not mentioned	BEST	Bare	Determination the efficiency of newly designed trap
Bielders et al., 2000	15 x 20	MWAC	Agriculture	Effect of land management on wind erosion
Buschiazzo et al., 1999	100 x 100	BSNE	Bare	Assessment of wind erosion in S. America
Funk, 2004	150 x150	SUSTRA	Bare	Validate WEPS wind erosion model
Ikazaki et al., 2011	113x 113	AMS & BSNE	Agriculture	Wind erosion effect on losing nutrient
Gomes et al., 2003	100 x 100	MWAC	Bare	Wind erosion data within agricultural field
Goossens and Gross, 2002	320 x 220	MWAC	Agriculture	
López, 1998	1.5 ha	None	Bare	
Rajot et al., 2002	Not mentioned	BSNE	Bare	Assessment of wind erosion in Sahel, Africa
Sterk and Spaan, 1997	55 x 70	MWAC	With residues	
Sterk et al., 1999	135 x 180	MWAC	Bare	
Stetler and Saxton, 1994	1600 x 1000	BSNE	Bare	Wind erosion data within dry land fields
Stout and Zobeck, 1996	360 x 250	BSNE	Bare	Wind erosion data within agricultural fields
Leenders et al., 2007	150 x 150	MWAC	With shrubs	Wind erosion data within pastoral fields

*BEST – cyclone-type trap; MWAC – Modified Wilson and Cooke; BSNE – Big Spring Number Eight; SUSTRA – Suspended Sediment Trap; AMS – Aeolian Material Sampler.

Table 3.2. Parameters required to gain insight into the aeolian mass transport at a land unit, required inputs for most wind erosion models.

Factor	Parameter	Why it is needed
Weather	Wind speed	To determine the wind threshold velocity
	Wind direction	Essential for determining of border effects
Soil	Texture	Soil and roughness parameters are important for determining the susceptibility of soil to wind erosion, and for determining the available loose materials at the surface.
	Soil moisture	
Roughness and crust	Roughness length	
	Crust thickness and strength	Most wind erosion models consider these parameters as key parameters in predicting the wind-blown mass transport from a bare surface
Vegetation/ residues	Percentage of surface covered with vegetation	These parameters determine the effectiveness of the vegetation in protecting the soil surface against erosive winds
	Height of vegetation	
	Vegetation pattern	

3.2.2 Study area and measurement plots

The region of the Khanasser Valley, Syria was chosen to test the method of the portable plot because it has a variety of land uses within a relatively small area. Also, it is possible to evaluate the border effect as the borders between some land units are relatively clear and distinct. The valley is located between the Al Hass and Shbeith mountains southeast of Aleppo city, Syria (Figure 3.1). The valley is rather flat with an average altitude of 350 m. Annual precipitation varies from 150 to 250 mm and the rainy season starts in October and ends in May (Masri et al., 2003; Youssef et al., 2012a, chapter 4).
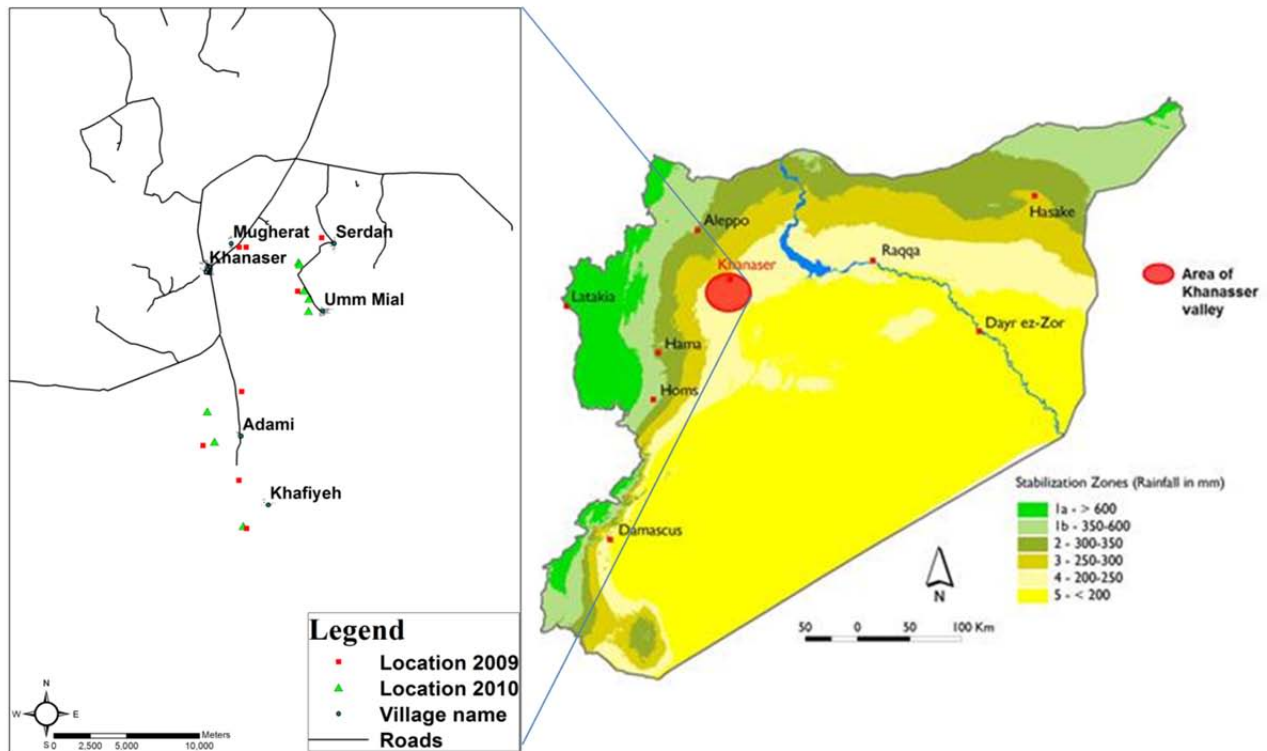
Figure 3.1. The location of Khanasser Valley in Syria (right), and the locations of the measurement plots in the valley.

In the wind erosion season, sediment transportation results mainly from the predominantly southerly or westerly winds; there are some exceptional strong wind events from other directions (Youssef et al., 2012a). The daily average wind speed at a height of 2 m may exceed 10 m s^{-1} (Masri et al., 2003) and the monthly average wind speed ranges from 3.5 m s^{-1} in the south up to 4.4 m s^{-1} in the north (Bruggeman et al., 2010). In an attempt to reduce wind erosion Atriplex halimus shrubs were planted at many locations throughout the valley. During the selection of the measurement locations, it was tried to include some of the re-vegetated locations. The sampling locations were selected following analyses of the general land uses in the Khanasser Valley region. In these analyses, we used a combination of previous land use maps prepared by the International Centre for Agricultural Research in the Dry Areas (ICARDA) and visual observations of the research sites. Depending on the rainfall amount Syria was divided into 5 stability zones (Figure 3.1, Youssef et al., 2012a, and chapter 4). Plots were chosen to represent the main land uses that can be found in the stability zones 4 and 5 in the Khansser valley region. Thus measurement locations were representing the following land uses:

1.   Intensively grazed fields (I.G), located in stability zone 4
2.   Partially grazed fields (P.G), located in stability zone 4
3.   Cultivated and/or bare fields (C&B), located in stability zone 4
4.   Combination of farming with shrub area (Sh.F). This area includes a few projects in the region, and located in stability zone 4

5. *Atriplex* protected area (Atri-). Within this area two main sub land uses be distinguished, the sandy area (Atri-s)(relatively small) and the crusty area (Atri-s) (relatively large), both zones are located in stability zone 5

6. Rangeland area: for the rangeland area (R.L), located in stability zone 5

Table 3.3 shows the main characteristics of the chosen plots in the study area.

Table 3.3. Characteristics of the measurement plots in the research site of Khanasser valley, Syria.

Name	Stability zone	§ Soil texture	% of surface covered with vegetation and rocks (P_{scy})	Crust	roughness C_{rr} (Chain method,-)	¥ Border effect	Threshold velocity*	Land use
I.G1	4	Clay-loam	< 3	No	4.3	SEB	3.8	Intensively grazed
I.G2	4	Sandy-loam	< 3	No	3.7	EB	3.8	
I.G3	4	Clay-loam	< 3	No	3.0	ITP	3.8	
P.G1	4	Clay-loam	7-10	No	2.9	ITP	4.6	Partially grazed
P.G2	4	Clay-loam	10-15	No	2.8	NE	5.0	
P.G3	4	Clay-loam	10-15	No	3.8	ITP	5.0	
C&B1	4	Clay-loam	0	No	2.2	EB	3.7	Cultivated and bare
C&B2	4	Clay-loam	0	No	7.2	ITP	3.7	
Sh.F1	4	Sandy-loam	25-30	No	1.1	EB	3.9	Farming with shrubs
Sh.F2	4	Clay-loam	30-35	Yes	2.6	ITP	7.6	
Sh.F3	4	Clay-loam	20-25	Yes	0.1	NE	6.3	
Atri-s	5	Silt-loam	20-25	No	1.0	ITP	6.3	Atriplex protected area
Atri-c1	5	Sandy-loam	35-40	Yes	0.4	ITP	8.2	
Atri-c2	5	Sandy-loam	35-40	Yes	0.4	ITP	8.2	
R.L1	5	Silt-loam	< 5	No	0.6	ITP	4.1	Rangeland area
R.L2	5	Silt-loam	< 5	Yes	0.6	ITP	4.1	

§ After soil texture was determined using the hydrometer method the soil type was determined using the Soil Texture Calculator (NRCS, 2010)

¥ The percentage of the surface covered with vegetation or residues was determined by eye for each plot

Λ: ITP: identical to the plot, NEB: non-erodible border, SEB: semi-erodible border, EP: erodible border

* The threshold velocity was determined as a function of the P_{scv} as explained in Youssef et al. (2012a), except the plots for the plots of Sh.F where values were derived from saltiphone data because these plots were a mixture of farming and shrubs

3.2.3 Measuring equipment and its setup

Figure 3.2 shows the equipment used for the measurement of meteorological data and the setup for the 16 MWAC (Wilson and Cooke 1980) catchers. The wind profile was measured using five anemometers (Cup-type anemometers, A100R, Campbell Scientific) recording wind speed at heights of 0.40, 1.00, 1.88, 3.00, and 4.00 m. A wind vane (model of W200P, Campbell Scientific), at a height of 2 m, recorded the wind direction (Figure 3.2 A and B). The wind profile was characterized by the Prandtl–von Kármán logarithmic equation (3.1).

$$u(z) = (\frac{u_*}{k})\ln(\frac{z}{z_0}) \qquad \text{For } z \gg z_0 \tag{3.1}$$

Where:

u(z) is the wind speed (m s^{-1}), at height z(m),

z_0 is the aerodynamic roughness height (m),
u_* is the wind shear velocity, and
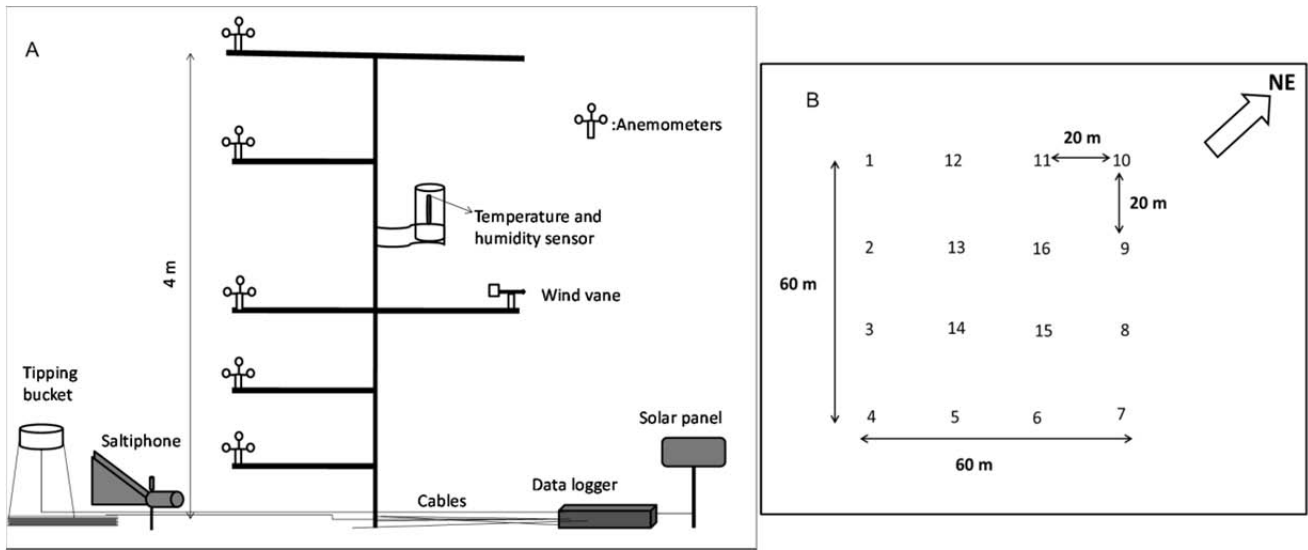k is the von Kármán's constant.

Figure 3.2A. Equipment used for recording climate parameters and saltation periods.
Figure 3.2B. The setup of the 16 MWAC catchers at each measurement plot.

A saltiphone (Spaan et al., 1991) recording the onset of particles during the events was used to determine the duration of saltation for each event. The other climate variables (the temperature, relative humidity, and soil moisture) were measured continuously during measurement periods. A CR1000 data logger (Campbell Scientific) was used to store sensor outputs at five minute intervals. The sampling methodology is explained in detail in Youssef et al. (2012a, chapter 4).

The MWAC catchers were installed on a regular grid to retrieve information on the spatial variability of the mass transport over the plot area (Figure 3.2B). Thus, the trend in aeolian mass transport within the plot along the downwind distance could be observed. Also, the values of the data collected from the catchers at each plot were averaged to provide information about the aeolian mass transport for the land use which the plot represented. This assumed that the average mass transport from all catchers was representative for the specific land unit.

The aeolian mass transport was measured on a weekly basis because the amount of sediment collected after a single wind event was very low for accurate weighing. The duration of the event as measured with the saltiphone was used to calculate the bulk aeolian mass flux. For most plots three measurement periods of on week for each were recorded. The approach of Sterk and Raats (1996) was followed to build up a flux profile by height as:

$$Q_z = \int_0^h \left\{ a(z+1)^{-b} + ce^{\left(\frac{-z}{d}\right)} \right\} \partial z \qquad\qquad [3.2]$$

Where a, b, c, and d are the regression coefficients of the model, h is the maximum transport height.
The values of the R-square (R^2) ranged from 0.50-0.98 for more than 70 % of the data from all catchers and for all events for the 16 plots.

3.2.4 Data analysis

During each measurement period, the characteristics of the event including averaged wind speed, maximum wind speed, averaged wind direction, were calculated for the duration of saltation. To have an idea about the mass transport for the whole plot during each event, the mass transport values collected by the 16 MWAC sediment catchers were averaged and the range of the values in addition to the standard deviation among these values were calculated (Table 3.4).

The wind value is widely used to show the power of an event as this value is the main factor describing the climate characteristics that cause wind erosion (Fryrear et al., 1998). Thus, it is important to determine the value of this factor for each event. The equation of wind value prepared by (Fryrear et al., 1998) was used to calculate the wind value with intervals of 5 minutes which is the interval of the wind data recorded during the measurements. Guo et al. (2012) showed that the interval times (over which wind speed is averaged) significantly affects the wind value calculations. Thus, as we used relatively short period interval times (5 minutes) in the current study, wind values for the events were relatvely high. However, as we used the same interval for all events a comparison between events was possible. Furthermore, to avoid the effect of land use on wind value calculations we use a fixed threshold velocity of 3.7 m s^{-1}, which is the minimum threshold velocity observed at all plots (Table 3.3). The effect of land cover on transport is analysed using a mass transport standardized for the power of an event, as will be described below, which requires a wind value representing the power of an event only, independent of the plot characteristics. Wind values W (kg s^3 m^{-4}) were calculated as:

$$W = \sum_{i=1}^{i=N} U_i (U_i - U_{tm})^2$$

[3.3]

Where:

U_i *is* the wind speed for the time step (i) at 2 m height (m s^{-1}), (only values larger than U_{tm} were used).

U_{tm} is the threshold velocity (3.7 m s^{-1}) considering as the minimum threshold velocity for our measurement plots. N is the number of wind speed observations with time step of 5 minutes during the week of measurements

The effect of land use on the total mass transport regardless the wind power is shown through the 'wind value-standardized mass transport' in which the value of mass transport for an event is divided by the wind value for this event and it is calculated as:

$$MS = M / W$$

Eq [3.4]

Where:

MS is the wind-value standardized mass transport (kg m^{-4} s^3), M (kg m^{-1}) is the mass transport and W is the wind value (m s^{-1})^3.

Insights into the effect of the border between neighbouring land units, were obtained through the analyses the distribution of the mass transports within the plots that are located at the border areas of two or more neighbouring land units. Geostatistical interpolation of the data was performed and maps showing the spatial variation of mass transport within the plots were created following the procedure explained in Sterk et al. (1998).

3.3 Results and discussion

3.3.1.1 General results

Table 3.4 provides the characteristics of the wind events and the mass transport values. The main wind directions were WSW, W and WNW. The average wind speed ranged from 4.6 m s^{-1} to 10.9 m s^{-1}. The maximum wind speed varied from less than 6.3 m s^{-1} to 12.9 m s^{-1}. The aeolian mass transport varied between land uses, plots, and weeks for each plot. The plots at the *Atriplex*-protected zone that have a crust on the surface (*Atri-c1 and Atri-c2* resulted in a mass transport of zero kg m^{-1}. For most weeks at most plots, the values of the range and the standard deviation (SD) of the mass transport values were high relative to the associated average values. The high values of the SD indicate a high variability in aeolian mass transport within the plot during each measurement period.

Table 3.4. Land use, wind parameters, duration of saltation and mass transport for each week of the measurements.

Land use	Plot name, village name	Week	Mean wind speed (m s^{-1}) ¥	Max. wind speed (m s^{-1})	Wind value [(m/s)^3 x10^3)]	Mean wind direction	Duration of saltation (sec, x 10^3)	Mass transport (kg m^{-1}) Mean	Range	SD
Intensively grazed (I.G)	I.G1 (Um Mial)	1	4.9	11.0	126.5	WSW	65.4	4.8	12.8	3.7
		2	4.6	10.1	79.9	WSW	6.2	1.6	5.4	1.6
		3	7.0	11.2	57.7	WSW	7.6	0.6	1.3	0.4
		4	7.0	9.7	33.3	WSW	3.5	1.1	4.2	1.2
	I.G2 (Mug NA)	1	6.6	10.3	49.3	SSW	49.5	3.5	5.0	1.3
		2	5.4	6.4	7.2	NNE	8.4	3.6	8.3	2.1
		3	5.6	8.0	3.2	ESE	9.0	2.3	5.0	1.2
	I.G3 (Serdah 1)	1	5.6	12.9	256.5	WSW	37.2	23.2	54.2	18.4
		2	7.5	10.3	86.5	W	12.0	0.3	0.8	0.2
		3	8.9	11.5	84.1	W	14.1	0.3	1.7	0.4
Partially grazed (P.G)	P.G1 (Serdah A)	1	8.8	11.5	351.1	WSW	28.1	1.1	5.3	1.9
		2	6.9	10.8	11.5	WSW	33.9	0.7	6.0	1.6
		3	7.0	10.7	5.2	WSW	5.8	1.2	2.6	0.7
	P.G2 (Um Mial F)	1	8.5	10.3	108.9	W	9.3	17.1	31.7	11.1
		2	9.1	10.5	136.4	WNW	23.4	15.5	32.3	11.1
		3	10.9	11.2	80.0	SE	0.6	3.0	6.0	1.9
	P.G3 (Um Mial P)	1	8.7	9.4	115.9	W	3.9	0.8	1.0	0.2
		2	8.8	10.0	140.9	W	29.1	1.1	3.3	0.8
		3	8.2	9.9	4.6	WNW	48.9	1.8	4.8	1.1
Cultivated (bare)	C&B1 (Serdah C)	1	6.9	9.6	182.9	WSW	9.4	1.9	7.2	1.9

(C&B)		2	7.9	8.9	115.9	WSW	7.2	1.0	4.0	1.2
		3	7.0	9.7	65.7	WNW	5.6	0.7	2.1	0.5
		4	6.9	6.9	34.4	WSW	1.3	1.0	2.0	0.6
	C&B2 (Serdah 2)	1	9.9	11.7	152.3	W	17.7	0.2	1.2	0.3
		2	6.2	7.8	54.8	W	1.8	0.1	0.3	0.1
		3	8.3	10.5	59.9	W	3.0	0.1	0.4	0.1
Farming with shrubs (Sh.F)	Sh.F1 (Mug A)	1	5.6	8.5	21.6	SSW	7.1	0.5	1.8	0.5
		2	5.8	8.8	29.2	SSW	13.8	8.6	18.5	4.8
		3	6.2	10.8	75.2	SSW	42.6	10.5	24.4	5.9
	Sh.F2 (Um Mial 3)	1	6.9	8.1	49.8	WNW	10.2	0.8	1.2	0.4
		2	7.6	8.7	67.2	WNW	108.0	0.0	0.0	0.0
		3	6.6	10.1	1.9	N	0.0	20.6	135.7	37.3
	Sh.F3 (Atriplex 4)	1	6.7	11.7	49.8	NNW	5.7	82.0	42.7	154.8
		2	5.3	8.1	67.2	W	0.9	0.0	0.4	0.1
		3	6.8	8.5	1.9	W	76.5	4.3	7.7	2.0
Atriplex (protected area) (Atri-)	Atri-protected (Atri-s)	1	6.9	9.2	20.7	ESE	61.2	3.5	19.8	4.9
		2	6.2	8.5	11.5	ESE	31.8	3.6	5.4	1.6
		3	5.3	6.3	5.2	SSW	75.8	0.7	1.3	0.4
	Atri-protected (Atri-c1)	1	Œ		No data		0.0	0	0	0
		2	6.0	7.8	No data	SSW	29.7	0	0	0
		3	Œ		No data		0.0	0	0	0
	Atri-protected (Atri-c2)	1	6.0	7.6	No data	W	0.6	0	0	0
		2	6.0	7.4	No data	WSW	0.3	0	0	0
		3	5.94	8.07	No data	WNW	0.7	0	0	0
Rangeland area (R.L)	R.L1 (Rangeland 1)	1	5.5	6.5	25.5	SSW	12.7	0.3	1.6	0.8
		2	6.1	8.6	2.4	SSW	35.4	68.4	99.1	25.5
		3	5.7	8.6	9.9	WSW	8.7	4.4	7.2	2.0
	R.L2 (Rangeland 2)	1	7.4	9.3	17.7	WNW	6.0	1.2	3.5	1.0
		2	6.8	9.2	17.2	WNW	3.6	0.0	0.0	0.0
		3	8.5	10.2	48.2	WNW	25.8	0.0	0.0	0.0

From table 3.4 it can be concluded that the re-vegetation projects that have been designed in the Khanasser Valley using the *Atriplex* shrubs indeed reduce the aeolian mass transport within this zone because we observed a zero mass transport in the re-vegetated areas, except for Atri-s. Atri-s has however a silt loam soil texture without crust and the Atriplex shrubs in this area were small and covered a low proportion of the surface. The extremely high value for the average mass transport of 82.0 kg m^{-1} at the farming with shrubs land use type (plot of Sh.F3) and the value of 68.4 kg m^{-1} at rangeland (plot R.L1) showed that there is a potential risk for catastrophic wind erosion at these land use types in the region.

3.3.1.2 *Wind profile*

Figure 3.3 shows the increase of the wind speed with an increase in the height from the soil surface. For 95% of the wind data, the fit (equation 3.1) resulted in an R-square (R^2) value between 0.85 and 0.95, despite the fluctuation in the wind speed during the time of measurement.
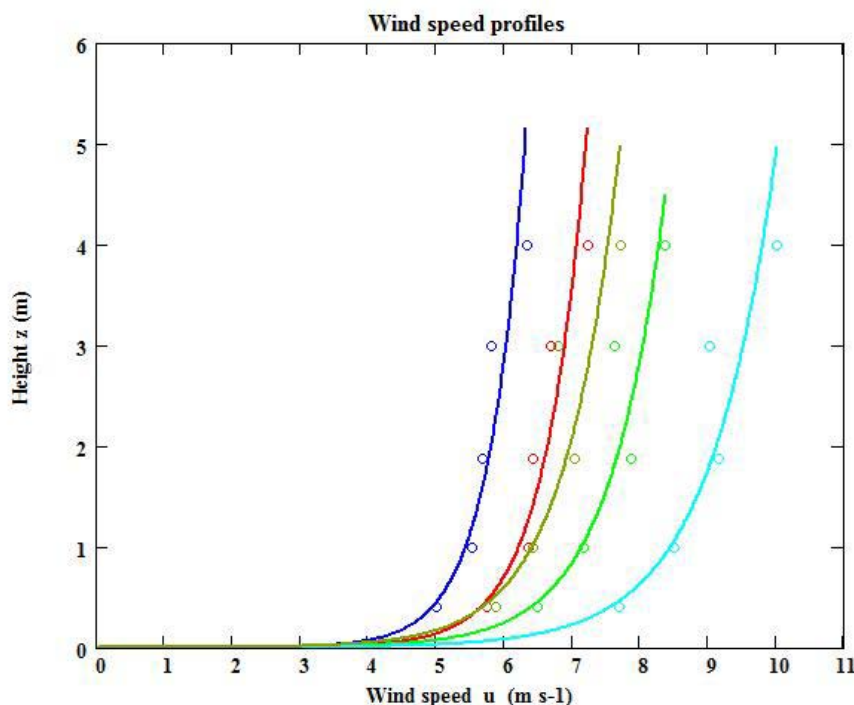

Figure 3.3: An example of the wind speed profile (measured at the heights of 0.40, 1.00, 1.88, 3.00, and 4.00 m) for different wind speeds during the measurements.

3.3.2 The effect of wind regime on the aeolian mass transport

Unexpectedly, when all data are analysed together, there is no correlation between the weekly wind value and mass transport (R^2 = 0.01, Figure 3.4). Theoretically, the amount of mass transport is related to the wind value (Fryrear et al., 1998) and thus, the results here do not fully agree with the theory as the correlation is almost zero. However, a possible relation between wind value and transport might be overshadowed by other factors, most importantly land use. To investigate this, the relationship is plotted for each land use separately (Figure 3.5).
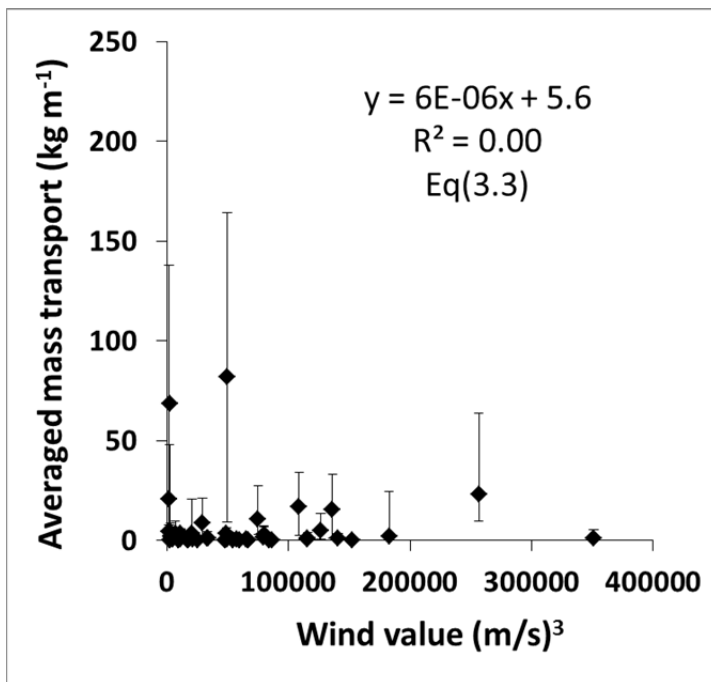
Figure 3.4. The relationship between the wind value (m s^{-1})^3 of a week and the mass transport (kg m^{-1}, averaged over 16 catchers) of the corresponding week, for all events and plots. Regression line left out because of the low R^2 value.

Figure 3.5 shows also that on bare fields (panel A (I.G), panel C (C&B)) and in the Atri-s field (Panel E) the wind value explains only 39-70 % of the average mass transport. For the land uses that have vegetation or residue and in the R.L the mass transport is not explained by the wind value (panels B(P.G), D (Sh.F) and F(R.L)). In land uses of I.G and C&B, the surface is not protected by the vegetation or residue, thus the effect of the wind is direct and the increase in wind power results in an increase in the aeolian mass transport in this land uses. However, there is 30-61 % of mass transport not explained with wind value and explained by other factors such as soil properties, roughness, soil moisture etc. For the Atri-s plot, although there were shrubs in the plot, the wind value explains 62 % of the mass transport and that most likely due to the high amount of erodible sediment within this plot and in the surrounding areas. So, strong wind events associated with higher mass transport.

In the land uses of P.G and Sh.F the soil surface was partially protected by the wind as these land uses have residues (i.e. P.G) or vegetation (i.e. Sh.F). Consequently the effect of the wind on the surface is not direct and thus mass transport in these land uses are not really explained by the wind value. Also, the low accuracy of measurement equipment may not show the effect of the wind on the surface (Figure 5 B and D). For the land use of R.L, the low amount of erodible sediment at the surface is most probably the factor behind the absent (weak) correlation between wind factor and mass transport. And here also, the low accuracy in the measurement equipment and the measurement errors may hide the effect of the wind value on mass transport.

Beside the explanation of the effect of wind value on mass transport, figure 3.5 also illustrates the variation (0 – 250 kg m^{-1}) of mass transport among events and among catchers for each plot (Figure 3.5). The range of the averaged mass transport for the land uses of Sh.F and the R.L is larger than 60 kg m^{-1} (Figure 3.6, D and F), while for the rest the variation range is less than 25 kg m^{-1}. The possible description for the high variation at the Sh.F land use can be the grazing for the shrubs at the end of the dry season and the change in wind speed especially the maximum wind speed (Table 3.4). These results imply that the vegetation can cause an increase in mass transport values when wind speed exceeds a certain limit. This agrees with findings of previous studies (Raupach, 1990; Raupach, 1992; Raupach et al., 1993; Michels et al., 1995; Sterk et al., 1998; Maurer et al., 2009) which reported that during a wind event, vegetation may increase the turbulence causing an increase in the soil movement around the vegetated area. For the land

use of R.L, the high variation in the mass transport among the wind events can be linked mainly to the availability of sediment. As in the rangeland areas, the amount of erodible sediment is limited and the sediment that can enter the measurement plot varies mainly with the wind direction. Thus, wind direction of SSW with average wind speed of 6.08 m s^{-1} and maximum wind speed of 8.6 m s^{-1} resulted mass transport of 68.4 kg m^{-1} (Table 3.4). However, with the wind direction of WNW even with average wind speed of 8.4 m s^{-1} and maximum wind speed of 10.2 m s^{-1} the measured mass transport was zero kg m^{-1} (Table 3.4).
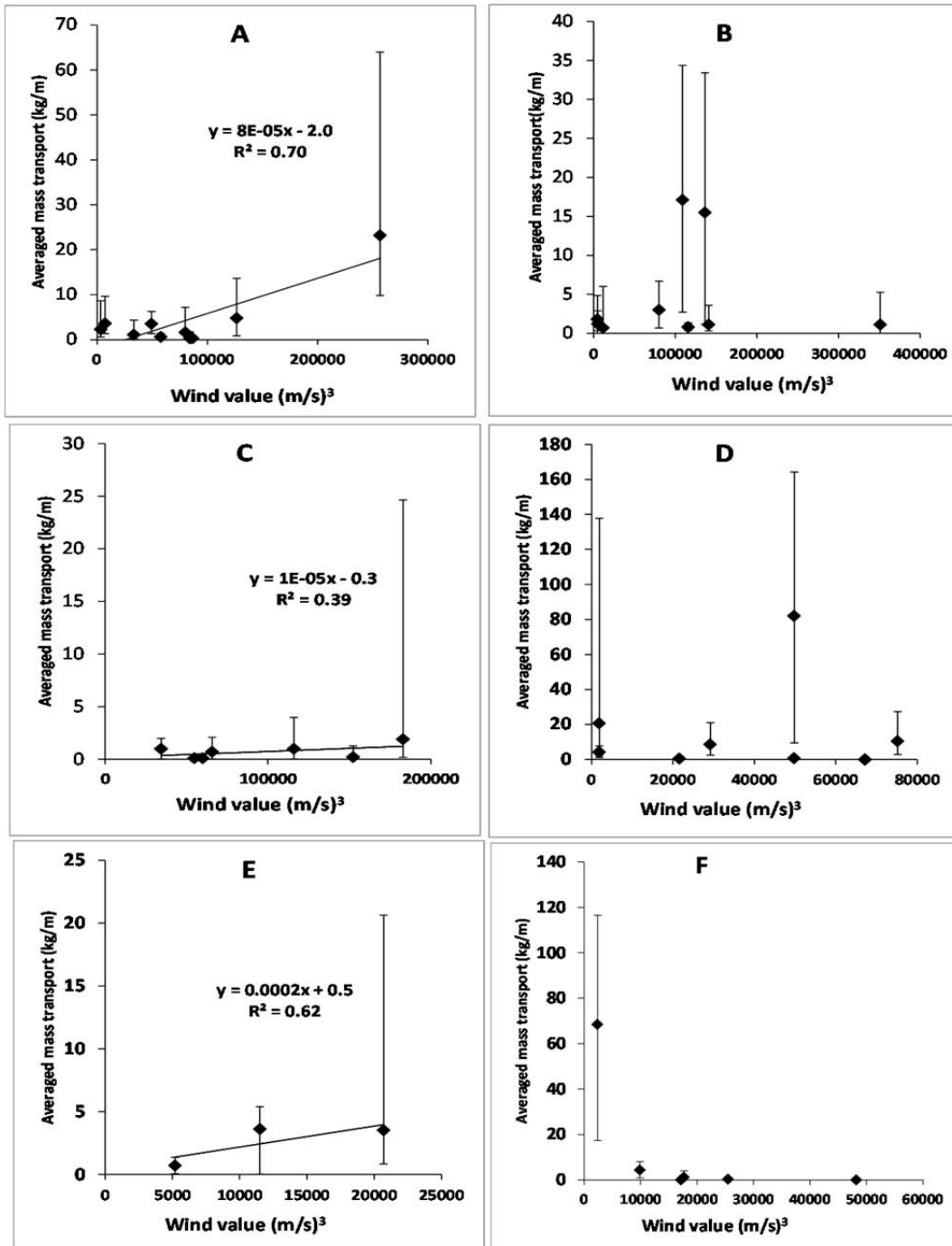
Figure 3.5. The relationship between wind value (m s^{-1})^3 and measured mass transport (kg m^{-1}) (averaged over 16 catchers) for each event and each plot. A): intensively grazed (I.G), B) partially grazed (P.G), C) cultivated (bare) (C&B), D) farming with shrubs (Sh.F), E) Atriplex-protected sandy area (Atri-s), F) rangeland area (R.L). The Atriplex-protected crusty area (Atri-c) is not included because wind data for plots were only available for one week (Table 3.4). Regressions shown for R^2 > 0.39. Vertical lines straddle the minimum and maximum value of the 16 catchers at the plot. Note the difference in y-axis between panels.

3.3.3 The effect of land use on aeolian mass transport

For most land use types, the effect of the wind value on mass transport is negligible or small, as was shown in the previous section and Figure 3.6. Thus, for the analysis of the effect of land use on mass transport, mass transport averaged over all events of each land use (Figure 3.6A) gives a good indication of the effect of land use on transport. However, as a weak relationship between wind value and mass transport exists for the intensively grazed and cultivated (bare) land use types, we also calculated average wind-value standardized mass transport for all land use types (Figure 3.6B).
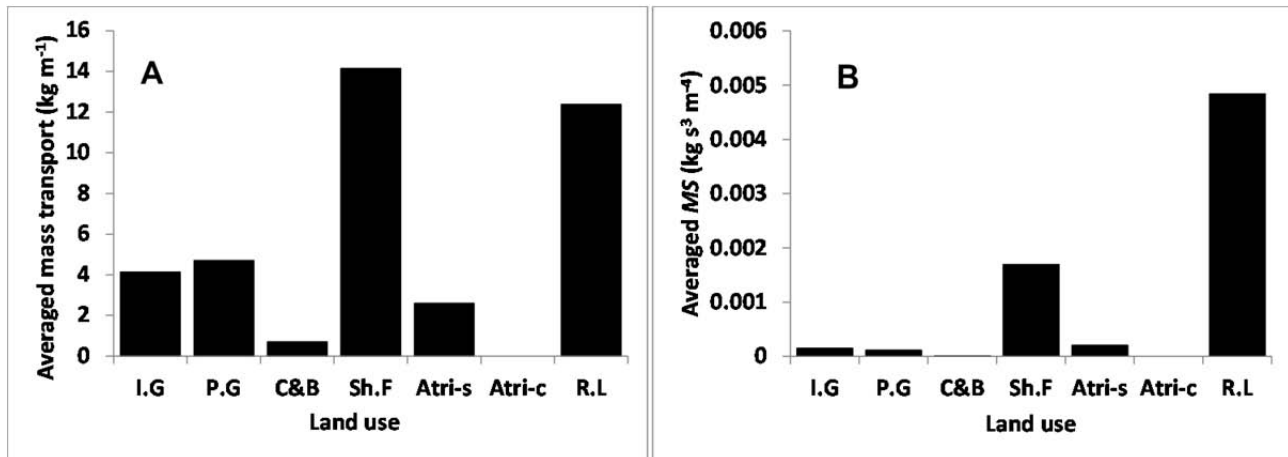

Figure 3.6. Effect of land use on mass transport. A) The mean (over all events) mass transport (kg m^{-1}) for each land use. B) The mean (over all events) wind value-standardized mass transport (MS) (kg s^{3} m^{-4}) for each land use. The land uses are: intensively grazed (I.G), partially grazed (P.G), cultivated (bare) (C&B), farming with shrubs (Sh.F), Atriplex-protected sandy area (Atri-s), Atriplex-protect crusty area (Atri-c) and rangeland area (R.L).

Figure 3.6A indicates the success of the project of planting Atriplex for controlling the wind erosion in the Khanasser region as the mean value of the mass transport in the rehabilitated rangeland is zero kg m^{-1} in the crusty area (Atri-c) and only 2.3 kg m^{-1} in the sandy area (Atri-s) (Figure 3.6A). Low values for the mean of the wind-value standardized mass transport (*MS*) for these land uses (Figure 3.6B) confirm this.

The results indicate that the grazing intensity seems to have a minor effect on the mass transport in the region. For mean mass transport, the value of intensively grazed and partially grazed areas is almost the same, while for *MS*, intensively grazed has a slightly higher value (Figure 3.6). So, there might be a minor effect of grazing on mass transport in the area, but results should be interpreted with care because the data set is small. An increase in mass transport with grazing intensity would be expected, because soil aggregates and/or crusts are pulverized by grazing and thus a higher mass transport is excepted for areas that are intensively grazed (Letnic, 2004).

The results show that the magnitude mass transport values of R.L and Sh.F is higher than the magnitude of the data with other land uses. As the R.L area does not have a vegetation cover, the area is open with flat topography where the wind can travel without interruptions, high mass transport is expected. At the end of the dry season, the major parts of agricultural area become out of vegetation and thus Sh.F spots become attractive zones for sheep as shrubs keep fodder for animals. The large number of sheep entering the Sh.F areas, most probably accelerate the mass transport rate resulting in a high magnitude mass transport value. Consequently, the highest mass transport was at the farming with shrubs land use type, having a mass transport even higher than at rangeland (Figure 3.6A). However, the mean *SM* value of rangeland is somewhat higher than for farming with shrubs. Theoretically, the latter situation would be expected as in rangeland there is no vegetation cover to protect the surface from erosive wind.

Again, results should be interpreted with care, as the data set is relatively small, and a larger number of field measurements would be required to confirm our findings.

To summarize, the rehabilitation with Atriplex for rangeland is an effective method to reduce wind erosion, the mixture of shrubs and farming is not the best method for dealing with this problem, and finally the use of wind-value standardized mass flux seems to be a good method for standardizing mass transport values collected with the portable plot method.

3.3.4 Border effects

Figures 3.7 and 3.8 show examples of the spatial distribution of aeolian sediment transport over the plot area representing two different border conditions. Figure 3.7 shows plot I.G1, located in the intensively grazed area. Most fields directly bordering the plot had a land use different from the plot itself. It is important here to mention that the wind direction fluctuated from WSW to WNW during the measurement periods although the averaged wind direction was WSW (Table 3.4). Thus, the average direction shown here is not fully represented by the wind directions during the measurements. Consequently, the non-erodible borders from the upwind direction also fluctuated when considering the change in the wind direction. Despite this condition, weekly averaged mass transport pattern shows a relation with wind direction (Figure 3.7B). The non-erodible border to the northwest of the plot results in an increase in mass transport over the plot from northwest to southeast, particularly for week 1, 2 and 4. Most likely, the strongest wind occurred from this direction. As the length of the plot was relatively small (60 m) it is not certain whether the maximum transport capacity was reached or not. The results here agree with the theory of Fryrear (1998) who showed an increase in the total mass transport from a non-erodible border.

Figure 3.8 shows an example of the distribution of aeolian sediment transport along the plot area for a plot that has borders with land uses that are identical to the plot itself. The figure shows that there is no clear trend in the distribution of the mass transport related to the wind direction. For one week of measurements the maximum transport capacity was observed at a point just to the east of the centre of the area. In another week the maximum transport occurred more to the left on the plot, but in both cases there was no clear trend from one of the edges of the plot to the other side of the plot. This can be explained by the fact that the surroundings of the plot were similar to the plot itself in soil and vegetation properties.

From the two examples in figure 3.7 and 3.8, it can be said that the spatial distribution of the mass transport within an area is related to the land use surrounding the area. Comparable results were found in wind tunnel studies of Youssef et al. (2012b, chapter 5) and Cornelis and Gabriels (2005), and in field observations of the effect of wind breaks (e.g., Skidmore and Hagen, 1977; Heisler and Dewalle, 1988).

Figure 3.7. Spatial pattern in mass transport (Kg m^{-1}) at plot I.G1. A) Map of the area surrounding plot, B) Aeolian mass transport distribution over the plot. WK1..4: week of measurement. Arrows (B) indicate the direction toward which the wind is blowing.
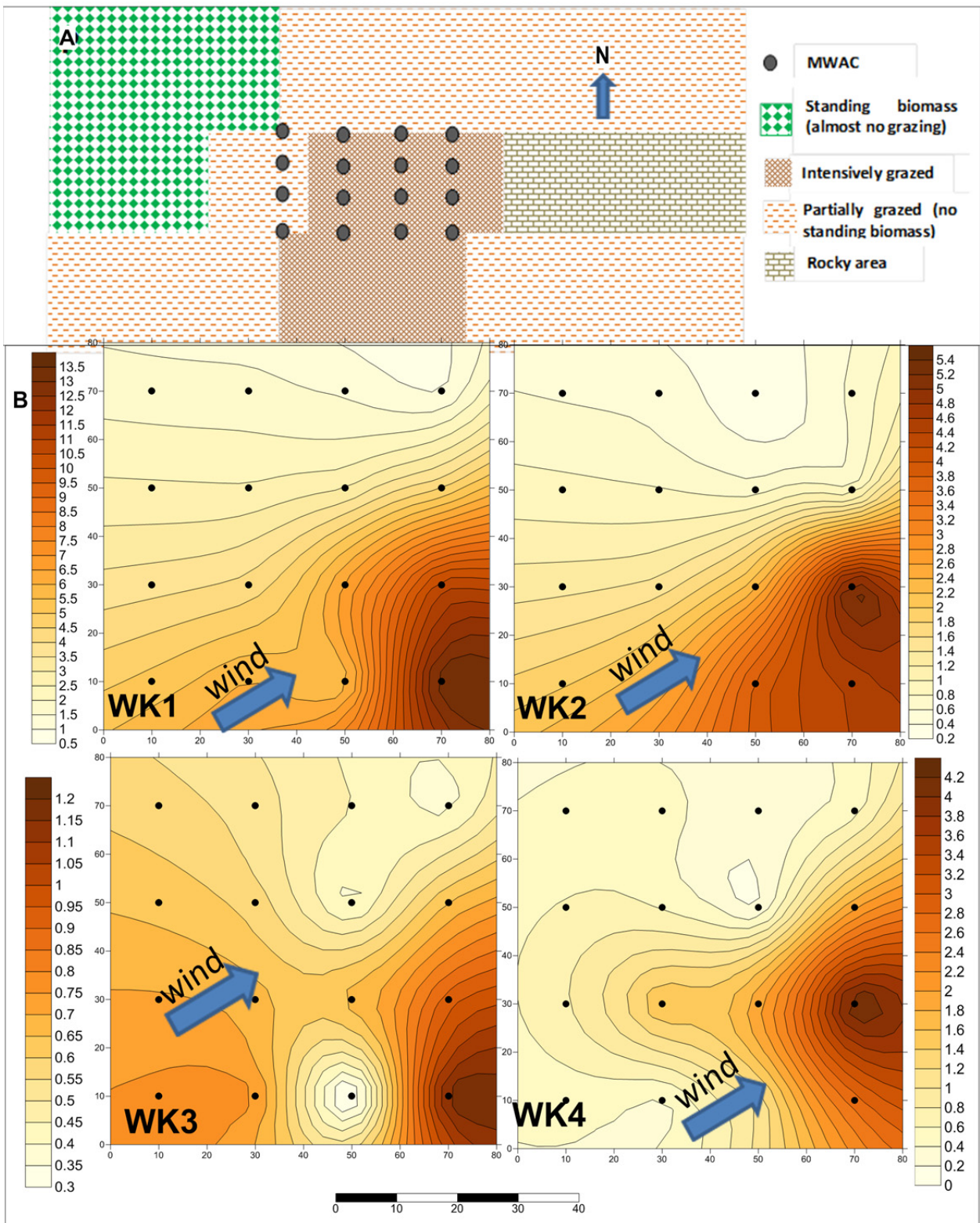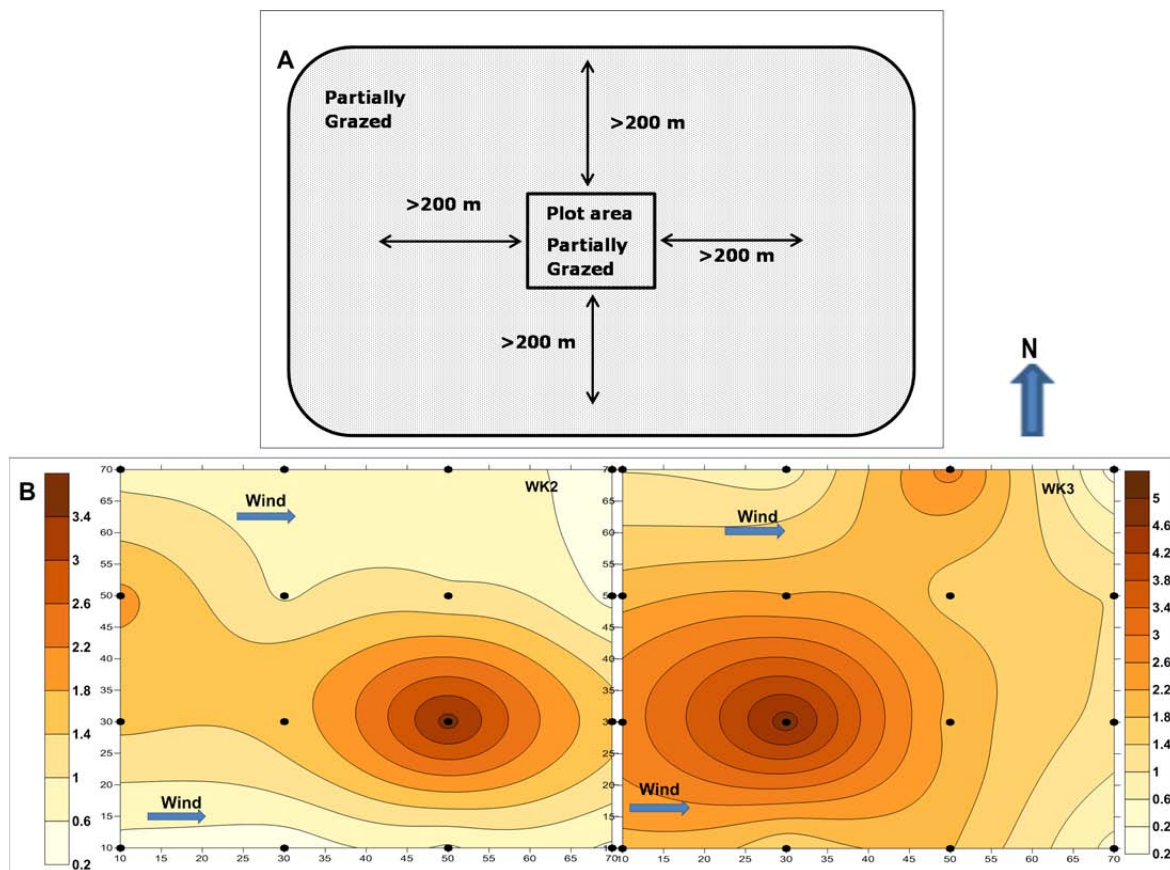
Figure 3.8. Spatial pattern in mass transport (kg m^{-1}) at plot P.G3. A) Map of the area surrounding plot, B) Aeolian mass transport distribution over the plot. Two weeks of measurements. Arrows (B) indicate the direction toward which the wind is blowing.

3.3.4 The use of data collected with the new measurement method

As the new method of sampling aeolian sediment transport provides data representing the main land uses in a region, it can support the modelling of wind erosion at the regional scale. We propose to approaches:

1) Scaling up a field scale model to a regional-scale model

In this approach, a field scale wind erosion model needs to be calibrated and validated against ground data for each land use type in a region. The calibrated and validated model then can be applied to the entire region to estimate mass transport. For example, the RWEQ model was calibrated and validated against ground data collected for the different land use types in the Khanasser Valley region (Youssef et al., 2012a, chapter 4). With a number of modifications, particularly by representing transport of sediment across borders, this approach can result in wind erosion predictions for a large region. I further explain and evaluate this approach in chapter 6. The main challenge in this approach is to retrieve input data to run the model for an entire region. This is because some of the model inputs show high variability and thus high-resolution data is required which makes the use of remote sensing techniques essential.

2) Validation of the existing regional scale models

There are a few regional scale wind erosion models that have been developed in the last decades (i.e. Butler et al., 1996; Webb et al., 2006). The main problem with these models is that they were never calibrated and validated against ground data because ground data representative for the regional scale were not available. The new sampling method using a portable plot proposed here may provide data that can be used for the calibration and validation of existing regional-scale wind erosion models. The calibration and validation of these models against ground data will improve their performance. The main problem in this approach is that the majority of current regional-scale wind erosion models were developed by only considering sediment transport in suspension. Thus, considerable modifications of these models

will be required before they can be tested against data collected with the current sampling method, because the proposed method mainly considers transport by saltation.

3.4 Conclusions

To improve understanding of wind erosion at the regional scale, we developed a new measurement method using portable plots. This method provides data on aeolian mass transport at multiple land use types in a region. In addition, the method provides information on spatial patterns in mass transport and the effect of borders between fields having different land covers. The portable plot method has the advantage that it maximizes the total number of measurement plots with limited equipment, time and budget. The method was tested in the Khansser valley region in Syria, and the results of this research identify the following findings:

- For intensely grazed and cultivated (bare) areas, weekly averaged aeolian mass transport is related to the weakly averaged power of the wind. For the remaining land use types no relations between wind power and transport were found, possibly due to the relatively small data set.

- The wind-value standardized mass transport suggested in this research can be a promising approach to understand the effect of land use on wind erosion processes regardless of the fluctuation in wind speed during the measurements periods.

- The spatial distribution of mass transport along a single land unit is related to the land unit type of directly neighbouring fields.

- The portable plot method provides information that can support the improvement of regional scale wind erosion models.

Chapter 4

Calibration of RWEQ in a Patchy Landscape: a First Step towards a Regional Scale Wind Erosion Model
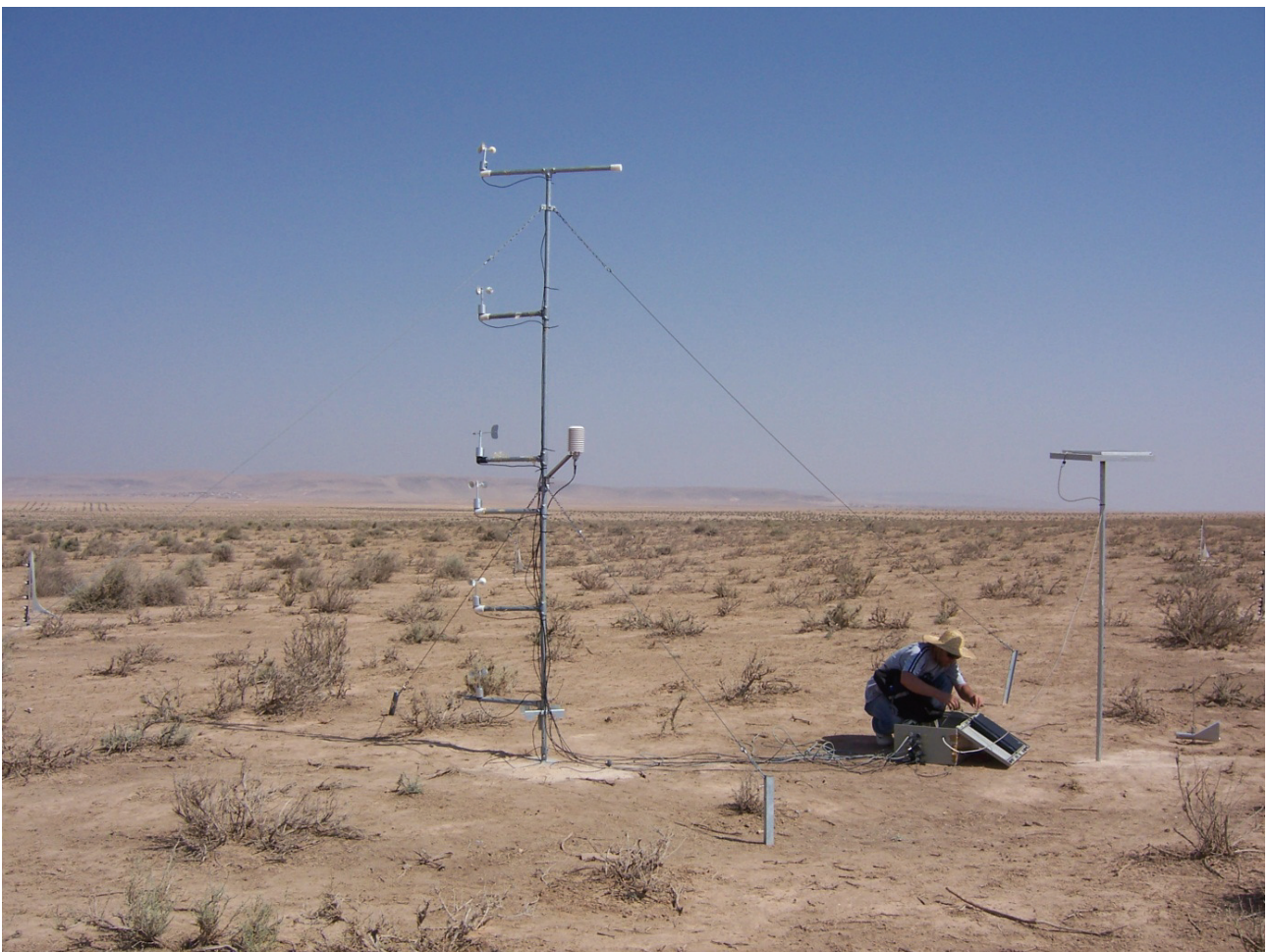
Calibration of RWEQ in a Patchy Landscape: a First Step towards a Regional Scale Wind Erosion Model

Abstract

Despite the fact that wind erosion seriously affects the sustainable use of land in a large part of the world, a validated wind erosion model that predicts windblown mass transport on a regional scale is lacking. The objectives of this research were to modify RWEQ (Revised Wind Erosion Equation) to estimate soil loss at a field scale in a way that it could operate at a regional scale, to calibrate the model using ground data collected from a field scale representing different land uses in Khanasser valley, Syria, and to estimate the total sediment transports (kg.m^{-1}) and soil losses (kg.m^{-2}) for farming fields.

We implemented a modified version of RWEQ that represents wind erosion as a transient process, using time steps of 6 hours. Beside this a number of adaptations including estimation of mass flux over the field boundaries, and the routing of sediment have been done. Originally, RWEQ was created and calibrated for application at the field scale in USA. Due to the adaptations imparted to the original RWEQ and the different environmental conditions in Syria, an intensive calibration process was required before applying the model to estimate the net soil loss from the experimental fields.

The results of this test showed that the modified version of RWEQ provided acceptable predictions for the average mass transport from the measurement plots with a linear regression coefficient R^2 of 0.48 and a value of 0.85 for the d-test, for the 20 wind events at the six tested plots.

Key words: Wind erosion modelling, RWEQ, Syria, Regional scale, Soil loss

4.1 Introduction

Wind erosion is an important problem in arid and semi-arid regions (Buschiazzo and Zobeck, 2008; Stroosnijder, 2007). Wind erosion significantly decreases soil productivity (Sterk et al., 1996; Visser and Sterk, 2007) and has negative effects on human health due to the harmful effects of dust particles on the respiratory system (Copeland et al., 2009; De Longueville et al., 2009). When conditions favourable for wind erosion are present, the process may result in large scale environmental disasters like the Dust Bowl in the USA in the 1930s, which affected more than 40 million hectares of lands (Cook et al., 2008). The amount of soil loss by wind erosion is affected by mainly meteorological conditions, vegetation cover, land management and soil properties (Leenders et al., 2005; Sterk and Spaan, 1997).

Minimizing soil loss is essential to reduce land degradation and to optimize crop yields. Thus, in regions that are vulnerable to wind erosion, prediction of soil loss at the regional scale is an important step in designing land use plans (Feng and Sharratt, 2007; Papadimitriou and Mairota, 1996). Despite this critical need for regional scale prediction of wind erosion, a limited number of regional scale models exist. In addition, most existing regional scale wind erosion models have not been calibrated and validated against the data of ground observations collected at a regional scale (Shao and Leslie, 1997; Zobeck et al., 2000). Therefore, regional scale wind erosion models and field sampling schemes are needed specifically at the regional scale. Clearly, there is a need for models that can run with data available at the regional scale. Regional data generaly consist of maps or remotely sensed information of land use, vegetation cover and soil type with resolution above 100 m. Thus, regional scale models should have size units comparable to an arable field (100 - 10000 m^2) with model equations for each unit that can be solved using limited attribute information. Such models could then predict soil loss for each arable field (i.e., model unit), taking into

account properties of the field itself and the spatial configuration of neighbouring fields. Regional scale modelling cannot be supported by real-time observations of mass transport or soil loss as it is infeasible to design and maintain sampling schemes that monitor wind erosion at the regional scale with models that are properly calibrated. To do so, field sampling schemes specifically directed towards calibration of (components of) regional scale models are required.

To cope with these challenges, we describe a methodology which combines modelling and field sampling efforts together. Thus, the objectives of this research are 1) to adjust an existing wind erosion model capable to predict soil loss at the scale of a field such that it could perform at a regional scale, using limited input data, 2) to calibrate the model against observations from a field monitoring scheme particularly designed for calibration of regional scale models with a size of model units comparable to arable fields and 3) to calculate total sediment transports (kg.m^{-2}) (loss or deposition) for arable fields. In this modelling work, the existing RWEQ model (Fryrear et al., 1998) was used as a starting point as it needs limited input data compared to mechanistic wind erosion models such as WEPS (Hagen, 2004) (Wind Erosion Prediction System). The RWEQ model was adjusted to prepare the model for simulation at the regional scale. RWEQ was translated into PCRaster to enable simulation of spatial variation in vegetation cover and eroding boundaries. Furthermore, the model was modified to take advantage of standard meteorological time series data by using transient temporal simulations. Also, net wind erosion over arable fields was calculated, which is essential for regional scale modelling. Key model parameters were found by an extensive brute force calibration technique using a new data set collected at six arable fields in the Khanasser region, Syria.

4.2   Material and methods

4.2.1 Study area

The Khanasser valley is situated between the Al Hass and Shbeith mountains, southeast of Aleppo city, Syria (Figure 4.1). At an altitude of 350 m above sea level, the valley is rather flat. Annual rainfall ranges from 150 to 250 mm and the rainy season starts in October and ends in May (Masri et al., 2003). Wind in the dry season (from June to September) travels from south to west with exceptional large wind events from other directions. During the dry season, the daily average wind speed (at 2 m height) is high and may exceed 10 m.s^{-1} (Masri et al., 2003). Monthly average wind speed in the valley varies from 3.5 m.s^{-1} in the south up to 4.4 m.s^{-1} in the north (Bruggeman et al., 2010).
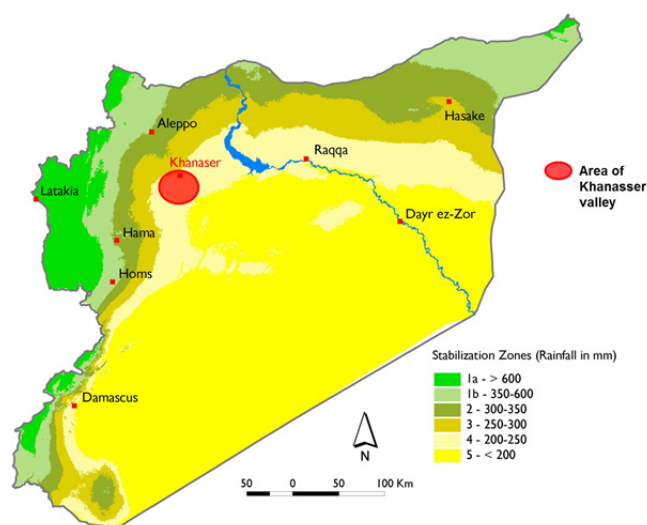

Figure 4.1. The location of Khanasser valley, and the stability zones in Syria (ICARDA, 2005).

Calcisols, Gypsisols, Leptisols, and Cambisols are the main soil types in the valley (Masri et al., 2003). These soils are well-drained and have Clay-Loam to Sandy-Loam texture. The intensive agricultural and livestock activities and poor management of limited natural resources are dominant problems in the valley. These land use conditions resulted in a significant increase in the land degradation in the valley (ICARDA, 2005).

Wind erosion is one of the most dominant land degradation problems threatening not only the agricultural and livestock activities but also the settlements in the valley (Thomas and Turkelboom, 2008). According to the annual rainfall, Syria can be divided into 5 stability zones. In stability zone 4, the annual rainfall is 200-250 mm and the main land use is dry farming (mainly cereals). In stability zone 5, the annual rainfall is less than 200 mm and the land use varies from pastures to rangelands where cultivation activities are currently prohibited. This research is carried out in stability zones 4 and 5 in Khanasser valley. In zone 4, the agricultural fields were divided equally among farmers in a way that all fields have access to the small number of roads which are oriented north-south. As a result of this division the fields are 50 - 80 m in width and 2000 – 4000 m in length in the east-west direction. The plough direction follows the field direction (east-west) in order to reduce the cost and time of ploughing activities. The research was carried out using a "portable" plot approach, to allow for a number of different locations to be handled with a relatively small set of equipment. For this research, data from six measurement plots were used (Table 4.1). No special treatments on the surface of the measurement plots were applied before or during the measurement periods. Furthermore, most plots did not obtain a non-eroding boundary. Consequently, sediment could freely blow into and out of the plot without obstructions.

Between June and September 2009, measurements on vegetation characteristics, soil parameters, climate and wind-blown mass transports were taken to evaluate wind erosion for a period of three weeks per field. After each period the research set up was broken down and transferred to the next plot. At each site the wind profile was measured using five anemometers gauging wind speeds at 0.4, 1, 1.9, 3.0 and 4.0 m heights. A wind vane recorded wind direction (degrees) as well. A saltiphone (Spaan and van den Abeele, 1991) was used to determine the onset of wind-blown mass transport and the total duration of saltation. Furthermore, the temperature, relative humidity and soil moisture were measured. All sensors were connected to a CR1000 data logger, which stored sensor outputs at 5 minute intervals. Information on solar radiation was obtained from measurements performed by ICARDA over long periods (Bruggeman et al., 2010).

Table 4.1. Description of the wind erosion measurement plots with their zones, crops, soil textures and land uses in the Khanasser valley, Syria.

Name of Plot	Zone	Crop	Soil [*]	Land use
Serdah *A*	4	Wheat	Clay-Loam	Harvested field with partially grazing; standing silhouette
Serdah *C*	4	Camion	Clay-Loam	Harvested field, bare, no standing silhouette,
Mugherat *A*	4	Wheat with Atriplex	Sandy-Loam	Extensive farming with shrubs of Atriplex, harvested field, no standing silhouette
Mugherat *NA*	4	Wheat	Sandy-Loam	Harvested field with Intensive grazing, no standing silhouette,
Um Mial	4	Barley	Clay-Loam	Harvested field with Intensive grazing, no standing silhouette,
Adami Gazelle	5	Atriplex reserve	Silt-Loam	Reserve area with Atriplex with partial grazing,

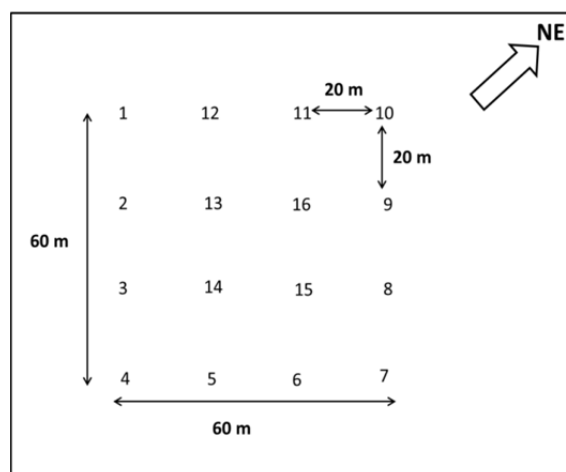* Soil type was determined with the Soil Texture Calculator (NRCS, 2010).

Figure 4.2. A sample of a measurement plot with positions of 16 MWAC catchers.

Vegetation characteristics (surface coverage, height), soil properties (texture, organic matter and calcium carbonate) and soil surface roughness (ridge spacing, ridge height) were determined at the start of the experiments for each plot. Due to the dry conditions and absence of management activities, it was assumed that values of these parameters did not change during the sampling period. Soil properties were obtained by analysis of eight soil samples for each plot in the laboratories of ICARDA. Thus, for each plot, the values of soil texture, OM and CaCO3 were obtained using the hydrometer method, the method of Walkley and Black (Walkley and Black, 1934) and the acid neutralization method, respectively. The roughness and the vegetation characteristics were collected through direct field observations. Each plot (60 x 60m) was divided into 144 parcels with (5 x5 m) area for each parcel. At each parcel five observations were recorded for the vegetation height, vegetation cover and residues, the random roughness using the chain method (Saleh, 1993) and the oriented roughness.

For the measurement of wind-blown sediment fluxes, 16 MWAC catchers were set-up in a regular grid on a 60 x 60 m plot (Figure 4.2). This set up of catchers provided a transect of mass fluxes regardless of the wind direction. Furthermore, changes in the flux at the borders of fields were measured in this way because the small size of the plot allowed observation of sediments that blew into or out of the plot. Sediments were collected four times at Serdah C and Um Mial and three times at the other plots because of the restriction of the measurement time. The sediment was collected mainly on weekly-based with some exceptions due to some logistical issues during the start of the research. The total mass transport (kg.m^{-1}) was calculated through sampling the horizontal mass fluxes at 5 heights (on average 0.1, 0.3, 0.5, 0.8 and 1.0 m). Then, the approach of Sterk and Raats (1996) was applied to build up a flux profile by height.

4.2.2. The Revised Wind Erosion Equation
The RWEQ model was developed by Fryrear et al. (1998) in order to estimate soil loss from agricultural fields in the USA. The RWEQ model not only is the best applicable methodology for the prediction of wind erosion at a field scale, but also provides information on erosion rates within the field (Fryrear et al., 1998). This paper only reports the key processes and equations of the RWEQ models, and for a complete description of all model equations the reader is referred to Fryrear at al. (1998). The RWEQ model makes estimates of sediment eroded and transported by wind between the soil surface and a height of 2 m for specified periods based on a single-event. The temporal interval used in RWEQ is 1 -15 days. The simulation area is a homogeneous circular or rectangular field bounded by a non-eroding boundary. The model calculates aeolian mass transport ($Q(z)$; kg m^{-1}) at downwind distance (z, m) in the field from the balance between wind erosivity and soil erodibility with equation 4.1.

$$Q(x) = Q_{max}\left[1 - e^{-\left(\frac{z}{S}\right)^2}\right]$$ [4.1]

Where:

Q_{max} (kg m^{-1}) is the maximum transport capacity and

S (m) is the critical field length defined as the distance at which the 63% of maximum transport capacity is reached.

The erosivity of the wind is expressed in the weather factor (W_F, kg.m^{-1}), which is calculated based on weather related input parameters. The erodibility of the soil is expressed in a crusting factor (C_F, -), erodible fraction (E_F, -), a combined crop factor (C_{OG}, -) and a single roughness factor (K_{tot}, -) (Figure 4.3). The erodibility and erosivity are combined in the calculation of maximum transport capacity (Q_{max}, kg.m^{-1}) and the critical field length (S, m), which are respectively calculated according to equation 4.2 and equation 4.3.

$$Q_{max} = \beta 1.(W_F.E_F.S_{CF}.K_{tot}.C_{OG}$$ [4.2]

$$S = 150.71 \cdot (W_F \cdot E_F \cdot S_{CF} \cdot K_{tot} \cdot C_{OG})^{-0.3711}$$ [4.3]

The values of S_{CF} and C_{OG} are calculated using the equations explained in Fryrear et al. (1998) and depending on the direct field observations for the crust, the vegetation and residues.
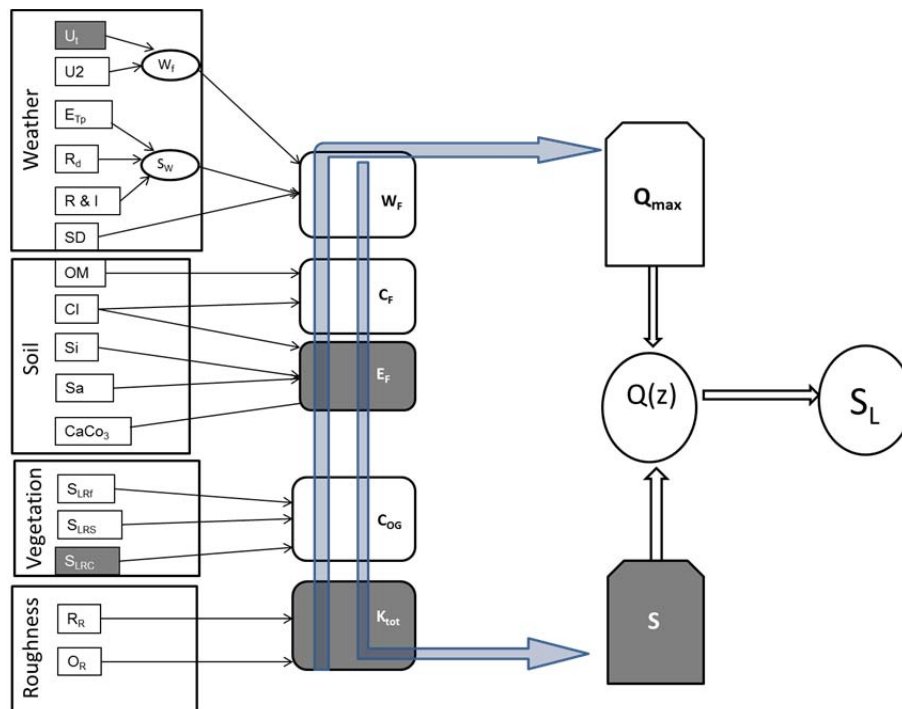
Figure 4.3. Illustration of calculation steps for soil loss SL and mass transport Q(z) in RWEQ.
U_t, threshold velocity at 2 m height; U2, wind speed at 2 m height; Wf, wind factor; E_{Tp}, potential relative evapotranspiration; R_d, number of rainfall/irrigation days; R&I, rainfall and irrigation; SD, snow depth; S_W, soil moisture; W_F, weather factor; OM, content of organic matter; Si, content of silt; Cl, content of clay; Sa, content of sand; CaCO$_3$, calcium carbonate ;C_F, crust factor; E_F, erodible fraction; S_{LRf}, flat residue; S_{LRs}, standing residue; S_{LRc}, crop cover; C_{OG}, combined crop factors; R_R, random roughness; O_R, orientated roughness and K_{tot}, single soil roughness factor. The highlighted boxes with white letters include the parameters that were calibrated.

The average soil loss (S_L; kg m^{-2}) at a specific point (z, m) in the field is explained as the first derivative of the mass flux equation (4.1) at the distance (z) (Fryrear et al., 1998) and given as:

$$S_{loss}(z) = \frac{2 \cdot z}{S^2} Q_{max} e^{-\left(\frac{z}{S}\right)^2}$$

[4.4]

Where:
z is the distance from the non-erodible border (m).

4.2.3 Translation of RWEQ into PCRaster

A major advantage of using RWEQ is that the model is relatively simple and requires a limited amount of input data, which makes the model relatively easy to be scaled up. In the development of RWEQ, the relation between soil loss and field length was determined for homogenous circular or rectangular fields. With the obtained relationship, soil loss from any field shape or size can be evaluated. The model inputs related to vegetation cover and soil roughness vary in temporal scale from daily to bi-weekly averages. Furthermore, the USA climate generator CLIGEN is used to simulate rainfall, wind speed, temperature and evaporation.

For the application of RWEQ in this research, it is necessary to take into account incoming and outgoing sediment fluxes at the edge of a field, to use measured input data for climate parameters and to take into account the presence of a non-homogeneous vegetation cover. Furthermore, for the application of RWEQ at a regional scale the model should be able to simulate mass transport over units with varying vegetation cover and patterns. In its current state RWEQ does not have the required flexibility and therefore, it was decided to rewrite RWEQ into the dynamic modelling language of PCRaster (Karssenberg and De Jong, 2005). PCRaster is an environmental modelling language embedded in a Geographical Information System, providing spatial and temporal functions that can be used to construct transient models.

Apart from the translation of RWEQ to PCRaster, additional adaptations to the model included 1) simulation of transport over the field boundaries and 2) the time step, which allowed using the model inputs and outputs in a time series format. Thus, at every time step, the model calculated the mass transport depending on weather inputs. As the assumption of the presence of a non-eroding boundary was invalid for the simulation area, it was decided to use the large scale land use map to determine the actual position of an upwind non-eroding boundary and adjust the simulation area such that it included the actual non–eroding boundary. To be able to account for the large variations in wind speed and wind direction within a day during the field measurements, a simulation time step of six hours was used, dividing a day in 4 periods, starting at 24-6h; 6-12h, 12-18h and 18-24h. The weather factor (W_F) was simulated for each time step separately. Average wind direction for each time step is used to calculate the distance of each grid cell to the upwind border of the plot. With these model adjustments, the model is made capable of calculating and showing mass transport related to the temporary climate variables and spatial field characteristics.

Table 4.2 shows the range of values of the main inputs of the model for one plot as an example to show the magnitude of the input values of the model.

Table 4.2. The range of values of main input parameters of RWEQ in PCRaster for the Serdah C measurement plot.

Factors	Input parameters	Parameter values
Weather factor ¥	Wind speed (m s^{-1})	3.0-7.0
(temporal variable)	Wind direction (degrees)	137-252
	Temperature (degree Celsius)	23-38
	Solar radiation (Cal cm^{-2})	155.0
Soil and erodible factor	Content of Organic matter (%)	1.3-1.6
(spatial variable)	Content of clay (%)	15-26
	Content of sand (%)	45-65
	Soil moisture (%)	1.0-4.0
Roughness and crust factor	Plough ridge spacing (cm)	35-40
(spatial variable)	Plough ridge height (cm)	8-10
	Soil roughness (chain method)	1.2-3.5
Vegetation/residues factor	Covered surface (%)	7-30
(spatial variable)	Height of vegetation or silhouette (cm)	2-5

¥ The presented input parameters for the weather factor are the wind events 4-11 Aug and 11-18 Aug, 2009.

4.2.4 Model calibration

Because RWEQ was developed and calibrated for application at field scale in the USA (Van Pelt et al., 2004), and since this research attempted to significantly adjust it to apply at fields in Syria, the RWEQ in PCRaster required a thorough calibration. As weather, soil, vegetation and roughness are the main factors of the RWEQ model (Figure 4.3), it was decided to use one parameter from each of these factors in the calibration process. Therefore, six calibration parameters, involved in the determination of the critical field length (S, m), the threshold wind velocity (U_t, m s^{-1}), the erodible fraction (E_F), the crop canopy (S_{LRC}) and the soil roughness factor (K_{tot}), were used in this calibration.

For the critical field length (S) the two fixed parameter values used in the original RWEQ model (Fryrear et al., 1998) were replaced by calibration parameters, and S was calculated with equation 4.5.

$$S = \mu_{Sa} \cdot (W_F \cdot E_F \cdot S_{CF} \cdot K_{tot} \cdot C_{OG})^{-\mu_{Sb}}$$ [4.5]

Where:

μ_{Sa} and μ_{Sb} are the parameters of calibration for the critical field length equation.

The threshold wind velocity (U_t m s^{-1}) is used in the calculation of the wind value (W_f). Although in the original RWEQ this threshold is considered a constant value, field observations proved that the threshold velocity was related to the percentage of vegetation cover (Figure 4.4). The relation given by equation 4.6 was therefore used in the calculation of the threshold velocity in our model

$$U_t = 0.13 \cdot R_E + \mu_{U_t}$$ [4.6]

Where:
R_E is the percentage of the soil surface covered with vegetation, and
μ_{Ut} is a calibration parameter for the threshold velocity.

Depending on the threshold velocity and the wind speed at 2 m height the wind value (m/sec)^3 is calculated according to equation 4.7 (Fryrear et al., 1998).

$$W = \sum_{i=1}^{i=N} U_{2,t=i}(U_{2,t=i} - U_t)^2 \qquad\qquad [4.7]$$

Where:

$U_{2,\,t=i}$ is the wind speed at 2 m height during observation number i,

U_t is the threshold velocity, and

N is the number of wind speed observations (*i*) in a time period of 1-15 days in the original version of the RWEQ and 6 hours in our adapted version.

The wind factor (W_f, (m s^{-1})^3) was calculated according to equation 4.8 (Fryrear et al., 1998).

$$W_f = \frac{W}{500} \cdot N_d \qquad\qquad [4.8]$$

Where:

W is the wind value (m s^{-1})^3,

N_d is the number of days in the period of measurements (15 days in the original version of the RWEQ and 0.25 day in our adapted version)
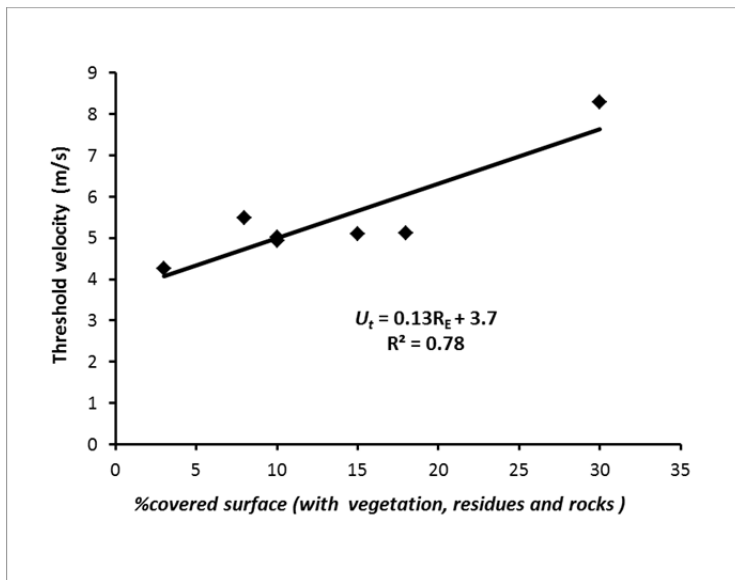
Figure 4.4. The relationship between the percentage covered surface (with vegetation, residues and rocks) and the threshold wind velocity.

The soil erodible fraction (E_F) depends on the soil texture (sand (S_A), Silt (S_i) and Clay content (C_L)), the content of organic matter (*OM*) and the calcium carbonate (*CaCO₃*) and by including the calibration parameter μE_F, E_F is calculated according to equation 4.9 (Fryrear et al., 1998).

$$E_F = \frac{\mu E_F + 0.31 S_A + 0.17 S_i + 0.33 \dfrac{S_A}{C_L} - 2.59 OM - 0.95 CaCO_3}{100} \qquad\qquad [4.9]$$

Where:

S_A is the content of sand (%),

S_i is the content of silt (%),

C_L is the content of clay (%),

OM is the organic matter (%) and

$CaCO_3$ is percentage of the calcium carbonate of the soil samples (%).

The crop canopy factor (S_{LRc}) is calculated as a function of the soil that is covered with a crop canopy (C_C), and incorporating the calibration parameter u_{slrc}, S_{LRc} is calculated according to equation 4.10 (Fryrear et al., 1998).

$$S_{LRc} = e^{-\mu_{Slrc}(c_c^{0.7366})}$$

[4.10]

The soil roughness factor is estimated with equation 4.11.

$$K_{tot} = e^{(1.86 \cdot K_{rmod} - 2.41 \cdot K_{rmod}^{0.934} - \mu_{K_{tot}} \cdot C_{rr})}$$

[4.11]

Where:

K_{rmod} is the modified roughness factor,

μ_{Ktot}, is the calibration parameter for the roughness factor and

C_{rr} is the measured chain roughness (Saleh, 1993).

The model was calibrated against data from all events and plots together. We followed this approach in order to find a single set of parameters that is applicable under a wide range of land use, soil type, and weather conditions. This is essential for application of the model at the regional scale because the range of environmental conditions will be large, and further calibration at the regional scale will not be feasible. We used a brute force technique for calibration. This technique calibrates the model by providing it a wide range of parameter inputs, running it for each parameter set, and selecting the model run that has a minimum value of the objective function. Here we use the mean square error as objective function, as described below. For each calibration parameter, we selected five different values falling within a range that can be considered physically possible. Then, the calibration was done for all sets of possible combinations of parameter values, resulting in approximately 15×10^3 number of calibration runs. This procedure was iterated a number of times, each time narrowing the range of acceptable parameter values. In the first calibration step, the ranges around the original values used in the RWEQ manual (Fryrear et al., 1998) were used. Then, to reduce the search space the ranges were reduced. The objective function was calculated as follows. First, MSE_v was calculated according to equation 4.12.

$$MSE_v = \sum_{v=1}^{v=16} \frac{(Q_{observed,v} - Q_{predicted,v})^2}{16}$$

[4.12]

Where:

$Q_{observed,v}$ is the measured mass transport of catcher v (each plot includes 16 catchers),

$Q_{predicted,v}$ is the predicted total mass transport by the model for catcher v and

the number of 16 is the total number of catchers used in one measurement plot.

Second, the value of MSE_{tot} for all events was determined with equation 4.13.

$$MSE_{tot} = \sum_{v=1}^{v=j} 1 \ldots j (MSE_v)$$ [4.13]

Where:

MSE_v is the mean square error of plot v, with $v = 1 \ldots j$, with j the number of plots and events.

4.2.5 Statistical analysis

The d test (Willmott, 1981), which was also employed by Feng and Sharratt (2007) for testing the (WEPS) model was used to evaluate the model performance. The d value is calculated according to equation 4.14.

$$d = 1 - \left[\frac{\sum_{v=1}^{v=n}(Q_{p_v} - Q_{o_v})^2}{\sum_{v=1}^{v=n}\left(|Q_{p_v} - Q_{oM}| + |Q_{o_v} - Q_{oM}|\right)^2} \right]$$ [4.14]

Where:

Q_{pv} is the predicted value, for plot v

Q_{ov} is the observed or measured value for plot v

n is the number of observations at all events and all plots

Q_{oM} is the mean measured value and, d ranges from 0 to 1.

4.3   Results and discussion

4.3.1   General results of field measurements

The characteristics of the wind events for given time (which was one week for most events) and the measured mass transports for each event are given in Table 4.3.

The averages of wind speeds and wind directions varied among the plots and events. The maximum of average wind speed over all events was recorded at the Serdah *A* measurement plot for the event of 9-30 July. Despite the fact that the main wind direction was WSW for most events, there was an important number of events for which the wind direction was different. For example, at the Adami Gazelle plot ESE and SSW were the main wind directions during the measurement periods. The results of the measured mass transport are not parallel with the wind speed. That is because total mass transport from a field depends not only on weather characteristics but also on vegetation cover, soil properties and soil roughness. Thus, at the Serdah *A* while the average of wind speed for the event of 9-30 July was 8.8 m s^{-1} which was the highest average speed among all events, the measured mass transport for this event was 1.1 kg m^{-1} which was relatively low compared to higher mass transports measured at few other events. On the other hand, the average wind speed during the event of 28-4 August at Um Mial was 4.6 m s^{-1} representing the minimum average wind speed among all events that resulted in 1.6 kg.m^{-1} for mass transport, which was relatively higher value compared with the other events.

Table 4.3. The average of mass transports ($Q_{average}$) measured at an event base from six measurement plots .

Site	Date	Dur (hh: min)	WS (m s^{-1})	Wind factor (m s^{-1})^3	WD (degree)	$Q_{average}$ (kgm^{-1})	$Q'_{average}$ g.cm^{-1}.day^{-1}
Serdah A	9-30 July	7:48	8.8	789.0	WSW	1.1	0.5
	30July-6 Aug	9:25	6.9	8.7	WSW	0.7	1.0
	6-13 Aug	1:37	7.0	3.9	WSW	1.2	1.7
Serdah C	16-28 Jul	2:36	6.9	177.5	WSW	1.9	1.6
	28 Jul - 4 Aug	2:00	7.9	132.6	WSW	1.0	1.4
	4- 11 Aug	1:34	7.0	53.0	WNW	0.7	1.1
	11-18 Aug	0:21	6.9	30.7	WSW	1.0	1.5
MugheratA	13-20 Aug	1:58	5.6	17.0	SSW	0.5	0.7
	20-27 Aug	3:50	5.8	25.4	SSW	8.6	12.3
	27Aug-3 Sept	11:50	6.2	102.8	SSW	10.5	15.1
Mugherat NA*	3-10 Sept	13:45	6.6	126.4	SSW	3.5	5.0
	10-18 Sept	2:20	5.4	13.9	NNE	3.6	5.1
	18-25 Sept	2:30	5.6	9.1	ESE	2.3	3.3
Um Mial	16-28 July	18:10	4.9	83.1	WSW	4.8	4.0
	28-4 Aug	1:43	4.6	65.7	WSW	1.6	2.3
	4-11 Aug	2:06	7.0	31.5	WSW	0.6	0.8
	11-19 Aug	0:58	7.0	23.7	WSW	1.1	1.6
Adami Gazelle	9-16 Sept	17:0	6.9	42.3	ESE	3.5	5.0
	16-23 Sept	8:50	6.2	26.6	ESE	3.6	5.1
	23-30 Sept	21:03	5.3	6.2	SSW	0.7	1.0

Dur, duration; WS, average wind speed during each wind event; WD, average wind direction during each wind event; $Q_{average}$, the average of total mass transport (kg m^{-1}) and Q´ $_{average}$ the average of mass flux (g cm^{-1} day^{-1}) .

4.3.2 Results of model calibration

Table 4.4 shows the original model parameter values, the range used for each parameter, the results of the calibration process and the MSE_{tot}.

The resulting parameters were used in the adjusted model to calculate the spatial mass transport and soil loss over simulated units. Figure 4.5 shows an example for the model prediction of the spatial mass (kg.m^{-1}) transport for four wind events over the Um Mial measurement plot.

Figure 4.5 clearly depicts that the estimated spatial mass transports during the four wind events have similar patterns although the values of mass transports varied from one event to another. The similarity in the patterns of spatial mass transports resulted from the dominant wind direction during the measurement period, which was WSW (Table 4.3), while the differences between mass transports values stemmed from the differences in wind speed for each event. The average mass transports calculated by RWEQ for each plot and each event are illustrated in table 4.5.

Table 4.4. The results of calibration together with the original parameters (Fryrear et al., 1998) and their ranges from the 20 events totally observed in 6 plots.

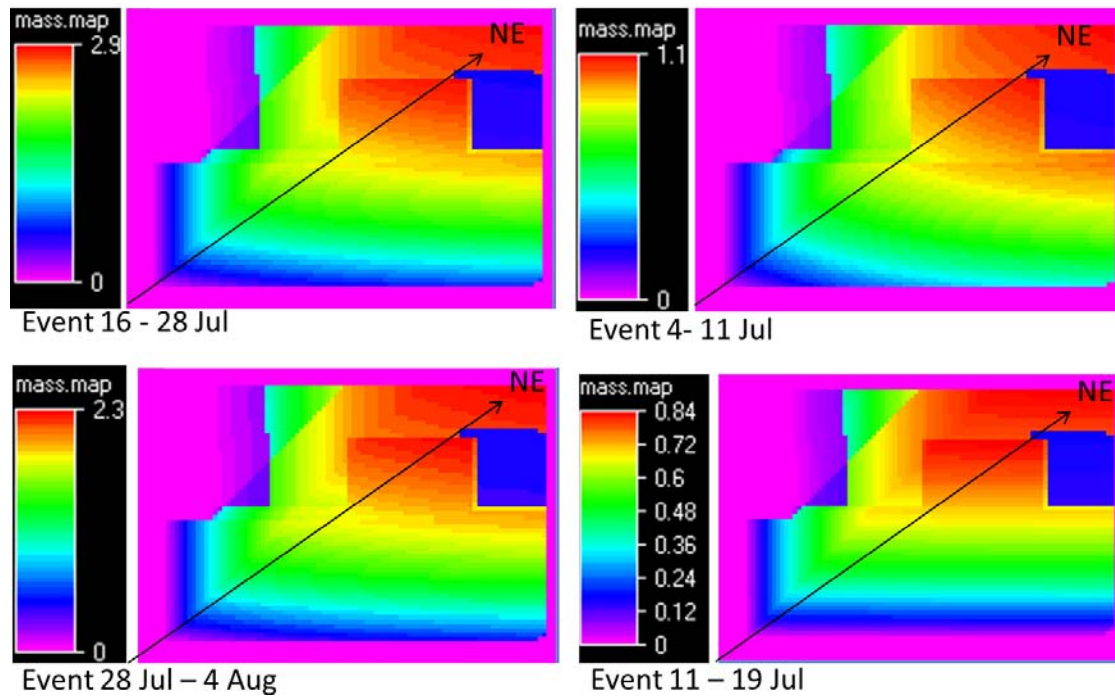| Parameters (-)	Original values (-)	Range tested (-)	Calibration Results (-)	MSE_{tot} (-)
μ_{Sa}	150.71	100 – 350	300	
μ_{Sb}	0.3711	0.03 - 0.17	0.03	
μ_{Ut}	-	3 - 4.2	3	208.3
μ_{E_F}	29.09	4 -14	6	
μ_{SLRC}	5.614	1.2 - 2.7	1.7	
μ_{Ktot}	0.124	0.03 - 0.11	0.03	

Figure 4.5. Spatial distribution of the predicted total mass transport (kg.m^{-1}) by the model for all wind events of Um Mail measurement plot in Khanasser valley, Syria.

Figure 4.6 shows the relation between the model prediction of spatial mass transports (using the calibration results) and the observed mass transports for 20 wind events at the six measurement plots.

The correlation between measured and predicted mass transports for Um Mial, Mugherat A and Serdah C is rather high compared to other plots. However, the correlation between measured and predicted mass transports for the Serdah A and Mugherat NA measurement plots were quite poor. Proper measurement of mass transport is hampered by the occurrence of dust devils which result in an overestimation by the measurements of the real transport. Here, we did not intend to measure dust devil because it is a rather small scale process and thus, it was excluded in this research. This can be the cause of the poor correlation between observed and modelled transports for the Serdah A, that resulted in higher values of the measured mass transport than that predicted by the model. In addition, for the Mugherat NA plot, the poor correlation could have been due to the entrance of sheep to the plot area during the measurement time which unexpectedly accelerated the soil movement and consequently the measured mass transport. As the Mugherat NA plot was close to the settlement, it was difficult to protect the plot from grazing during the measurement period.

The averages of measured and predicted mass transports over the plot are shown in Figure 4.7. The correlation between the measured and predicted mass transports was acceptable due to the number of processes and parameters employed in the model script. As it is clearly shown in Figure 4.7, the correlation between measured and predicted mass transports was improved after averaging over the plot. This improvement of correlation when averaging the mass flux over the plot can be related to the reduction of the value of the standard deviation due to the decreasing of the number of points located far from the correlation line. These results indicated that there is the possibility of applying the average of model outputs (Bierkens et al., 2000) for upscaling the model. Upscaling the model to a regional scale was planned to be the next step of this research.
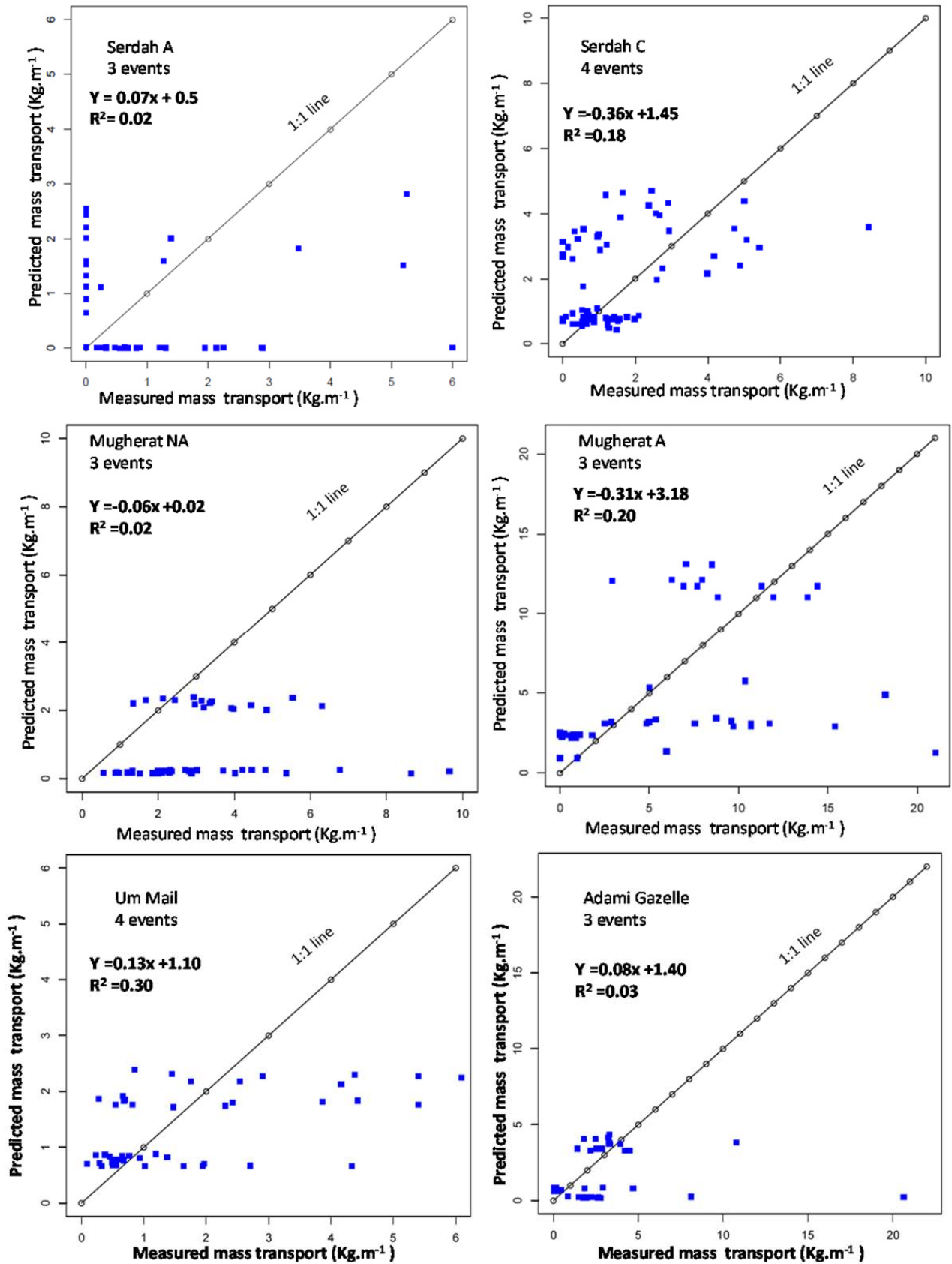
Figure 4.6. Using the calibration results, the relation between the measured and predicted mass transports (kg m^{-1}) of every measurement plot for the full measurement time. Each dot represents one catcher.
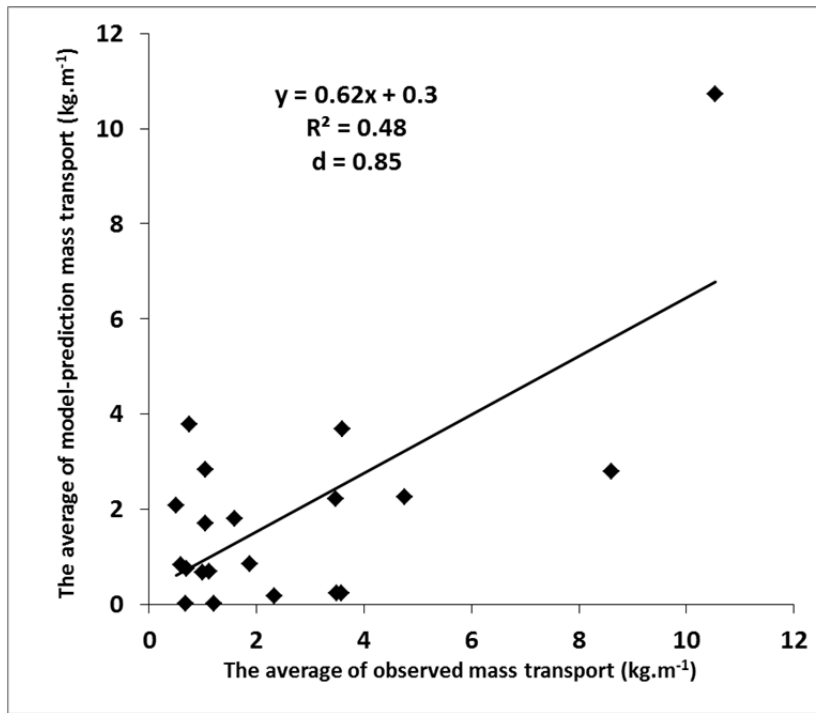
Figure 4.7. Using the calibration results, the relation between the average values of the measured and predicted mass transports by the model (kg m⁻¹).

4.3.3 Outputs of the calibrated RWEQ

Mass transport

Table 4.5 illustrates the average mass transport $Q(x)$ (kg m^{-1}) and $Q'(x)$ (g cm^{-1} day^{-1}) calculated by the model (Equation 4.1) for each wind event and the mean values of mass transport at the six measurement plots over the full measurement period (which was three weeks for most of the plots). It is notable in that there are differences in the predicted mass transports among plots and also among the events for each plot. It can be seen that the highest average mass transport for three weeks was at Mugheart A plot (5.20 kg m^{-1}). The high wind speed recorded over a short time during the measurement periods was the principal cause. For example, during the wind events of 27 Aug-3 Sep, for one time step of six hours the average wind speed was 9.0 m s^{-1}, causing a total mass transport around five kg.m^{-1} over the simulated unit. The minimum average mass transport at the Serdah A measurement plot was 0.2 kg m^{-1}, and was linked to the well vegetated surrounding area and the high amount of residues on the soil surface. While comparing the results of this research with those obtained by ICARDA 2003 in the Khanasser valley region (Masri et al., 2003), our results show a higher mass transport . To enable the compression between the two studies we use the unit of g cm $^{-1}$ day^{-1} for the mass flux as it was used by the mentioned study of ICARDA. Thus, in the region the mass flux varied from 0.1 to 0.3 g cm^{-1} day^{-1}in the results of ICARDA while the measured mass flux was between 0.5 and 15.1 g cm^{-1} day^{-1} in the current study and the model predicted the mass flux was from 0.01 up to 15.3 g cm^{-1} day^{-1}. The lower mass flux of the research done by ICARDA was because they used a measurement period of 12 weeks when computing the mass flux at one plot. In the calculation of mass flux it is essential to use the real event time with units of kg m^{-1} s^{-1} or g cm^{-1} s^{-1} (Sterk and Raats, 1996). In the current research the exact time of saltation was obtained through the use of a saltiphone that recorded the saltation period correctly. Thus, only saltiphone-recorded periods were used when calculating the mass flux.

Table 4.5. The average mass transport calculated by the model for the 6 measurement plots.

Site	Date	*Wind factor (m s^{-1})^3*	Q(x) average (kg m^{-1})		Q´(x) average g cm^{-1} day^{-1} ¥	
			Each event	Average	Each event	Average
Serdah *A*	9-30 July	789.0	1.7		0.8	
	30July-6 Aug	8.7	0.0	0.6	0.0	0.3
	6-13 Aug	3.9	0.0		0.0	
Serdah *C*	16-28 Jul	177.5	0.8		0.7	
	28 Jul-4 Aug	132.6	0.7	2.0	1.0	2.8
	4- 11 Aug	53.0	3.8		5.4	
	11-18 Aug	30.7	2.8		4.0	
Mugherat *A*	13-20 Aug	17.0	2.1		3.0	
	20-27 Aug	25.4	2.8	5.2	4.0	7.4
	27Aug-3 Sept	102.8	10.7		15.3	
Mugherat *NA*	3-10Sept	126.4	2.2		3.2	
	10-18 Sept	13.9	0.2	0.9	0.3	1.2
	18-25 Sept	9.1	0.2		0.2	
Um Mial	16-28 Jul	83.1	2.3		1.9	
	28-4 Aug	65.7	1.8	1.4	2.6	1.7
	4-11 Aug	31.5	0.8		1.4	
	11-19 Aug	23.7	0.7		1.0	
Adami Gazelle	9-16 Sept	42.3	0.2		0.3	
	16-23 Sept	26.6	3.7	1.6	5.3	2.2
	23-30 Sept	6.2	0.7		1.1	

¥ This unit g cm^{-1} day^{-1} was used to enable comparing the results of this research with results of previous studies.

Soil loss

Using the calibrated model the soil loss from each measurement plot was calculated. The spatial distribution of the net soil loss (kg.m^{-2}) from the Um Mial measurement plot for the event of 11 -19 Aug is given as an example of this calculation (Figure 4.8). Table 4.6 gives the average net soil loss from the 6 measurement plot at 20 wind events.
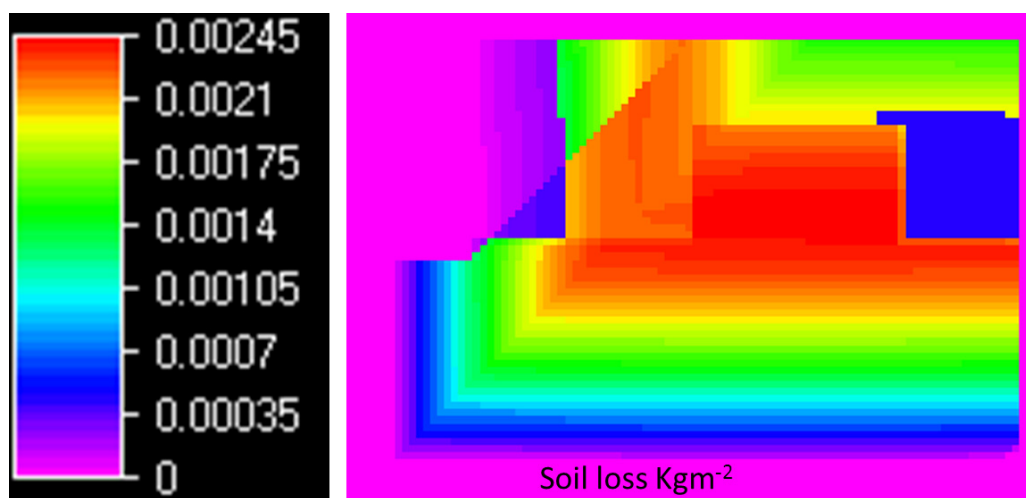

Figure 4.8. The soil loss map of Um Mial plot and surrounding area for the wind event of 11 -19 of Aug, 2009.

63

Table 4.6. The average soil loss (g m^{-2}) calculated by the model for the 6 measurement plots.

Site	Date	Soil loss (g m^{-2})	
		Each event	Average
Serdah A	9-30 July	2.8	0.94
	30July-6 Aug	0.0	
	6-13 Aug	0.0	
Serdah C	16-28 Jul	11.9	6.4
	28 Jul 4 Aug	8.9	
	4- 11 Aug	2.6	
	11-18 Aug	2.2	
Mugherat A	13-20 Aug	7.1	18.5
	20-27 Aug	9.6	
	27Aug-3 Sept	38.8	
Mugherat NA	3-10Sept	7.5	2.9
	10-18 Sept	0.8	
	18-25 Sept	0.5	
Um Mial	16-28 Jul	7.3	4.5
	28-4 Aug	5.9	
	4-11 Aug	2.6	
	11-19 Aug	2.3	
Adami Gazelle	9-16 Sept	0.7	5.6
	16-23 Sept	13.5	
	23-30 Sept	2.6	

The model results of net soil loss show that the values fluctuate among the plots and among the wind events at each plot (Table 4.5). Parallel to results of mass transports, the highest soil loss was predicted at the plot of Mugherat *A* with a value of 18.5 g m^{-2} (Table 4.6) for the average of 3 wind events. The minimum soil loss was predicted at the Serdah A measurement plot with a value of 0.94 g m^{-2}. Moreover, among wind events, the minimum value of soil loss was predicted for the events of 30 Jul − 6 Aug and 6 − 13 Aug at Serdah *A* with values of 0.0 g m^{-2} and the maximum value was predicted for the event of 27Aug-3 Sept at Mugherat *A* with value of 38.8 g m^{-2}.

4.4   Conclusion

In this study, the RWEQ wind erosion model was adjusted and calibrated against ground data collected from six simulated units in stabilization zones 4 and 5 in Khanasser valley, Syria.

The original RWEQ model was mainly created to estimate the soil loss from agricultural field in the USA. It considers the simulated unit to be homogenous, and that it has clear non-eroding borders and it uses the average of weather data over a period of 1 -15 days. These specific conditions do not exist in the area used for this study. Moreover, the weather parameters change continually in the region examined, thus, averaging over such a long period may result in unrepresented parameters for weather characteristics. Therefore, adjustments to the original RWEQ model were applied in the current study. The adjustments include the simulation of sediment flux over the field boundaries and the time step which was narrowed to six hours. This allowed the adjusted model to calculate the mass transport depending on weather inputs over these six hours.

Mass fluxes were observed using 16 MWAC catchers on a grid set-up on a 60 x 60 m plot. The weather, soil, vegetation and roughness are the main factors of the RWEQ model, and because of that, one parameter from each of these factors was calibrated using the extensive brute force calibration technique. Six calibration parameters, which were included in the determination of the critical field length (*S*, m), the

threshold wind velocity (U_t, m s^{-1}), the erodible fraction ($E_{F,}$ -), the crop canopy (S_{LRC}, -) and the soil roughness factor (K_{tot}, -), were used in this calibration.

With the calibrated model it is possible to calculate the mass transport and the net soil loss from simulated area units. The model results were tested against ground data collected from the study area. The results of this test showed that the coefficient of determination for the linear regression equation between measured and predicted average mass transports by the model at the simulated units at 20 wind events was (R^2=0.48, d=0.85). This correlation is acceptable compared with previous tests of the RWEQ model. Finally, we realize that for regional scale modelling it is important to calculate total soil loss over a plot. This was the reason behind aggregating model results over each simulated unit to calculate total soil loss using the RWEQ in PCRaster.

Chapter 5

The effect of vegetation patterns on wind-blown mass transport at the regional scale: A wind-tunnel experiment

The effect of vegetation patterns on wind-blown mass transport at the regional scale: A wind tunnel experiment

Abstract

Wind erosion is a global environmental problem. Re-vegetating land is a commonly used method to reduce the negative effects of wind erosion. However, there is limited knowledge on the effect of vegetation pattern on wind-blown mass transport. The objective of this study was to investigate the effect of vegetation pattern on this phenomenon within a land unit and at the border between land units. Wind tunnel experiments were conducted with artificial shrubs representing *Atriplex halimus.* Wind runs at a speed of 11 m s^{-1} were conducted and sand translocation was measured after 200-230 second using a graph paper prepared for this purpose.

This research showed that: 1) the transport within a land unit is affected by the neighbouring land units and by the vegetation pattern within both the unit itself and the neighbouring land units; 2) re-vegetation plans for degraded land can take into account the 'streets' effect (zones of erosion areas similar to streets); 3) the effect of neighbouring land units includes sheltering effect and the regulation of sediment passing from one land unit to the neighbouring land units and 4) in addition to investigation of the general effect of vegetation pattern on erosion and deposition within the region, it is important to investigate the redistribution of sediment at smaller scales depending on the scope of the project.

Key words: wind erosion, vegetation pattern, wind-blown mass transport, wind tunnel

5.1 Introduction

Many arid and semi-arid areas in the world suffer from the consequences of wind erosion (Cornelis, 2006; Stroosnijder, 2007). Airborne dust particles pollute the air and can cause health problems to the inhabitants (Thomas and Turkelboom, 2008), saltating grains can cause crop damage, and the removal of the topsoil reduces soil fertility, eventually resulting in degraded areas (Nanney et al., 1993). To minimize sediment transport and reduce the erosive forces of wind, re-vegetation of degraded land is a widely used approach (Leenders, 2006; Wang et al., 2011; Zhao et al., 2011). A minimal vegetation cover providing optimal protection against wind erosion reduces costly re-vegetation efforts and competition for limited water resources. Leenders et al. (2007) indicated that the parkland system, in which a combination of trees and shrubs are distributed over an area, provides potential for regional-scale protection against the negative impact of wind erosion. This study investigates the effect of vegetation and its pattern on the wind-blown sand transport.

A large number of studies have reported that vegetation has the capacity to decrease soil loss by wind as it reduces wind speed and soil erodibility, and increases the entrapment of eroded material (Van De Ven et al., 1989; Sterk et al., 1998; Udo and Takewaka, 2007; Abdourhamane et al., 2011; Leenders et al., 2011; Munson et al., 2011). Research on stabilization of moving sand dunes has also linked reduction of sand movement to the increased trapping capacity of vegetation cover (Hesse et al., 2004; Chang et al., 2011; Drenova, 2011; Floyd and Gill, 2011). Lancaster and Baas (1998) showed that vegetation increases both the aerodynamic roughness length and the threshold wind shear velocity. Leenders et al. (2007), in their study of the effect of dispersed shrubs and trees on wind erosion in an agricultural field in the Sahel of Africa, showed that shrubs decrease the total mass flux by trapping soil particles and trees decrease the wind speed and, thus, the erosive force. Therefore, for optimal protection of the soil surface in agricultural

fields, a combination of shrubs and trees is recommended. Studies have also shown that attention should be given to the percentage of cover in order to prevent increased turbulence, which may lead to an increase in wind erosion (e.g. Sterk et al., 1998).

Knowledge about the effectiveness of vegetation in reducing wind-blown sediment transport is essential for designing approaches for re-vegetation of degraded land (King et al., 2005; Burri et al., 2011). However, research on the impact of vegetation on wind-blown sediment transport under field conditions alone is not sufficient as, under field conditions, the effect of vegetation cannot be isolated. Under such conditions it is affected by other factors such as soil properties, changes of vegetation during the measurement period, topography and soil surface conditions (Lopez et al., 1998). Thus, wind tunnel studies are a useful additional procedure for studying the relationship between vegetation and wind-blown sediment transport under controlled conditions (Gabriels et al., 1997; Cornelis and Gabriels, 2004).

Several wind tunnel experiments have been undertaken to improve understanding of the relationship between vegetation and wind erosion. These experiments used pieces of dead vegetation (Molina-Aiz et al., 2006), living vegetation (Burri et al., 2011), or artificial vegetation (Cornelis and Gabriels, 2005; Udo et al., 2008; Wuyts et al., 2008) as surrogates for real-world vegetation. These studies concluded that vegetation reduces the total wind-blown sediment transport and that the impact of vegetation on sediment transport changed with vegetation density and porosity. Udo and Takewaka (2007) concluded from their wind tunnel experiments that, in addition to the density, the height and flexibility of the vegetation are essential characteristics determining effectiveness in the reduction of wind-blown mass transport. The results of the wind tunnel study of Burri et al. (2011) showed an exponential decrease in mass flux with increasing vegetation cover, although with low vegetation cover (around 3%) an increase in the mass flux was observed. Li et al. (2008) simulated *Tamarix spp* shrubs growing in "Nabkha" dunes in a wind tunnel and observed sand transport around the simulated vegetation. They concluded that vegetation reduced air flow above the sand mounds, changed the wind profile upwind and downwind of the sand mound, and decreased the sand transport from the mound area. These studies have provided valuable insight; however have some limitations regarding scale.

To date, the majority of wind tunnel experiments regarding vegetation effects on wind-blown mass transport have focused on the simulation of field conditions at the plot or point scale (Musick et al., 1996; Udo and Takewaka, 2007; Li et al., 2008). These results are important for understanding the effect of vegetation on wind-blown mass transport at specific locations and the mechanisms by which the vegetation reduces the total mass transport around the vegetation element. However, for understanding the effects of vegetation on wind erosion at a regional scale, the results of these studies are insufficient. In regions vulnerable to wind erosion, land management activities in one land unit may affect wind erosion processes in neighbouring land units (Hupy, 2004; Leenders, 2006). Furthermore, erosion that occurs in one land unit affects the units located downwind. Todd et al. (2004), Fryrear et al. (1998) and Youssef et al. (2012a, chapter 4) studied the effect on the maximum sediment transport and reported a gradual increase in the mass flux from bare land downwind from a non-erodible border. Therefore, to understand the effect of vegetation at the regional scale, it is vital to generate data representing processes taking place along the entire land unit and at transitions between land units.

The objective of this study is to provide further understanding of the effect of vegetation cover and different vegetation patterns on the change in mass flux of wind-blown sediment at the regional scale through wind tunnel experiments. The main research questions are: 1) what is the change in wind-blown sediment transport at borders between bare and vegetated land? 2) What is the effect of vegetation pattern on the translocation of wind-blown mass transport across arable fields? 3) How does the vegetation pattern affect the size and spatial distribution of areas with erosion or deposition along land units? Answers to these questions will be discussed in the current paper.

5.2 Material and methods

5.2.1 Wind tunnel

This study was conducted in the wind tunnel of the International Centre for Eremology (ICE), Ghent University, Belgium. The dimensions of the wind tunnel are 12 m in length (8.50 m is used in this study), 1.2 m in width with an adjustable roof height of up to 3.20 m (Gabriels et al., 1997; Cornelis and Gabriels, 2004). Wooden spires and roughness cubes were used to create a boundary layer of 0.60 m at the upwind border of the experimental section which is 6 m from the entrance of the working section of the wind tunnel (Cornelis and Gabriels, 2004). Wind speed was measured with vane probe-type anemometers (Gabriels et al., 1997) placed at X = 5.85 m (measured from the entrance), and Y = 0.60 m (measured from the wall of the working section) positioned at heights of 0.02, 0.13, 0.27, 0.38, 1.10 m (Figure 5.1). Sediment was stored in a 2.50 m long; 0.50 m wide and 0.01 m deep tray. To create a roughness similar to that of sand, sandpaper was placed in an area up to 1.50 m in front of the tray and on the areas to its left and right (Figure 5.1).

As sand is very sensitive to wind erosion (Chandler et al., 2005), it was chosen for use in the present experiments. Beach sand was collected from the beach of Ter Heijde, Den Haag, the Netherlands, dried for two weeks, and subsequently filtered through a 1 mm sieve to remove shells. Table 5.1 shows that more than 95% of the sediment particle size falls within the 100 - 500 µm range, which corresponds to the particle class that is highly vulnerable to wind erosion (Chandler et al., 2005). The wind velocity during each run was 11 m s^{-1} at a height of 1.10 m above the (solid) sand paper and a distance of 6 m from the test section entrance. This corresponds to a shear velocity of 0.26 m s^{-1} determined following the procedure of Cornelis and Gabriels (2004).
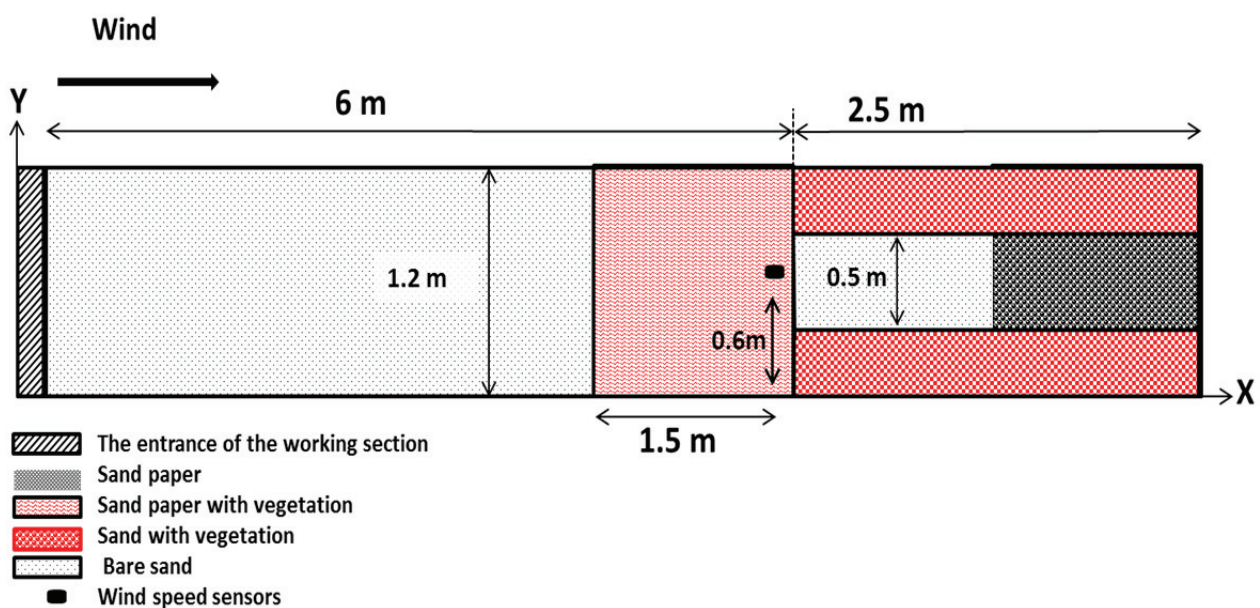

Figure 5.1. The setup of the wind-tunnel experiments at the ICE, Ghent Belgium.

Table 5.1. Particle size distribution of the sediment used in the wind tunnel experiment.

Fraction (µm)	<50	50-100	100-300	300-500	500-1000
Percentage (%)	0.1	1.3	20.5	75.3	3.2

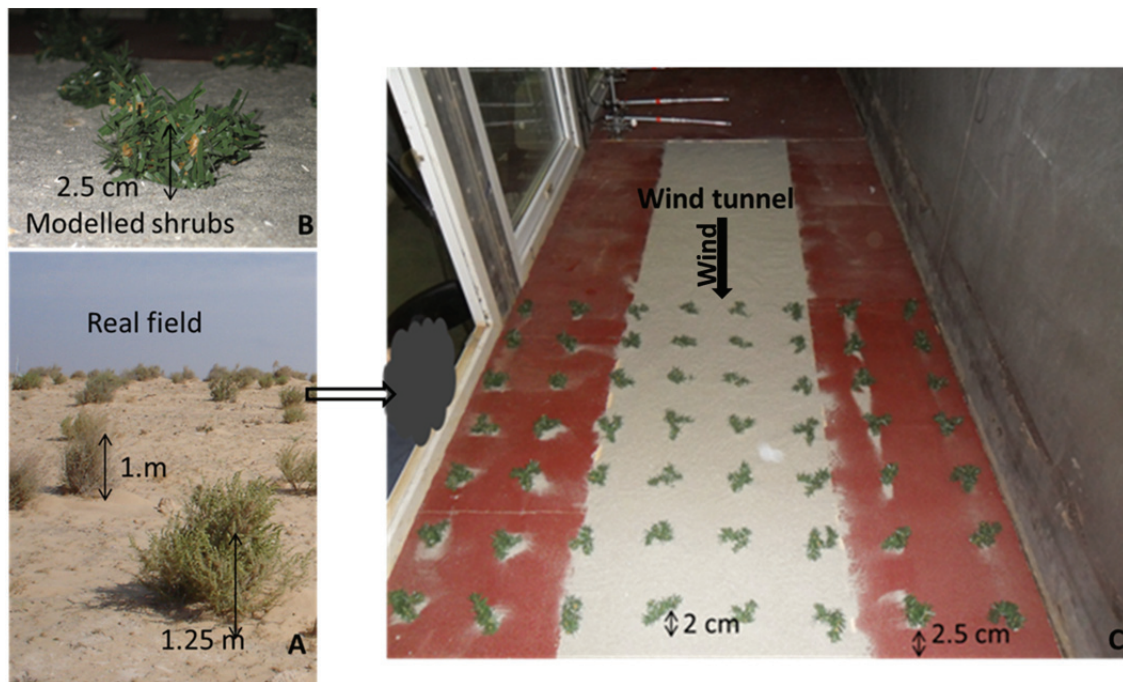*Figure 5.2.* (*A*)*: View of Atriplex shrubs in the field* (*B*)*: simulated shrubs in the tray and* (*C*)*: simulated shrubs in the wind tunnel*

5.2.2 Representation of vegetation

In arid and semiarid environments, *Atriplex halimus* is often used for re-vegetation of degraded land (Hassine and Lutts, 2010) because it has a low water requirement (less than 100-200 mm per year) (Martínez-Fernández and Walker, 2011). *Atriplex halimus* also resists saline conditions and survives a high grazing pressure (Ruiz-Mirazo and Robles, 2011). Therefore, in these experiments artificial plants with morphology similar to *Atriplex halimus* shrubs were used, applying a downscaling ratio of 1:50. This scale was chosen because it allowed accurate simulation of the height of *Atriplex halimus* and distances between shrubs in real fields under the dimensional and boundary layer conditions of the wind tunnel. The modelled shrubs were between 2.00 and 2.50 cm high, representing 1 and 1.25 m-high *Atriplex halimus* shrubs in the field (Figure 5.2A). The shrub model consisted of polyethylene ribbons attached to iron sticks (Figure 5.2B, C). Each shrub model has several sticks attached to each other at their lower end and fixed to a wooden board. The shrubs were then bent, to represent the shape of real *Atriplex halimus*. The fraction of the surface covered by the vegetation was 10 - 11% throughout the experiments.

Wind-driven sediment transport was observed under two scenarios (Figure 5.3). In the first scenario, the sediment movement from bare to vegetated land was simulated for four vegetation patterns. In the second scenario, the sediment movement from vegetated to bare land was simulated for one vegetation pattern. The patterns used (Figure 5.3) were:

1.   Pattern P.A: 36 individual modelled shrubs were positioned on a regular grid;
2.   Pattern P.B: 32 individual modelled shrubs are placed in a sequence of offsetting the second, fourth, sixth and eighth rows of shrubs in the Y direction;
3.   Pattern P.C: 18 patches (with two individual modelled shrubs for each patch) were distributed along the tray with rows of three patches perpendicular to the wind direction;
4.   Pattern P.D: 12 patches (with three individual modelled shrubs for each patch) were distributed along the tray with rows of two patches perpendicular to the wind direction;
5.   Pattern P.E: movement of sediment from vegetated to bare land was tested using shrubs in a regular grid shape.
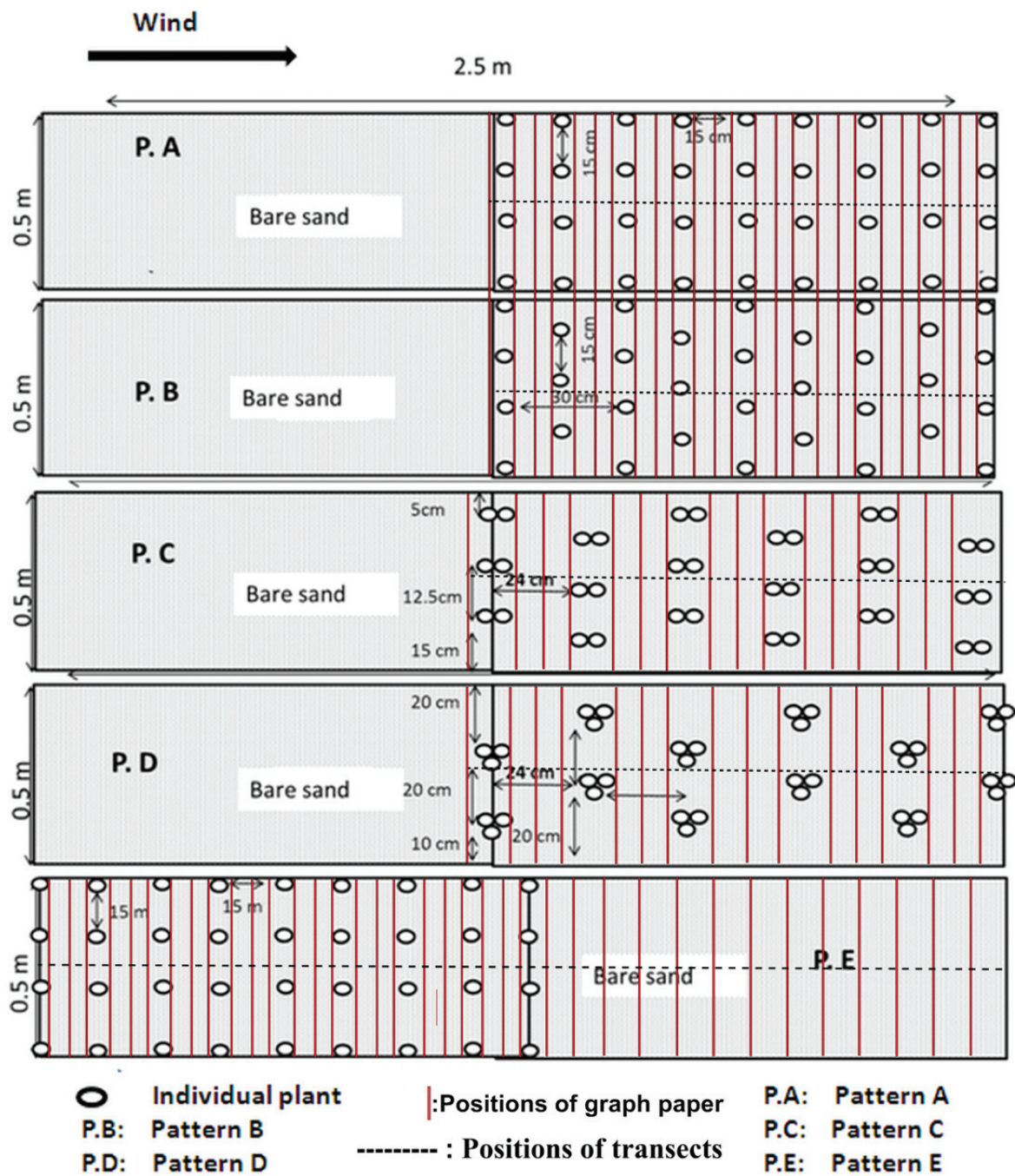
Figure 5.3. Layout and vegetation patterns tested in the wind tunnel experiments.

A decrease in the number of shrubs was compensated for by an increase in the width of a single shrub, and thus, the fraction of surface covered by vegetation remained the same for all patterns (Figure 5.3).

An average free-stream wind speed of 11 m s^{-1} (or shear velocity of 0.26 m s^{-1} above the surface) was chosen for all experiments. This wind speed provided movement of sand however, did not affect the shape of the modelled vegetation in the wind tunnel. Before each run, the surface in the tray was smoothed using a soft brush to create a homogenous sand height of 0.01 m. Each test lasted 200-230 seconds (except run 3 in P.D pattern) within this time period all sand in the bare (upwind) part of the tray was eroded in patterns P.A, P.B, P.C and P.D. We ran three replicates for each pattern.

To measure the sand height along the experimental tray a 0.50 x 0.25 m piece of 0.30 mm thick graph paper (coated to prevent destruction from the sand) was used. The graph paper was inserted carefully into the pre-wetted sand, perpendicular to the wind direction, and the sand topography was

drawn onto the paper. Pre-wetting the sand after each run prevented the surface from collapsing when inserting the graph paper. The height of the sand was first traced onto the graph paper, with the heights then read directly from the paper at 1 cm intervals resulting in 51 heights being recorded for each position of the paper in the tray. Figure 5.3 shows the positions at which the sand heights were measured relative to the position of vegetation elements. This measurement scheme resulted in 1275 measurement points for each run of patterns P.A and P.B, 816 for each run of patterns P.C and P.D and 1887 for each run of pattern P.E.

Geostatistical interpolation of the data was performed using a spherical variogram model (which best fitted the data), and maps showing the spatial variation of sand heights along the tray were created by ordinary point kriging (Chappell and Warren, 2003).

5.2.3 Key simulated parameters of turbulence and saltation with the existence of vegetation.

The simulation of wind-blown sediment in a wind tunnel is complicated because the parameters that affect the saltation process need to be either correctly represented or downscaled (White, 1996). Table 5.2 gives an overview of the key parameters affecting this study. We took these into consideration as follows:

1. The boundary layer and other aerodynamic criteria. Gabriels et al. (1997) showed that the boundary layer thickness of the ICE can be adjusted using wooden spires and roughness cubes. The boundary layer in this research was 0.70 m, which agrees with the boundary layer explained by White (1996). All other aerodynamic criteria for airflow were simulated correctly in the ICE wind tunnel (Gabriels et al., 1997; Dierickx et al., 2001).

2. The obstacle height, H: this parameter was downscaled by a ratio of 1:50. As noted, this scale was chosen because it allowed simulation of the height of *Atriplex halimus* and distance between shrubs in fields under the dimensional conditions of the boundary layer of the wind tunnel (the maximum height of simulated shrubs was 2.50 cm).

3. The roughness length, Z_0: to create roughness similar to sand on the floor of the wind tunnel, sand paper was affixed to the upwind area and sides of the sediment tray.

4. Particle diameter, D_p: According to White (1996), when simulating an obstacle 1 m in height, the particle diameter for simulation of sediment movements around the obstacle should be around 10 μm. This means that a correct simulation for this parameter is not possible because, due to the cohesive forces that connect particles of small size, particles with a 10 μm diameter will not be saltated (White, 1996). Thus, we applied the downscaling ratio of 1:1 for the D_p parameter to ensure that the saltation process would take place.

5. The reference height, h, of measured wind speed: In this research, the boundary layer was arranged to be 0.70 m and the wind speed was measured at heights of 0.02, 0.13, 0.27, and 0.38. Thus, the wind speed was measured within logarithmic portions of the wind tunnel (White, 1996). In addition, the free wind speed (above boundary layer) at a height of 1.10 m was measured for reference purpose (Gabriels et al., 1997).

6. The ratio of obstacle height to boundary layer (H/B_o): According to White (1996) if the ratio (H/B_o) for real field conditions is less than 0.2 (which is the case for our study, the ratio for the wind tunnel should also be less than 0.2. In our simulation the maximum value of the ratio (H/B_o) was 0.035. Although in general terms the simulation here obeys the requirements of downscaling as suggested by White (1996) (0.035 <0.2), the magnitude of the simulated and suggested values is quite different.

7. Time-scale T: White (1996) showed that the time effect in wind tunnel experiments is much shorter than under real field conditions, and that the necessary duration of experiments is proportional to the wind velocity applied. In our simulation, the time applied was (200-230 seconds) at the wind speed of 11 m s^{-1}. This period was sufficient to empty the majority of the sediment reservoir.

Table 5.2. Parameters of saltation and flow simulated in this research.

Parameter(s)	Importance of scaling and/or simulation principles
Aerodynamic criteria and boundary layer B_o (m)	Affect 1) the mean velocity and turbulence density and energy 2) roughness Reynolds number (R_{er},-) 3) Jensense length-scale criterion (Jensen, 1958) 4) the ratio (H/B_o) (White, 1996).
Obstacle height H (m):	The height should be under the dimensional conditions of the boundary layer (White, 1996).
Roughness length Z_0 (m)	Should be scaled exactly like field conditions to ensure $R_{er} > 2.5$ (White, 1996).
Particle diameter D_p (m)	Affect gravity, drag, Saffman and Mangnus forces that are essential forces in saltation process (Zou et al., 2007).
Reference height (h,-)	The height where wind speeds are measured should be within the logarithmic portions of the wind tunnel.
The ratio of obstacle height to boundary layer (H/B_o, -)	In aeolian saltation, the ratio (H/B_o) is less than 0.2 (White, 1996). And thus, that should be considered when simulate the field conditions.
Time scale T (seconds)	Generally simulated saltation time is shorter than the time of saltation at real field conditions.

5.3 Results

5.3.1 Spatial distribution along the experimental tray

For each pattern P.A, P.B, P.C and P.D, the spatial distribution of sand height along the tray was similar for runs 2 and 3 (Table 5.3). Based on the divergent standard deviations (σ) and the variation in pattern, run 1 can be considered as a preparation run. The difference between the results of run 1 and runs 2 and 3 can be explained by the probable change in trapping efficiency after a vegetation element has trapped some sediment. After run 1, although the shrubs were cleaned using a soft brush to remove the sand around them, part of the sand among the small leaves was not completely removed.

For pattern P.E, since no incoming sediment was simulated from the upwind border the spatial distribution of sand height along the tray was similar for runs 1 and 2. Run 3 was removed from the calculations because sand removed during runs 1 and 2 was not completely replaced before run 3. That was due to the difficulty of adding sand between the leaves of the model shrubs. This condition resulted in a large variation in the patterns of erosion and deposition between run 3 and both run 1 and 2.

The spatial distribution of sand height, averaged over run 2 and 3 for each bare sand to vegetation scenario and over run 1 and 2 for the vegetation to bare sand scenario, is shown in Figure 5.4. As the sand height along the tray was 1 cm before the test, values above 1 cm represent deposition and values below 1 cm represent erosion. The first 125 cm of the tray is not included for the bare sand to vegetation patterns as this part of the tray was empty after each run.

Table 5.3. Average sand height (cm) and standard deviation (σ) for each run (r1, r2 or r3) and vegetation pattern.

Pattern	P.A			P.B			P.C			P.D		
Run	r1	r2	r3	r1	r2	r3	r1	r2	r3	r1	r2	r3
Sand height	1.25	1.36	1.37	1.01	1.35	1.31	0.95	0.78	0.78	0.97	1.08	0.85
σ	0.16	0.21	0.21	0.15	0.21	0.18	0.15	0.16	0.13	0.14	0.11	0.11
Average*(σ)	0.21			0.20			0.15			0.11		

*the average (σ) is calculated from run 2 and 3, because run1 is considered to be a preparation run
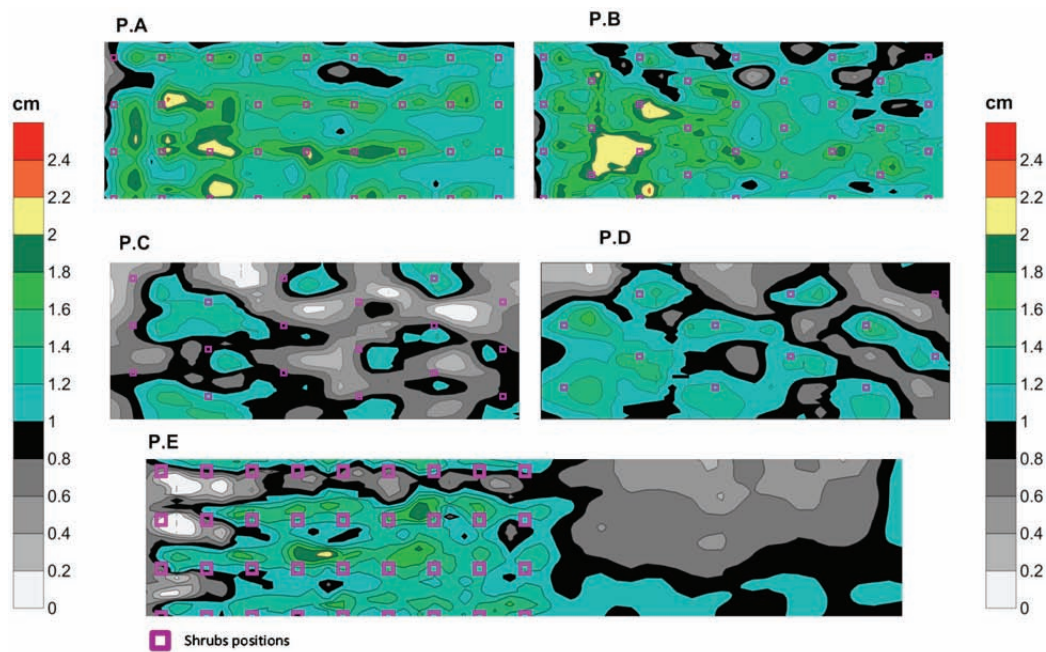
Figure 5.4. Spatial distribution of sediment height over the tray for the average (calculated as explained in the paragraph 5.3.1) of 2 runs for each vegetation pattern.

With pattern P.A, deposition occurred behind shrubs. The amount of deposition decreased from the upwind border to the downwind border of the vegetated unit. In the area between rows parallel to the wind direction, erosion occurred with a gradual increase in erosion towards the downwind border. These results are in the agreement with the field research findings of Bowker et al. (2008), who found similar 'streets' of erosion in the downwind direction between shrubs for several dust storms in the north Chihuahuan desert. In pattern P.B, high deposition behind shrubs was observed in the upwind half of the tray. From the fifth (perpendicular to wind direction) row of shrubs to the end of the tray, decreased deposition and some erosion was recorded.

For patterns P.C and P.D, erosion was dominant, although low levels of deposition were observed behind the vegetated patches. Pattern P.E shows distinct erosion features at the upwind border of the tray. After the third row of shrubs there was a gradual increase in the deposition up to the end of the vegetated part of the tray. In the bare part of the plot, erosion started at a distance of 5-10 cm, which is equal to approximately 2-5 times the height of the vegetation elements.

The average σ for patterns P.A and P.B (0.21 cm, 0.20 cm) is higher than the average σ for P.C and P.D (0.15 cm, 0.11 cm). Therefore, the patterns with lower numbers of vegetation elements (P.C and P.D) resulted in a more homogenous (gentler topography) surface than patterns with a larger number of vegetation elements (P.A and P.B).

5.3.2 Average sediment height for the tested area

To evaluate the general trend in erosion or deposition in the direction of the wind, transects parallel to the wind direction were calculated. For every 5 cm the mean of all sand heights was calculated and plotted (Figure 5.5). As in Figure 5.4, the first 125 cm is not included for patterns P.A, P.B, P.C and P.D, as this part of the tray was almost empty after each run.

Figure 5.5 shows that, for each of the patterns P.A, P.B, P.C and P.D, run 2 and run 3 gave comparable results, and that there are clear, consistent differences between the patterns. The minor differences can be attributed to the fluctuation of the wind speed during the runs.

Both patterns P.A and P.B show a small strip of erosion at the border between the bare and vegetated parts of the tray. As the shear velocity of the wind is reduced because of the presence of shrubs,

mass transport rates decline as well (compared to the larger transport rates that blew away all the sand from the upwind part of the tray). Net deposition occurs from just 2.50 to 120.00 cm downwind from the vegetation edge. The initially high and then downwind-decreasing deposition indicates a decrease in sediment concentration due to decreased sand supply since much of the sand was entrapped by the upwind vegetation. Deposition reaches the highest level at 20 cm downwind from the border. Beyond this, deposition decreases gradually and approaches equilibrium (neither erosion nor deposition) after 100 cm from the border.

In contrast to patterns P.A and P.B, pattern P.C resulted in net erosion continuing downwind for the entire length of the vegetation zone. The more sparsely distributed shrubs likely provided less frictional resistance, which would allow shear velocity to remain high, resulting in higher erosion rates. The continued erosion in pattern P.C along the first 15 cm from the vegetation edge indicates that the vegetation elements were too sparse to protect the area from erosion, even though the percentage of surface cover was similar to that of patterns P.A and P.B.
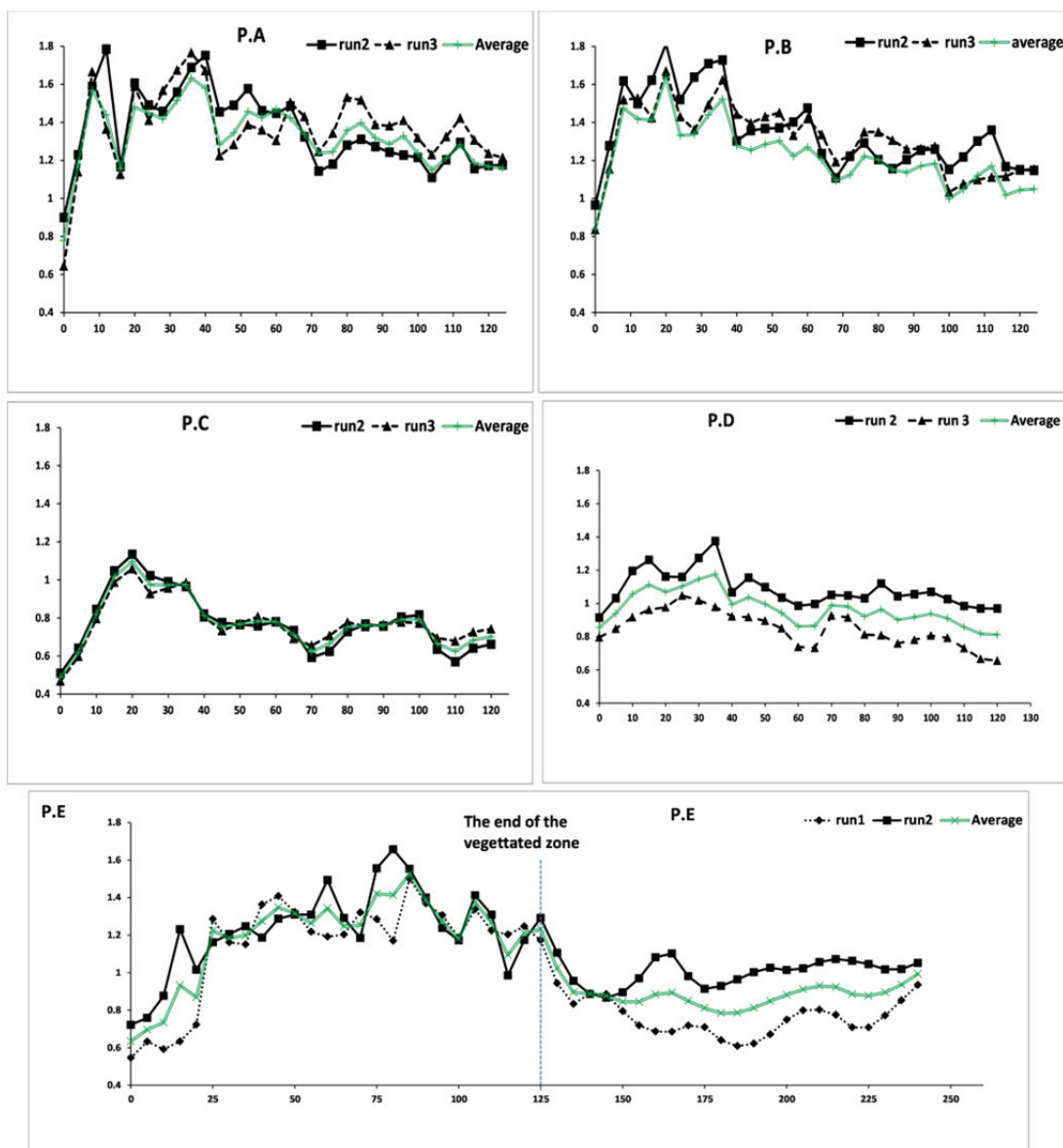
X axis: Downwind distance from the edge of the vegetated part of the tray (cm)
Y axis: The average of sand heights (cm)

Figure 5.5. Average sand heights along the downwind distance for runs 2 and 3 of each vegetation pattern.

In pattern P.D, sand heights for run 2 and 3 deviated on average 0.23 cm (Table 5.3) but the same general pattern was observed. The difference is probably due to the difference in the duration of the wind speed above 10.50 m s^{-1} between the two runs - 216 seconds for run 2 and 306 seconds for run 3. With longer duration a higher amount of sediment is eroded. Also in this pattern both runs still show erosion in the first 10 cm after the border, after which deposition occurs in run 2 and less erosion occurs in run 3. At the distance of 50 cm downwind from the vegetation edge, the airflow of run 2 appears to reach an equilibrium with no further significant erosion or deposition observed to the end of the tray. The results of run 3 show an increase in erosion from 35 cm up to 65 cm, followed by a decrease in erosion between 65 cm and 85 cm. From 85 cm to the end of the tray erosion again increased.

In the vegetated part of pattern P.E (vegetation to bare sand scenario), net deposition begins 10-20 cm from the border of the vegetated field. As observed in P.A, which had a similar vegetation pattern, the shrubs resulted in reduced shear velocity, and hence reduced erosion compared to a bare field. However, there was no compensation for the erosion that did occur, as was the case in P.A., because there was no sediment source upwind of the vegetated unit in the P.E setup.

5.3.3 Sand height with distance along a longitudinal transect at Y=0.60 m

For more details on the sand height distribution along the tray, a 1 cm wide (Y direction) transect for sand heights along the middle of the tray (Y = 0.60 m, middle of the wind tunnel) was calculated using the average of two replications for each pattern (Figure 5.6).

X axis: Downwind distance from the edge of the vegetated part of the tray (cm)
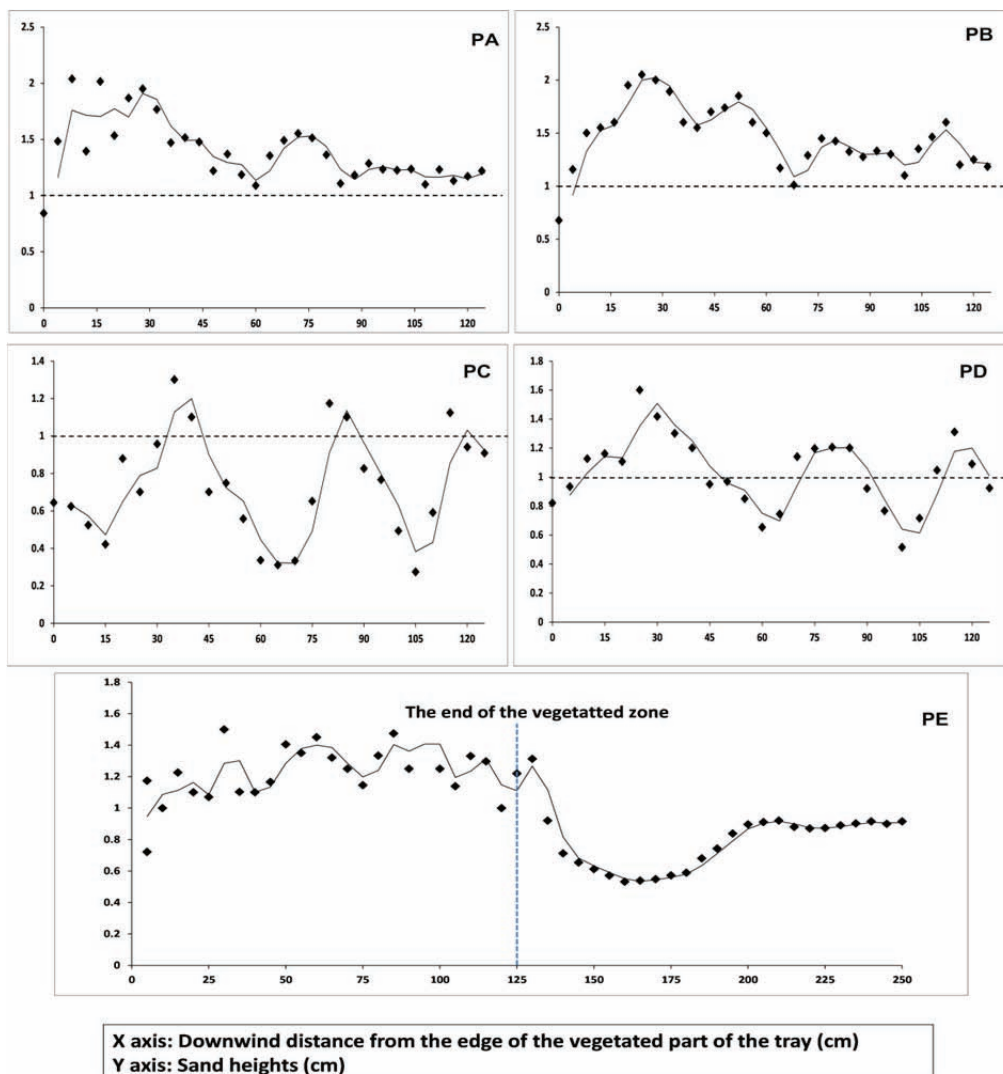Y axis: Sand heights (cm)

Figure 5.6. Transect of sand heights along the downwind distance (average of two replicates).

Figure 5.6 shows that with patterns P.A and P.B, after a small strip of net erosion at the upwind border, net deposition can be observed along the entire length of the tray. With pattern P.C, two small zones of net deposition occur at distances of 30 to 45 cm and 80 to 90 cm. Outside these zones, net erosion was observed along the transect for pattern P.C. In the case of the P.D pattern, in the first 45 cm deposition was dominant, after which distance associated with net erosion is almost equal to that associated with net deposition. With pattern P.E, net erosion in the first 15 cm was generally followed by net deposition within the vegetated area, whereas net erosion was dominant within the bare sand area.

5.3.4 Erosion and deposition along the tested area

In the framework of land protection projects, the full impact of erosion or deposition must be known in order to choose a suitable vegetation pattern. And thus, it is not only important to know the general trend of erosion or deposition along a land unit with certain vegetation characteristics, it is also essential to know the size of areas associated with erosion or deposition and the severity of the erosion or deposition within the region. To gain insight into the intensity of the mass transport effects, sand height was classified into five classes indicating the severity of erosion or deposition (Table 5.4). Figure 5.7 shows the results of applying this classification for the average of two replicates for each vegetation pattern. It should be noticed that only the vegetated part of the tray was analysed.

**Table 5.4. Classification of erosion and deposition upon sand heights.**

Sand height	Explanation	Symbol
0-0.45 cm	Intense erosion	*I E*
0.45-0.90 cm	Erosion	*E*
0.90-1.10 cm	Balance	*B*
1.10-1.80 cm	Deposition	*D*
1.80 -2.50 cm	Intense deposition	*I D*

Figure 5.7 shows that although a large percentage of cells were associated with deposition for patterns P.A and P.B, erosion also occurred at a small scale within these patterns. It should be noticed that in P.A., despite the potential risk of the corridor ('street') effect, erosion was observed in just 4.5% of the cells, whereas in P.B erosion was observed in 8.2% of the cells. In pattern P.C erosion was quite high accounting for 56.3% of the cells, whereas in pattern P.D erosion was lower (37.8%) and deposition was higher (34.7%) (comparing with the erosion and deposition percentage in P.C pattern). Although P.E has the same vegetation pattern as P.A, the percentage of cells associated with erosion was quite higher in P.E (26.4%) than in P.A (4.5%).

5.4   Discussion

5.4.1 Large-scale considerations

The effect of borders between different land units on the wind driven mass flux is essential for understanding regional-scale wind erosion. The variability of wind-blown mass flux found in this study in bare and vegetated fields along the dominant wind direction identifies a significant concept related to the border effect:
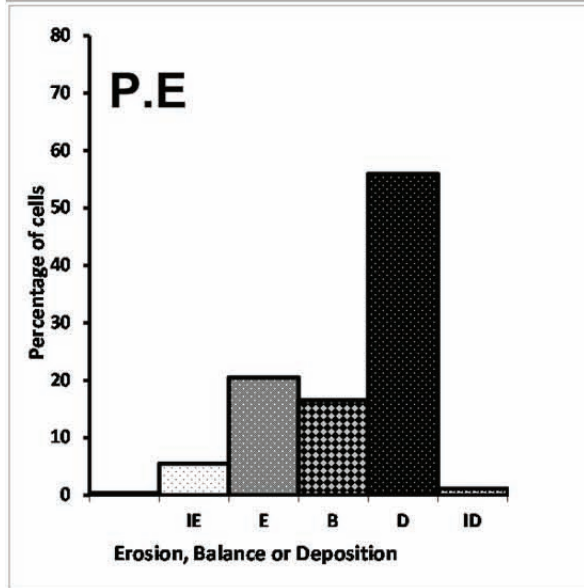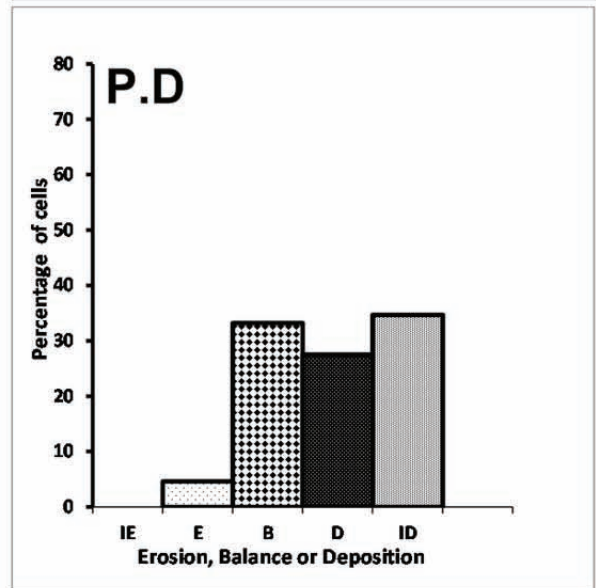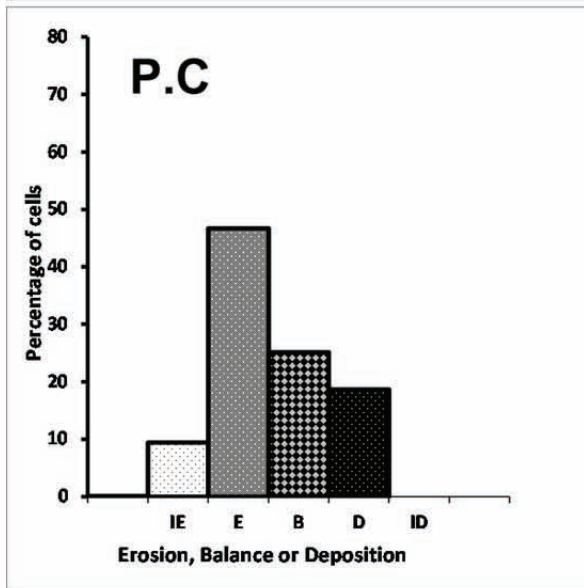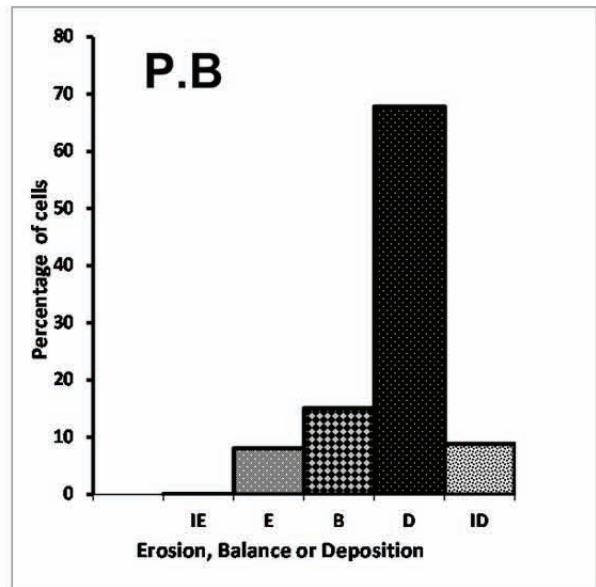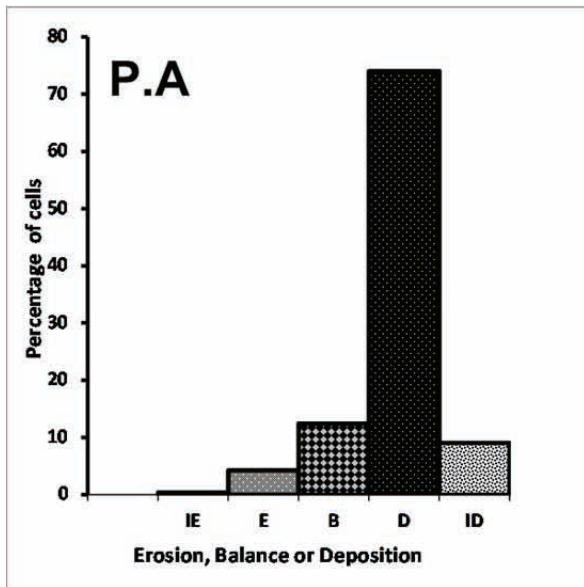
Figure 5.7. Percentage of cells (1 pixel is 4 cm x 1cm) with erosion, balance, or deposition along the tray for the average of three replications. Where IE, Intense erosion; E, Erosion; B, Balance; D, Deposition and ID, Intense deposition (per table 5.4)

Sediment transport between bare and vegetated land units

According to the theory of Fryrear et al. (1998), when sediment travels over a bare land unit, it is expected that the absolute maximum transport is reached after a certain distance under the condition that the field length is not limited. When crossing a border with vegetation, the theory states that deposition occurs until a new transport process is started. In fact the vegetation causes a decrease in sediment concentration downwind from the vegetation edge because it traps a significant amount of the moving sediment. Patterns P.A, P.B and run 2 for pattern P.D show results that are in agreement with this theory. A sediment-laden air flow reaches the border of vegetation, after which deposition occurs and at the end equilibrium is established. Although for patterns P.A. and P.B equilibrium was not fully reached, the trend clearly shows decreasing deposition. This result is also in agreement with the findings of Chen et al. (1995), Gash (1986), Irvine et al. (1997) and Wuyts et al. (2008) who reported that both the effect of vegetation on reducing wind speed and the trapping capacity of the vegetation increase inside the vegetated area from the upwind borders.

The results obtained with pattern P.C and run 3 of P.D are not in agreement with the theory. With the P.C pattern, sediment transport within the vegetated area is higher than within the bare area (Figure 5.8). And for pattern P.D, while in run 2 the pattern and percentage cover were sufficient to reach an equilibrium between erosion and deposition, in run 3 (higher average wind speed) more erosion occurred. Several previous studies have indicated that limited surface cover (5 - 7.5%) combined with a certain minimum wind speed can increase wind-blown mass fluxes (Raupach, 1990; Raupach, 1992; Raupach et al., 1993; Michels et al., 1995; Sterk et al., 1998; Maurer et al., 2009) due to the increased turbulence caused by the limited vegetation cover. The effect of the wind speed on the increased mass flux is illustrated in the difference between run 2 and 3 for pattern P.D. However, these studies did not mention the effect of the spatial distribution of the vegetative cover. Although the vegetative coverage was the same (11%) for all patterns, pattern P.C clearly showed an increase in mass transport, and with a higher average wind speed run 3 for pattern P.D also showed this increase in mass transport. These results lead to the conclusion that vegetation pattern is another factor that can cause an increase in the wind-blown mass flux, most probably due to an increase in turbulence. Therefore, in a region with a given cover, scattered patches of vegetation may exacerbate wind erosion especially under high wind speeds.

5.4.2 *Small-scale considerations*

Not only is regional scale investigation of the effect of vegetation pattern on general erosion or deposition important, investigation into the effects at small scales is also needed. In this study, none of the vegetation patterns protected the sediment surface sufficiently to completely halt wind-driven mass transport. The small-scale effects of vegetation found in this study are:

a) 'Street' effect: This effect refers to the formation of zones of erosion similar to streets. This effect was apparent in the P.A pattern where rows of vegetation were parallel to the wind direction. In their research, Bowker et al. (2008) reported similar 'streets' of erosion in the downwind direction between shrubs for several dust storms in the north Chihuahuan desert. This effect should be taken into account when designing re-vegetation projects. Thus, if the aim of the project is to prevent sediment from reaching a certain area, pattern P.B might be a more effective pattern than P.A. However, if the aim is to reduce sediment movement along the entire region, pattern P.A can be used. Therefore, taking into account the dominant wind direction, the vegetation pattern of rows of shrubs or trees may result in erosion zones similar to the shape of streets. This allows part of the sediment to reach the protected area, but the total sediment movement is reduced.
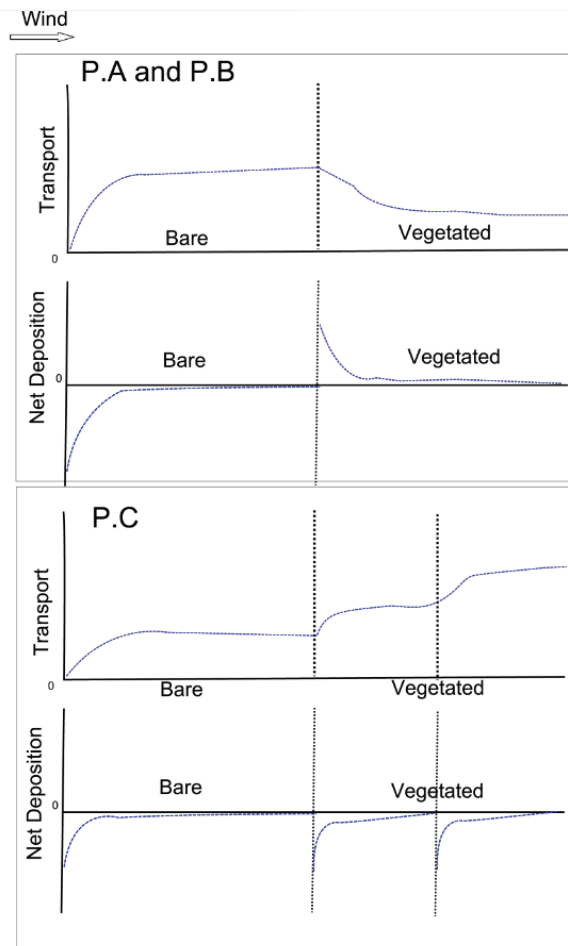
Figure 5.8. Transport and deposition scheme for bare and vegetated land units.

b) The spatial sequence of erosion and deposition. Although over all, patterns P.C and P.D are mainly associated with erosion, the transects shown in Figure 5.6 show that a spatial sequencing of erosion and deposition can occur – rather than just one or the other. Deposition can be linked to the redistribution of sand on both sides of vegetation 'elements' in the Y direction perpendicular to wind direction. This small-scale deposition is not clear and can be neglected when considering things at the regional scale. However, when the focus of the protection project is involves the effect of wind-blown mass flux at the micro-scale, these zones of erosion and deposition may carry specific importance.

c) Sheltering zone. The small sheltering zone of one land unit on a neighbouring land unit, i.e. the sheltering effect of wind breaks, has been determined by several studies to be 10 – 20 times the height of the vegetation (Skidmore and Hagen, 1977; Heisler and Dewalle, 1988; Cornelis and Gabriels, 2005). In this study, the size of protection zone shows that the shelter-effect of one land unit on a neighbouring land unit is similar to the effect of wind breaks. And thus, the findings of this study support these earlier findings. This can be seen clearly in the P.E pattern, where the height of vegetation used is 2.00-2.50 cm and the sheltered area is 20-25 cm (Figure 5.5). This explains why a zone of deposition was observed directly behind the border of vegetated area within the bare area in the P.E pattern (Figure 5.5).

5.4.3 Size of areas associated with erosion or deposition

Depending on the aim of the re-vegetation project, the size of the area with net erosion or net deposition should be considered. Especially when protecting settlements, the exact distribution of sediment can be very important. Our results from testing the four vegetation pattern scenarios show that patterns P.A, P.B and P.E are characterized by deposition, pattern P.C is characterized by erosion, and P.D is mainly characterized by a net balance.

The number of vegetation elements per area appears to play a role in the overall effect. The higher number of vegetation 'elements' in pattern P.C (18) compared to pattern P.B (32) resulted in a decrease in the percentage of cells with erosion from 56.3% in P.C to 8.2% in P.B. These results agree with Leenders et al. (2007) and Bowker et al. (2006; 2007) who concluded that, after wind events, deposition behind each individual vegetation element was observed. Thus, a higher number of vegetation elements results in a higher deposition rate. However our study also showed that an increase in the number of vegetation elements - from 12 in P.D to 18 in P.C – can result in an increase in the percentage of cells with erosion from 34.7% in P.D to around 56.2% in P.C. And this indicated that certain vegetation pattern caused an increase in the erosion rate comparing to other pattern although the % of surface covered with vegetation is identical for all patterns.

Moreover, the 'depositional with limited erosion' patterns (P.A and P.B) and 'erosional with limited deposition' pattern (P.C) is a significant finding and should be taken into account when deciding which vegetation pattern to use for re-vegetating degraded land.

The higher percentage of cells with erosion in pattern P.E (26.4%) compared to pattern P.A (5%), is an important indicator of border effects. Thus, in pattern P.E, the vegetated part of the tray faced the wind first and thus no incoming sediment was simulated, while in the P.A pattern the wind first blew over the bare area and then over the vegetated area. The differences in borders between the two scenarios resulted in huge differences in the size of areas associated with erosion and deposition.

5.5 Conclusion

Wind erosion is a critical environmental problem that threatens the human life in the arid (semi) arid regions. Vegetation cover is the key factor for protecting soil surface from erosive wind. In this study, a set of wind tunnel experiments was performed to investigate the effect of vegetation pattern on wind-blown sediment transport. A scale of 1:50 was used to represent *Atriplex halimus* shrubs. The main findings of this research were: (1) vegetation pattern has a significant effect on wind-blown mass transport, due to the effect of the vegetation on wind-flow turbulence ; (2) whereas the vegetation pattern of rows parallel to the dominant wind direction decreases the total mass transport in a region, it may not provide the required protection for areas of consideration; (3) in regions vulnerable to wind erosion, the effect of neighbouring land units includes the effect on wind speed and the regulation of sediment flowing from one land unit to the neighbouring land units. The current study has provided some insights on the behaviour of wind-blown sediment transport in both vegetated, bare land units and at the border between these units. But the results of the current paper are limited to simulated vegetation, to the size of sediment used and to the applied wind speed. And therefore, for deeper understanding of the effects of vegetation cover and patterns on wind-blown sediment transportation, we think further simulations should be conducted using:

- sediment from the regions where the simulated vegetation grows,
- different ranges of wind speed,
- additional variations of vegetation patterns as found in the areas where the vegetation grows.

Chapter 6

A new process-based regional scale wind erosion model (RS-WEQ): the effect of land cover patterns on wind erosion

A new process-based regional scale wind erosion model (RS-WEQ): the effect of land cover patterns on wind erosion

Abstract

Although wind erosion is a global scale problem, a calibrated and validated regional scale wind erosion model that represents soil transport by saltation does not exist, even though saltation is an important transport mode. Here, we propose model equations for saltation that can be used to represent wind erosion along a sequence of different arable fields in a region, taking into account mass fluxes across borders of arable fields. These equations were coded in Python resulting in the new 'Regional Scale Wind Erosion Equation' (RS-WEQ). Although the RWEQ model (Revised wind erosion equation) was the starting point for the development of this regional scale model, the current model is not restricted in its application to a single field. RS-WEQ predicts mass flux, soil loss and deposition for all land covers in a region, including the spatial pattern of these variables within arable fields. RS-WEQ was run using scenarios that represent main land covers in dry regions in general and in Khanasser valley, Syria specifically. Outputs of RS-WEQ showed that the wind speed, field length and land cover affect the region averaged mass flux, soil loss and deposition, and the intensity distribution of these variables inside the region. Specifically, the model results show that the region averaged mass flux and related abrasion risk increase with an increase in wind speed and field length. RS-WEQ also indicates that soil loss and deposition decrease with an increase in field length. As the model equations are relatively simple resulting in short run times even when run over large areas, the model has potential to be applied to map wind erosion over large areas, possibly up to continental scale when provided with remotely sensed data.

6.1   Introduction

Wind erosion is a serious environmental problem, especially in arid and semi-arid regions (Morgan, 2005; Shao, 2008; Sivakumar et al., 2005; Stroosnijder, 2005) and has potential negative effects on human health (Thomas and Turkelboom, 2008). Abrasion due to wind erosion damages crops and natural vegetation (Woodruff, 1956). Moreover, the amount of nutrients that can be lost as a result of wind erosion, mainly through saltation and suspension, declines soil productivity (McTainsh and Pitblado, 1987; Visser and Sterk, 2007; Visser et al., 2005c). The deposition of eroded sediment may cause crop burial (Csavina et al., 2010; Cuadros et al., 2010; Li et al., 2009; Qi et al., 2011; Wilson et al., 2011) and can block roads (Xue et al., 2008). Dust storms are the most obvious large-scale wind erosion process (Leslie and Speer, 2006) and they may cause large-scale disasters similar to what happened with the Dust Bowl in the USA in the 1930s which affected more than 400000 km^2 of land (Cook et al., 2008).

Researchers who studied the disaster of the Dust Bowl reported that the main causes of this catastrophic event were drought and intensive agriculture without adequate vegetation cover (Baveye et al., 2011; Romm, 2011). Vegetation cover is an important factor in the protection of soil against erosive winds (Burri et al., 2011; Sterk and Spaan, 1997; Van De Ven et al., 1989). Thus, a change in vegetation cover in an area that is vulnerable to wind erosion has direct impact on wind erosion. The effect of vegetation cover on the wind erosion process, with an emphasis on saltation, has been studied by a large number of researchers (i.e. Van De Ven et al., 1989; Hagen, 1996; Sterk and Spaan, 1997; Leenders et al., 2005; Visser et al., 2005c). In general, these studies concluded that vegetation has the potential to decrease soil loss due to wind erosion through the protection of the soil surface, the reduction of the wind speed, and the trapping of saltating particles. According to Leenders (2006), scattered natural vegetation can be effective in reducing large-scale wind-blown sediment transport. In agricultural regions, the wind erosion

problem is strongly linked to the land cover and land management (Fryrear et al., 1998). The amount of incoming and outgoing sediment into or from a field is interrelated with the surrounding area (Hupy, 2004; Leenders, 2006; Youssef et al., 2012b, chapter 5). As a region includes several different land covers, modelling the interrelation between neighbouring land units from the perspective of sediment transportation and deposition is required for better understanding and quantifying of wind erosion at the regional scale.

In the 1920s and 1930s, the soil conservation movement has been initiated in the USA (Morgan, 2005). From that time up to date myriad researches on soil erosion and soil conservation have been carried out in different parts in the world (Morgan, 2005). Part of these studies used models as a helpful tool for improving our understanding of the soil erosion processes (Campbell and Palmer, 2010). Wind erosion modelling started in 1965, with the development of the wind erosion equation (WEQ) (Woodruff and Siddoway, 1965). The WEQ and the majority of wind erosion models that have been developed later on (e.g., RWEQ, WEPS - Wind Erosion Prediction System) were calibrated and validated against data collected at relatively small scales (plot, field or village) (Fryrear et al., 1998; Hagen, 1991; Youssef et al., 2012a, chapter 4). These models use parameters representing climate, soil, roughness and vegetation to calculate the mass flux and soil loss from the simulated field. In field scale models, like RWEQ, the simulated field often has a non-eroding border (Fryrear et al., 1998). In the estimation of the mass flux and soil loss, these models assume that the non-eroding border isolates the field from the neighbouring areas and therefore the effect of the incoming and outgoing sediment into or from the simulated field are generally ignored. However, the intensity of wind-blown mass transport at a specific field is related to the land use in the surrounding fields (as noted above). Thus, the assumption of isolated fields does not hold when applying these field scale models at the regional scale. Furthermore, although sediment deposition has an obvious negative effect on plant growth and soil properties (Zou et al., 2007), the majority of wind erosion models (including RWEQ) do not take the deposition into account and they mainly focus on the negative effect of wind erosion due to abrasion and soil loss.

The improvement of remote sensing (RS) technology in the last few years has advanced large-scale wind erosion predictions (Lu and Shao, 2001; Pacheco et al., 2010; Yan et al., 2005). These attempts usually integrate modelling tools with dust cloud observations extracted from satellite images (Washington et al., 2003). Although these predictions provide an estimation of wind erosion at regional or even continental scales, they have a certain degree of uncertainty (Shao, 2008; Shao and Leslie, 1997). This is mainly because these approaches do not fully allow quantifying sediment transport by saltation, and instead they consider mainly the suspension process for model validation. Saltation however has the largest contribution to total soil loss and is the main process causing crop damage by abrasion (Sterk, 1997; Visser and Sterk, 2007). So, current approaches need to be extended with regional scale models that account for saltation and abrasion (Baker et al 2009).

Although wind erosion is a serious environmental problem, a regional-scale model that takes into account the saltation mode of the transport process as a central transport mode does not exist. In fact, the complexity of the wind erosion process and the interrelation between neighbouring land covers in a region makes the prediction of wind erosion at the large scale rather difficult (Zobeck et al., 2000). As the vegetation cover is one of the most important parameters in protecting the soil surface from the forces of the wind, a regional scale model is required that considers saltation, and represents transitions in vegetation cover. The objective of this paper is to progress the insight on the effect of land cover on the saltation flux at the regional scale. To reach this objective, we developed the new regional scale model RS-WEQ (Saltation Flux Regional Scale Model) that considers the saltation process, taking into account vegetation cover transitions between fields. We use this model to address the following questions: (1) What is the effect of vegetation cover and pattern and field length on mass flux, soil loss, and soil deposition? (2) In the framework of reducing wind erosion at regional scale, what is the optimal land use pattern and field length?

6.2 Material and methods

6.2.1 RWEQ Model

The RWEQ model was developed by Fryrear et al. (1998) for the estimation of soil loss from agricultural fields in the USA. The model calculates soil loss for an individual field, including the downwind trend in soil loss and sediment flux within the field (Fryrear et al., 1998). RWEQ calculates aeolian mass transport ($Q(x)$, kgm^{-1}) and soil loss ($S_{loss}(x)$, kg m^{-2}) at a distance (x, m) away from the upwind border with equation 6.1 and 6.2.

$$Q(x) = Q_{max}\left[1 - e^{-\left(\frac{x}{S}\right)^2}\right] \hspace{4cm} [6.1]$$

$$S_{loss}(x) = \frac{2.x}{S^2} Q_{max} e^{-\left(\frac{x}{S}\right)^2} \hspace{4cm} [6.2]$$

Where:
Q_{max} (kg m^{-1}) is the maximum transport capacity and
S (m) is the critical field length defined as the distance at which the 63% of the maximum transport capacity is reached.

In RWEQ, these are calculated according to equation 6.3 and 6.4.

$$Q_{max} = \beta 1.(W_F.E_F.S_{CF}.K_{tot}.C_{OG}) \hspace{3cm} [6.3]$$

$$S = \beta 2 \cdot (W_F \cdot E_F \cdot S_{CF} \cdot K_{tot} \cdot C_{OG})^{-\beta 3} \hspace{2.5cm} [6.4]$$

Where:
$\beta 1$, $\beta 2$ and $\beta 3$ are the model parameters,
W_F is the weather factor,
E_F is the erodible fraction,
S_{CF} is the crusting factor,
C_{OG} is the combined crop factor and
K_{tot} is a single roughness factor.

The reader is referred to Fryrear et al. (1998) or to Youssef et al 2012a (Chapter 4), for a detailed explanation of these factors.

6.2.2 Extensions to RWEQ for regional scale modelling

RWEQ simulates mass flux and soil loss over a single field assuming a non-eroding boundary at the upwind border of the field, which implies the incoming sediment flux is assumed zero. For regional scale modelling, cross-boundary fluxes need to be considered between a large set of fields. To represent this, we define a

one-dimensional model that simulates mass flux along a transect in downwind direction, with a set of n fields positioned at the transect. Mass flux is simulated for each field i, $i = 1, 2, .., n$, with a field length in the wind direction of l_i (m). The value of i increases in the wind direction, and the same calculations are done for each field, starting with field $i = 1$. The aim is to model the mass flux $Q_i(x_i)$, ($kg\ m^{-1}\ s^{-1}$), soil loss rate $SL_i(x_i)$ (t ha^{-1} yr^{-1}) and the deposition rate $D_i(x_i)$, (t ha^{-1} yr^{-1}) for each field i, with x_i the distance (m) from the upwind border of field i. Following RWEQ, we define a maximum transport capacity $Q_{max,i}$, for each field. When the incoming mass flux $Q_{i-1}(l_{i-1})$, which is the outgoing mass flux of the upwind field, is less than $Q_{max,i}$, the flux will increase in downwind distance and erosion occurs on field i, else deposition occurs. In the case of erosion, we assume the mass flux equation has the same form as equation 6.1 used by RWEQ, but modify it to account for an incoming mass flux at the upwind border by introducing a distance-to-border variable (z_i, m). In the case of deposition we assume a similar quadratic equation introducing a critical field length U_i for deposition, analogue with the critical field length used for erosion. The calculation of the mass flux at field i become:

$$Q_i(x_i) = \begin{cases} Q_{max,i}\left(1 - e^{-\left(\frac{x_i - z_i}{S_i}\right)^2}\right), & \text{for } Q_{i-1}(l_{i-1}) < Q_{max,i} \\ \left(Q_{i-1}(l_{i-1}) - Q_{max,i}\right)e^{-\left(\frac{x_i}{U_i}\right)^2} + Q_{max,i}, & \text{for } Q_{i-1}(l_{i-1}) \geq Q_{max,i} \end{cases} \quad \text{, for each } i \quad [6.5]$$

Where:
S_i (m) is the critical field length of field i.

In the case of ($Q_{i-1}(li-1) < Q_{max,i}$, z_i needs to be calculated. Given $Q_i(0)$ should equal $Q_{i-1}(l_{i-1})$ Equation 6.5 for the case with erosion can be solved for z_i:

$$z_i = -\sqrt{-s_i^2 \ln\left(1 - \frac{Q_{i-1}(l_{i-1})}{Q_{max,i}}\right)} \quad [6.6]$$

Deposition is calculated according to Skidmore (1986), assuming that the vegetation affects the wind speed over a distance of 15-20 times its height. The critical field length U_i for deposition used in the model is 15 m considering the average height of the natural vegetation and crops is around 0.90-1.00 m in a dry region. By differentiating Equation 6.5 we retrieve equations for deposition rate:

$$D_i(x_i) = \begin{cases} -\left(\frac{2z_i}{s_i^2} - \frac{2}{s_i^2}x_i\right)Q_{max,i}e^{-\left(\frac{x_i - z_i}{S_i}\right)^2}, & \text{for } Q_{i-1}(l_{i-1}) < Q_{max,i} \\ -\frac{2}{-U_i^2}x_i\left(Q_{i-1}(l_{i-1}) - Q_{max,i}\right)x_i e^{-\left(\frac{x_i}{D_i}\right)^2}, & \text{for } Q_{i-1}(l_{i-1}) \geq Q_{max,i} \end{cases} \quad \text{For each } i \quad [6.7]$$

Similar to RWEQ, RS-WEQ calculates the mass flux and soil loss of the simulated fields depending on the land cover (vegetation density and height) for each independent field, soil properties (texture and soil moisture) for each simulated field, surface conditions (mainly random roughness) for each simulated field and climate variables (wind, air density and solar radiation). In the current model, we do not model the change in the climate variables along the region. However, we consider the effect of one land unit on the neighbouring units by consideration of incoming or outgoing sediments. Here we run RS-WEQ for wind events with a duration of 6 hours, chosen because our calibration of the RWEQ model was done over the same time span (Youssef et al., 2012a, chapter 4), and we use calibrated RWEQ values in our model, (see section 6.2.3).

6.2.3 Scenarios for running the prepared model

To run the RS-WEQ model spatial-erodibility and weather parameters are needed (Equation 6.3 and 6.4). These were derived for a set of land use scenarios that are often found in (semi-) arid regions. In this research RS-WEQ was tested on bare fields, wheat fields and Atriplex fields. The parameters $\beta 1$, $\beta 2$ and $\beta 3$ have been recalculated for the RWEQ model calibration by Youssef et al. (2012a, chapter 4) as shown in table 6.1. These values were used in RS-WEQ also.

Table 6.1. The recently-calculated parameters for the RWEQ model.

Parameters	Original values (Fryrear et al., 1998)	Calibration results (Youssef et al., 2012a)
β1	109	109
B2	150.71	300
β2	0.3711	0.03

The Q_{max} and S parameters were calculated using Equation 6.3 and 6.4 and the field data reported in (Youssef et al ., 2012a, chapter 4) were used to obtain the value for each parameter (table 6.2).

Table 6.2. Parameters of the RWEQ model for bare, wheat and Atriplex fields.

Land use	E_F*	S_{CF}	K'	C_{OG}
Bare (B)	0.208	0.908	0.95	0.96
Wheat (W)	0.208	0.908	0.85	0.85
Atriplex (A)	0.208	0.908	0.90	0.65

* E_F is the erodible fraction, S_{CF} is the soil and crusting factor, C_{OG} is the combined crop factor and a K' is the single roughness factor

Parameters for weather factors were chosen for three main wind speeds, which simulate the wind speed that may cause sediment transport. Weather factors were created for wind speeds of 10, 12.5 and 15 m. Using the spatial-erodibility and weather parameters for each land use the Q_{max} and S were calculated (Youssef et al., 2012a, chapter 4). Table 6.3 shows the Q_{max} and S calculated for each simulated land use.

Table 6.3. Q_{max} and S for the simulated land covers.

Land use	W_{F1}=7.35		W_{F2}=20.68		W_{F3}=44.13	
	Q_{max} (Kg m^{-1})	S (m)	Q_{max} (Kg m^{-1})	S (m)	Q_{max} (m)	S (m)
Bare (B)	138.10	137.39	388.41	94.05	828.61	71.00
Wheat (W)	109.41	150.50	307.70	102.54	656.43	77.41
Atriplex (A)	88.58	162.77	249.14	110.89	531.51	83.71

Scenarios were defined with field lengths of 50, 150 and 450 m. These values were chosen since they represent field lengths that can be found in agricultural areas in general and especially in the region of Khanasser valley, Syria where the RWEQ model was recently calibrated and validated. Three main scenarios for field sequences (Table 6.3) were tested for each field length and for each wind speed. Therefore, all combinations of pattern, field length and wind speeds were run.

6.2.4 Criteria for evaluating model outputs

Mass flux

RS-WEQ results were evaluated using criteria for mass flux causing plant damage, and soil loss affecting the soil productivity. Baker (2007) and Baker et al. (2009), studied the effect of mass flux density on plant development using two main plant parameters; the net assimilation rate (NAR, $g\ m^{-2}\ Tu^{-1}$) and the relative growth rate (RGR, $g\ m^{-2}\ Tu^{-1}$) in which Tu is thermal units (°C) calculated according to equation 6.8.

$$Tu = (T_{\max} + T_{\min})/2 - T_b \hspace{5cm} [6.8]$$

Where:

T_{max} (°C) and T_{min} (°C) are the maximum and minimum daily air temperatures respectively, and

T_b (°C) is the base temperature considered by Baker et al. (2009) to be 15.5 °C

The study showed that both *NAR* and *RGR* decreased linearly with an increase in mass flux. Based on this study, we identify three classes of abrasion (due to mass flux) associated with increasing degrees of plant damage. These classes are: *low*, representing a mass flux causing shrinkage of leafs compared to untreated plants, *moderate*, causing plants to be shorter and having a more shrubby shape compared to untreated plants, and *high*, in which the mass flux fully destroys plant leafs resulting in a bare stem without obvious leafs (Baker et al., 2009). Table 6.4 provides an overview of the three abrasion classes and the related fluxes. The flux application in the experiments of Baker (2007) and Baker et al. (2009) ranged from 10-40 minutes. The mentioned experiments were executed in a wind tunnel, where a continuous flux over bare sand was applied. As already mentioned, in this research we use the RS-WEQ model with a wind event duration of 6 hours. We assume here, that the damage in the wind tunnel experiments from 10-40 minutes is comparable to the damage of 6 hours in real field conditions (represented by our model). Of course this is a somewhat arbitrary assumption, but better data, in particular field data, on damage by mass flux are currently not available. The identified classes were used to evaluate RS-WEQ output on abrasion damage to plants.

Table 6.4. Classes of plant damage due to sediment mass flux. After Baker (2007).

Flux range (kg m^{-1} s^{-1})	*NAR* (g m^{-2} Tu^{-1})	*RGR* (g m^{-2} Tu^{-1})	Flux class
0-0.015	0.760-0.772	6.75-6.86	*Low*
0.015-0.03	0.772-0.785	6.86-6.98	*Moderate*
0.03-0.045	0.785-0.797	6.98-7.10	*High*

* *Tu*: is thermal units (°C)

Soil loss

Data for classification of soil loss due to wind erosion are rather sparse. Klik et al. (2004), showed that soil loss in Austria ranges from 0.0-5.4 t ha^{-1} yr^{-1}. Cornelis et al. (2010) showed that the annual actual soil loss in Flanders, Belgium ranges from 0-40.9 t ha^{-1} yr^{-1} with an average of 0.9 t ha^{-1} yr^{-1}. Bilbro and Fryrear (1985) evaluated soil loss due to wind erosion for six crops in the USA and they found that the soil loss ranged from 12 t ha^{-1} yr^{-1} with "kafir" crop to 83 t ha^{-1} yr^{-1} with cotton (Bilbro and Fryrear, 1985). Gupta and Rama (1996) studied the soil loss due to wind erosion in the arid regions in India and they reported that soil loss due to strong wind in the arid conditions can exceed 5400 t ha^{-1} yr^{-1} (Gupta and Rama, 1996). The focus of this research is on (semi) arid regions with a low population density, a small supply of nutrients through fertilizing, and low-income levels of local farmers. With this assumption the soil loss has a critical impact on soil productivity and thus, the tolerance of soil loss should be low. The soil loss classes were identified as low, which corresponds to deposition values of 0 up to -5 t ha^{-1} yr^{-1}, where negative values indicate soil loss; moderate, corresponding to -5 up to -50 t ha^{-1} yr^{-1}; and high, corresponding to values below -50 t ha^{-1} yr^{-1}. Ranges are given by negative values as in our model negative deposition values refer to soil loss. As the deposition is not considered seriously by previous wind erosion models and studies, details on the quantity and severity of deposition are not available. Therefore, we consider in this study the deposition and soil loss to have comparable absolute values and thus we identified the deposition classes as: low 0-5, moderate 5-50, and high > 50 t ha^{-1} yr^{-1}

In an analysis of meteorological data for the region of Khanasser valley (as an example of Mediterranean dry regions) it was found that the duration of wind speed above 10 m s^{-1} is about 12-15 hours per year, for a wind speed above 12.5 m s^{-1} it is about 10 hours per year, and wind speeds above 15 m s^{-1} occur for less than 2 hours per year (Youssef et al., 2012a, chapter 4). Thus, to generate annual wind erosion, RS-WEQ was run for a period of 6 hours for all scenarios, assuming two of such wind events per year in the conversion of RS-WEQ output in kg m^{-2} 6^{-1} hours to kg m^{-2} yr^1. Soil loss and deposition (t ha^{-1} yr^{-1}) were calculated along the modelled transect. To avoid a border effect at the border of the region (no-incoming sediment) the first 450 m in upwind section of the transect was excluded from model output analyses. Sediment fluxes and soil deposition and loss were calculated for each 1 m cell along the transect. The region averaged soil loss was calculated according to equation 6.9.

$$E_{Sloss} = \frac{TE}{N_{tot}}$$

[6.9]

Where:

E_{Sloss} is the average soil loss in t ha^{-1} yr^{-1},

TE (t ha^{-1} yr^{-1}) is the sum of deposition values (Equation 6.7) of all cells along the transect, summing cells with negative values (i.e., erosion) only,

N_{tot}: total number of cells along the transect.

Note that region averaged soil deposition is the same as region averaged soil loss.

The percentage of cells associated with each class (low, moderate or severe) of erosion along the measurement distance was calculated according to equation 6.10.

$$P_d = 100 \left(\frac{N_d}{N_{tot}} \right)$$

[6.10]

Where:

P_d is the percentage of cells associated with erosion in class d,

N_d is the number of cells associated with erosion under class d.

The same procedure was followed to calculate the percentage of cells associated with deposition along the transect.

6.3 Results

6.3.1 Comparison between RWEQ and RS-WEQ

Figure 6.1 compares the prediction of mass flux using RWEQ and RS-WEQ. The figure shows a simulation with a sequence of bare (B), Atriplex (A) and wheat (W) land covers. It is shown that RWEQ predicts the mass flux for each land cover with the assumption of the existence of the non-erodible border at the edge of the simulated field from the upwind direction. However, RS-WEQ takes border effects into account, resulting in non-zero mass fluxes at borders of fields. Furthermore, RS-WEQ simulates both erosion and deposition. In the bare field, mass flux increases with downwind distance and erosion occurs. In the Atriplex field mass flux decreases with distance, because the Q_{max} of Atriplex is lower than the incoming flux of the field from the bare soil. This reduction in flux with distance results in deposition of soil material in the Atriplex field. In the wheat field the mass flux increases, because the Q_{max} of the wheat field is higher than its incoming flux.
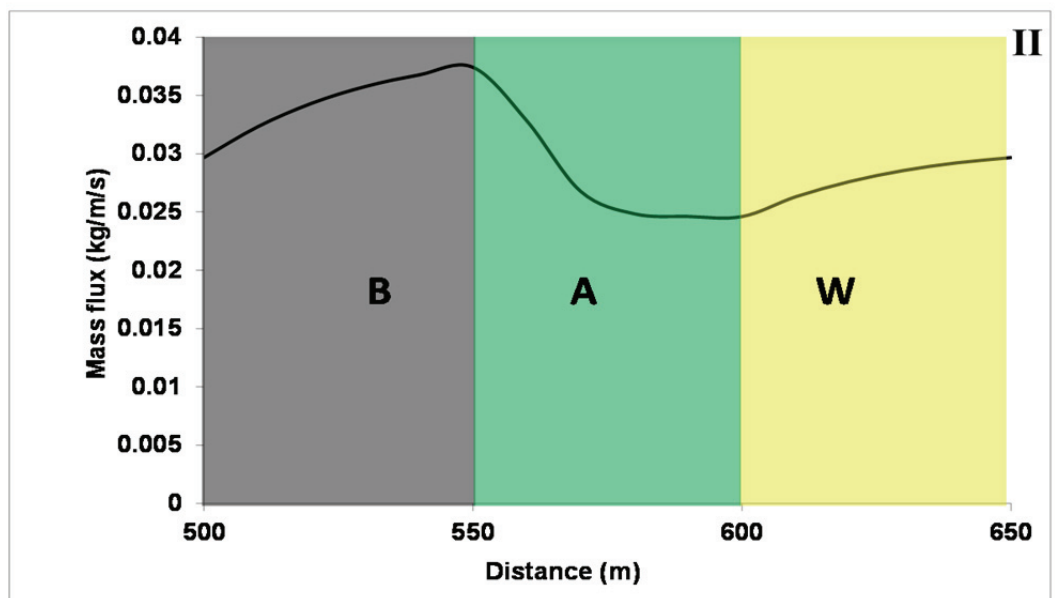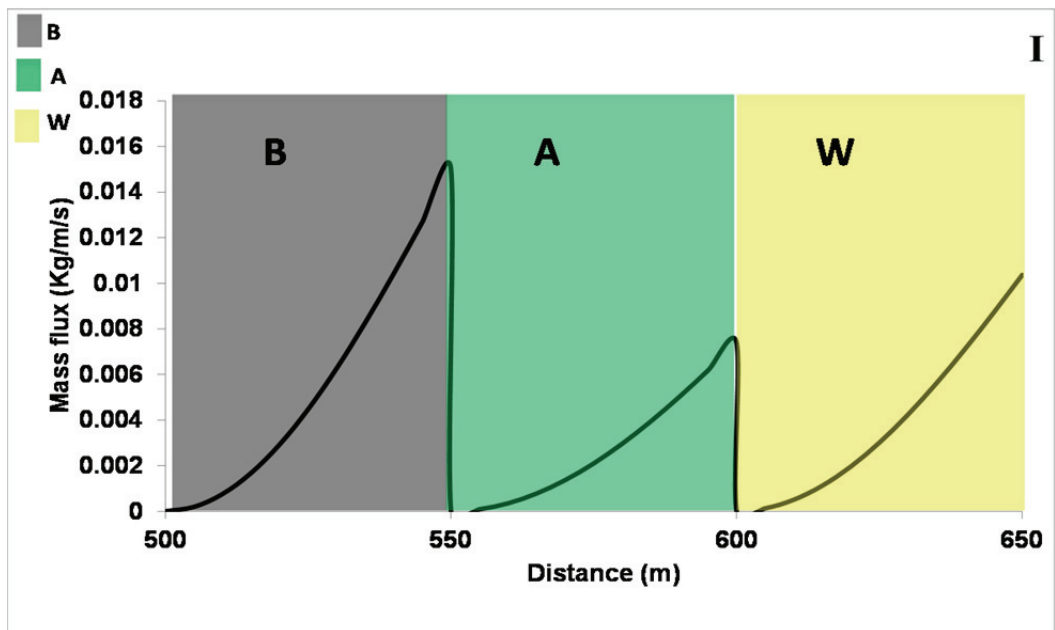
Figure 6.1. I: RWEQ model predictions for the aeolian mass flux for the neighbouring land units of bare (B), Atriplex (A) and wheat (W). II: RS-WEQ predictions for the mass flux taking for B, A and W.
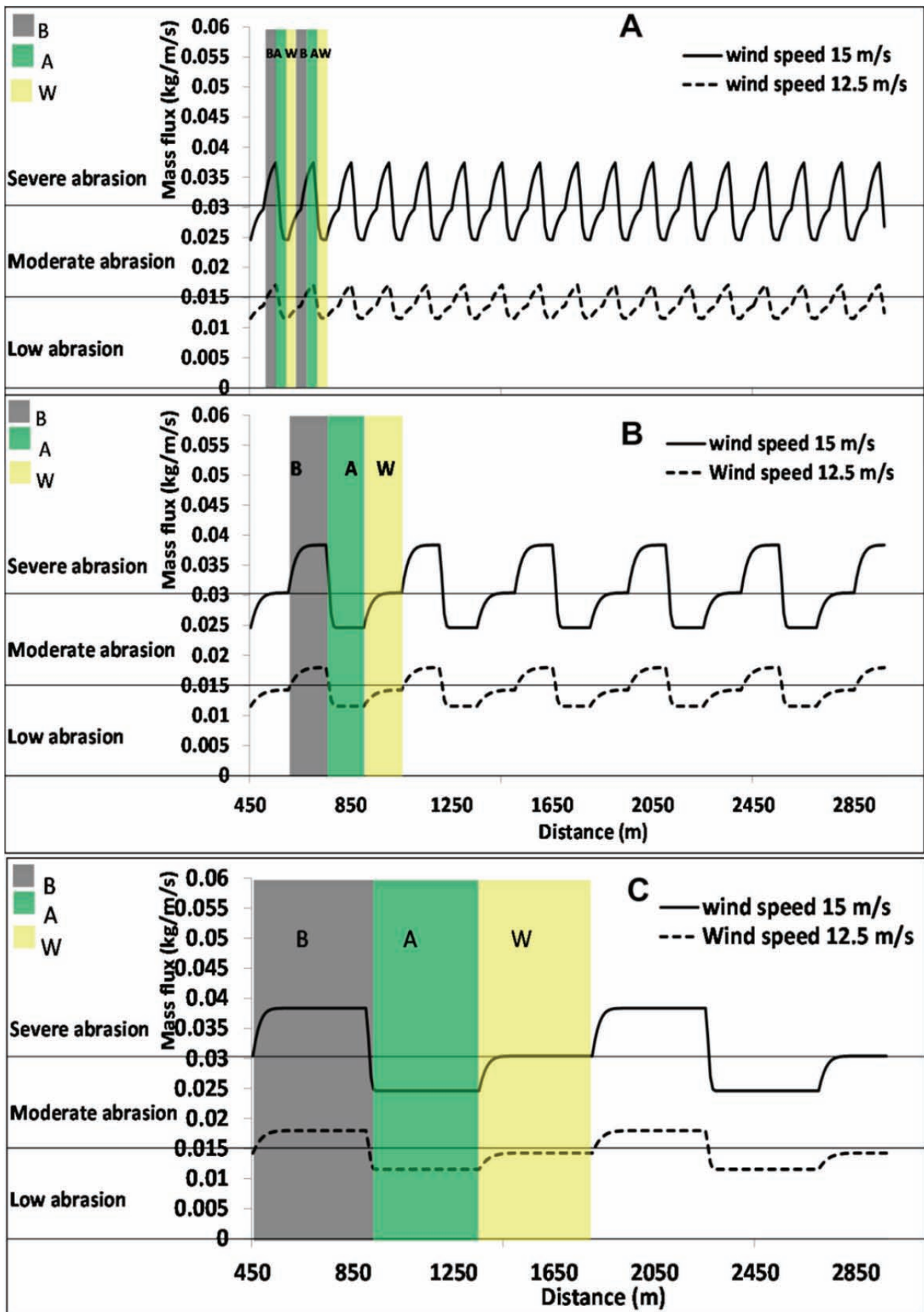
Figure 6.2. Mass flux and abrasion classes with wind speeds of 12.5 m s^{-1} 15 m s^{-1}. A: field lengths of 50 m, B: field lengths of 150 m and C: field lengths of 450 m. B, A, W stand for bare, Atriplex and wheat respectively.

6.3.2 Mass flux and abrasion

For all boundary conditions of incoming fluxes at the upwind border of the region, the wind-blown mass flux reaches a steady-state, repetitive, pattern within a few hundred meters of the border of the region. So, for large regions, edge effects at the border of a region occur on a small proportion of the region and will thus have a small contribution to the total wind erosion in region. So, we focus here on mass fluxes outside the area undergoing edge effects, which occur in by far the largest part of a region. As shown for the BAW scenario in Figure 6.2, which is regarding the pattern in mass flux representative for the other scenarios, the wind-blown mass flux varies considerably in downwind direction. At a field length of 150 or 450 m fluxes almost reach the maximum transport capacity for all fields. At 50 m field length the maximum fetch is too small to completely reach the maximum transport capacity, but variation of mass fluxes in downwind direction is still considerable.

Due to the large spatial variation in mass flux, a single wind speed mostly results in mass flux values that fall in two different abrasion classes at different positions along the transect. This is the case for the BAW scenario at a wind speed of 12.5 and 15 m s^{-1} (Figure 6.2) and for most other scenarios at these wind speeds. In addition to this spatial variation in abrasion, a large variation in abrasion between wind events may occur. For example, whereas the mass flux values fall in the low and moderate abrasion classes with a wind speed of 12.5 m s^{-1}, moderate or severe abrasion may occur at a wind speed of 15 m s^{-1}, as shown in Figure 6.2. The figure also shows that the field length has effect on the mass flux, but this effect is not large enough to cause a change in abrasion classes. For example, at a wind speed of 15 m s^{-1} abrasion was moderate or high at all field lengths considered.

The mass flux averaged over a region changes with vegetation pattern and field length. The effect of these properties on mass flux is however small compared to the relatively large changes in region averaged mass flux when the wind speed is changed. Figure 6.3 shows that the differences in mass flux between the WB, BWA and WBA scenarios are small. Average values of the BW pattern are somewhat higher than those of BWA and WBA, which can be explained by the occurrence of Atriplex fields in the BWA and WBA scenarios, having a lower maximum mass flux. It is also shown that the difference in the order of the land cover types may have negligible effect; the region averaged mass fluxes of the BWA and WBA pattern are almost identical. Although field length has a relatively small effect, the average mass flux values increase with increasing field lengths, particularly at short field lengths; the increase in the mean mass flux values due to the increase in field length from 50 m to 150 m is around 3-5 times the increase in mass flux due to the increase in field length from 150 m to 450 m (Figure 6.3).

As abrasion is a significant factor affecting plant growth in wind erosion regions (Baker et al 2009), details on the severity of abrasion due to wind-blown mass flux and the effect of land use patterns on it is needed. Figure 6.4 shows the proportion of the region that falls in the abrasion classes low, moderate, and high, respectively. The relative effects of land cover pattern, field length, and wind speed is comparable to those found for the region averaged mass flux. Atriplex in the BWA and WBA scenarios reduces the proportion of the higher abrasion classes compared to the BW scenario. The effect of field length is small. In most situations, longer fields result in a somewhat larger proportion of the higher abrasion damage class (WBA scenario, 15 m s^{-1} wind speed), which is expected considering that region averaged erosion increases with field length. In some situations, however, the higher abrasion class may decrease in proportion even while region averaged flux increases with field length. This is the case for the BW scenario, 12.5 m s^{-1} wind speed, and is explained by a shift in the intensity of the flux within the classes. By far the largest effect on abrasion intensity has wind speed. An increase in wind speed from 10 m s^{-1} to 15 m s^{-1} results in a shift from low abrasion to moderate or high abrasion for all land cover patterns and field lengths.
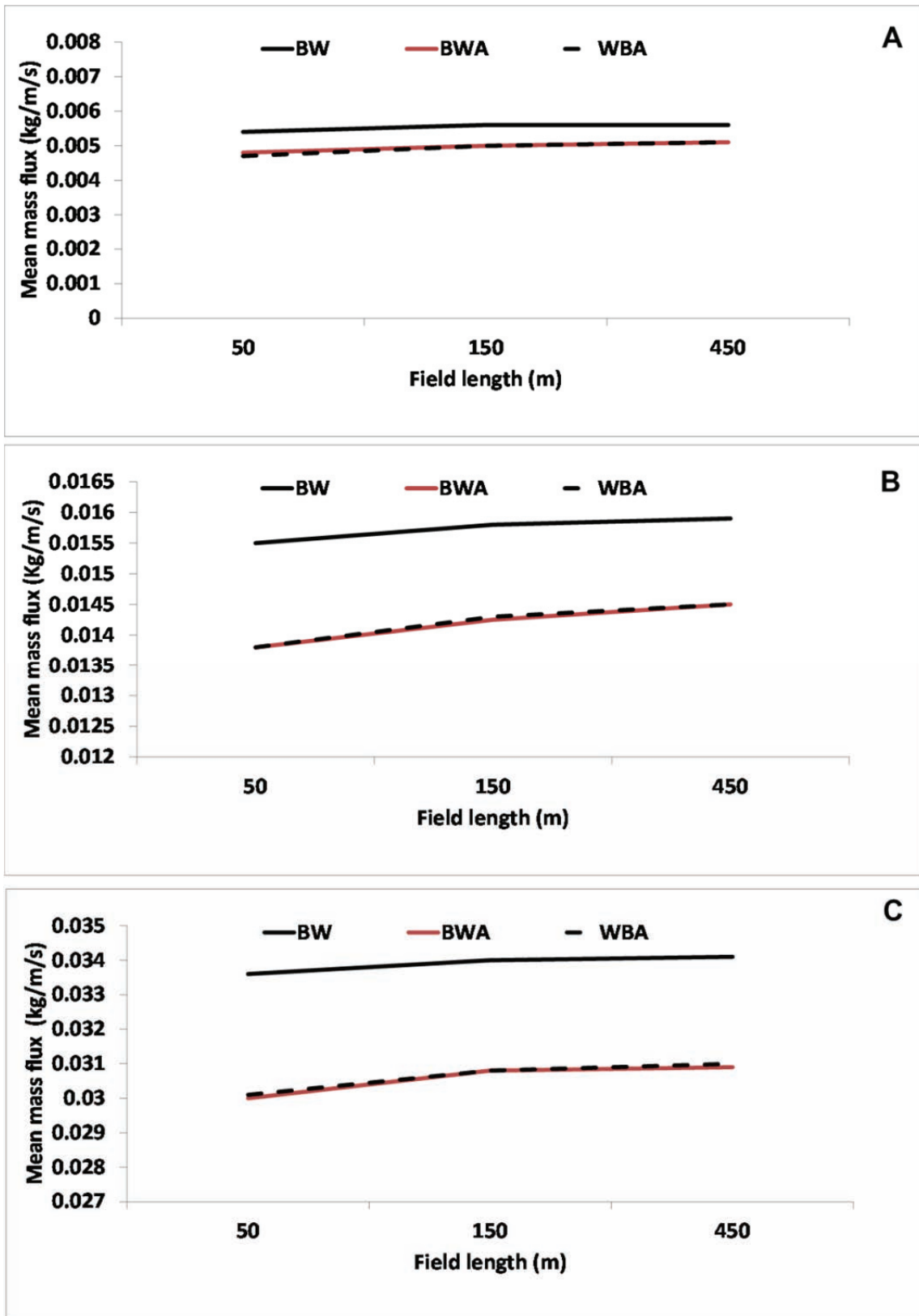
Figure 6.3. Mean mass fluxes (abrasion) for scenarios WB, BWA, and WBA, for the field lengths of 50 m, 150. A: wind speed 10 m s^{-1}, B: wind speed 12.5 m s^{-1} and C: wind speed 15 m s^{-1}.
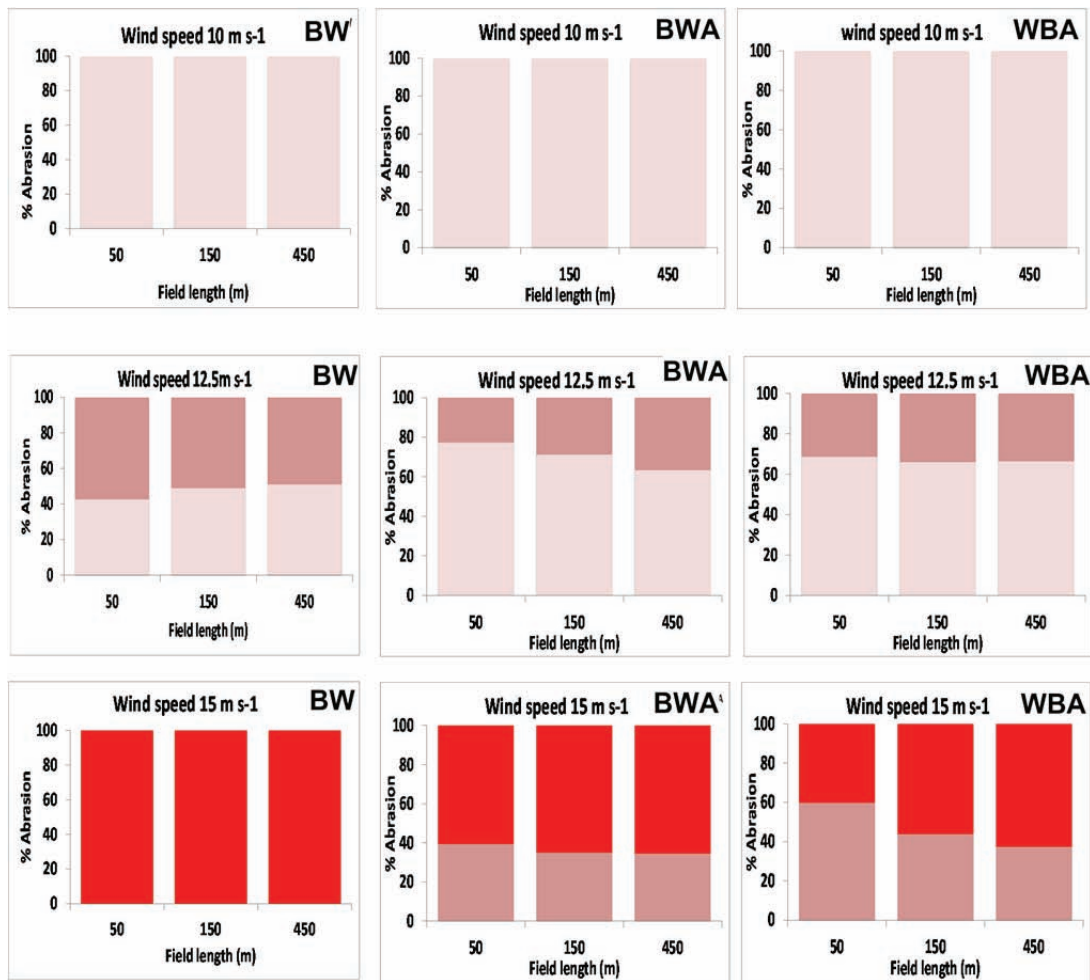
Figure 6.4. The percentage of the region falling in the abrasion classes high, moderate and low for all scenarios and wind speeds.

As mentioned in the methods section, a wind flux in the low abrasion class causes shrinking plant leafs, moderate abrasion causes smaller plants and reduced production and with high abrasion plant leaves will be completely destroyed (Baker et al., 2009). Applying these criteria to our results indicates that at a wind speed of 10 m s^{-1}, damage due to abrasion is limited to shrinking leafs for all scenarios. At a wind speed of 12.5 m s^{-1} all scenarios cause comparable damage to the plant ranging from low to moderate. At a wind speed of 15 m s^{-1}, damage for scenario BW is critical and biomass production will be minimal. For scenario BWA and WBA the damage ranges from moderate to high and thus, quite low production is expected from these scenarios under this wind speed.

6.3.3 Erosion and deposition

Although region averaged soil loss and deposition is by definition the same, Figure 6.5 shows that deposition occurs over a smaller proportion of the region than erosion, and where deposition occurs, it generally occurs at a higher rate than erosion. Wind speed has a large influence on erosion and deposition, and peak values approximately double when wind speed is increased from 12.5 m s^{-1} to 15 m s^{-1} (Figure 6.5). As peaks in erosion or deposition occur directly at the upwind border of fields, field length has no effect on the range of erosion and deposition values occurring in the region. However, on average, erosion or deposition decreases with field length. This is due to the fact that most erosion or deposition occurs close to the upwind border of fields, and thus, at larger field lengths, relatively large areas undergo negligible erosion or deposition, as is the case at a field length of 150 m (Figure 6.5).
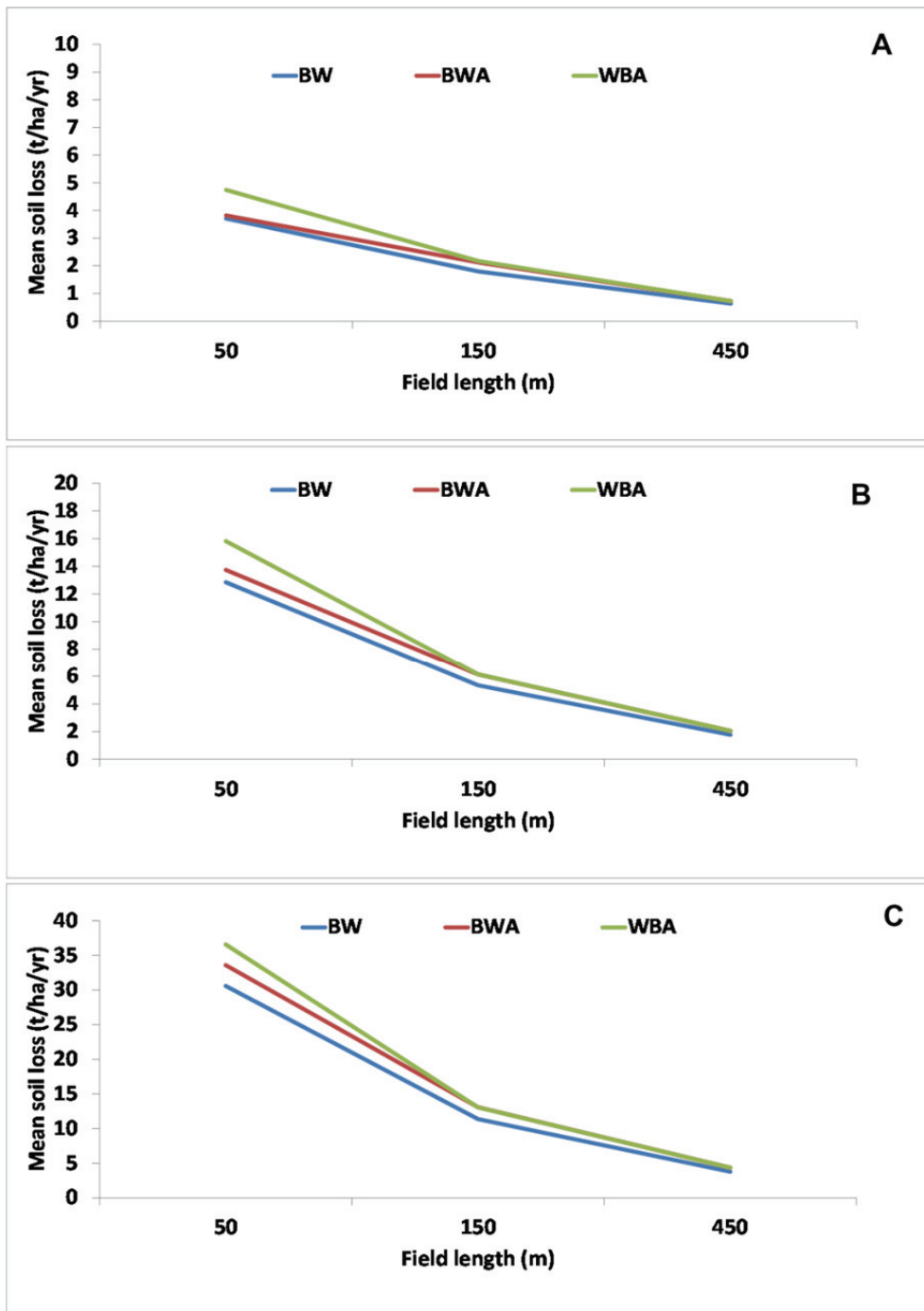
Figure 6.6 Region averaged soil loss for scenarios BW, BWA, and WBA, for field lengths of 50 m, 150 m and 450 m. A: wind speed 10 m s⁻¹, B: wind speed 10 m s⁻¹ and C: wind speed 10 m s⁻¹. Note that region averaged deposition is equal to region averaged soil loss.
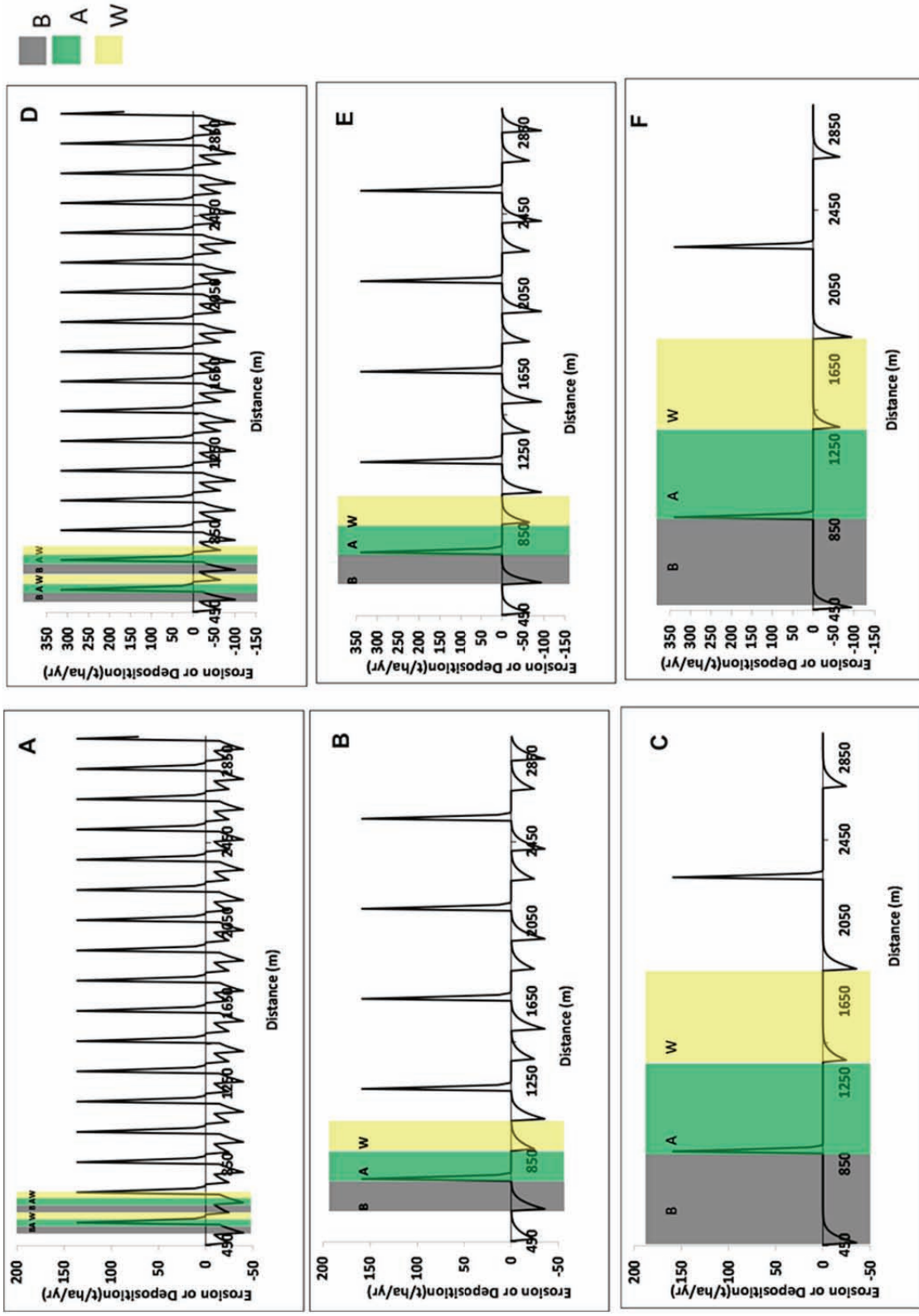
Figure 6.5. Soil loss and deposition for the scenario WBA for field lengths of 50 m, 150, and 450 m, with a wind speed of 12.5 m s⁻¹ (A, B and C) and 15 m s⁻¹ (D, E and F). Positive values indicate deposition, negative values erosion.

This negative relation between field length and soil loss (erosion) is clearly shown by the region averaged erosion values in Figure 6.6. Average erosion at a field length of 50 m is 4-8 times higher than the value at a field length of 450 m, and the largest effect of field length occurs at high wind speeds. Note again, that the same holds for region-averaged deposition, as this is equal to region averaged erosion. In addition, Figure 6.6 shows that the mean values of soil loss and deposition increase with increasing wind speed, which is expected because the capacity of winds to erode and carry sediment increases with wind speed. Compared to the effect of field length and wind speed, the land cover pattern has a small effect on soil loss and deposition. The BW pattern is associated with slightly lower region averaged values compared to the scenarios that include Atriplex.

Figure 6.7 provides the proportion of the region that falls in the erosion and deposition intensity classes, respectively. For the runs shown, the proportion of the region that undergoes erosion (i.e., all shades of red in the figure) is between 30 and 70%. Variation in this value mainly occurs between land cover patterns, where the BWA pattern has the smallest proportion with erosion, approximately 30% of the region. For each land cover pattern, the proportion of the region with erosion is relatively constant with field length and wind speed.

As high erosion or deposition values are particularly important for soil productivity and plant growth, the distribution of the intensity of erosion carries specific importance. For erosion, the intensity increases with wind speed and decreases with field length, as shown in Figure 6.7. Furthermore, the effect of land use pattern can be seen by the lower proportion of high erosion values with the BW pattern compared to the patterns that include Atriplex. The results regarding the deposition show trends that are comparable to those of erosion.

To sum up, average erosion increases mainly with field length and wind speed, which is caused not so much by an increase in the relative area with erosion, but by an increase in the intensity of erosion within the area with erosion. The land cover pattern may have an effect on the distribution of erosion over the different intensity classes, as shown in Figure 6.7, but the region-averaged erosion is hardly affected by the land cover pattern.

6.4   Discussion and conclusions

In this study, we developed a regional scale model (RS-WEQ) that considers saltation as the main transport mode, represents erosion and deposition over a pattern of arable fields, and takes the interrelation between neighbouring land units into account. Scenarios representing land covers occurring in a region with a dry climate were used to run RS-WEQ. Unlike many other field models, our model is capable of representing wind erosion over a sequence of fields, taking into account mass fluxes across the border of fields. This results in a completely different pattern of mass fluxes (and erosion) compared to models that assume closed borders, as was shown by our comparison with RWEQ (Figure 6.1). The new model indicates that for regional scale wind erosion modelling it is essential to represent sediment fluxes over field borders. In addition, our model indicates that the mass flux, soil loss and deposition in a region are affected by the field length, vegetation cover, land use pattern, and wind speed. More specifically, an increase in wind speed and field length results in an increase in the mean mass flux and related abrasion risk. Also, an increase in field length results in a decrease in the quantity of soil loss and deposition. Furthermore, it was shown that with a wind speed of 15 m s^{-1} the area associated with a high soil loss is larger for series of short fields than with a series of long fields.
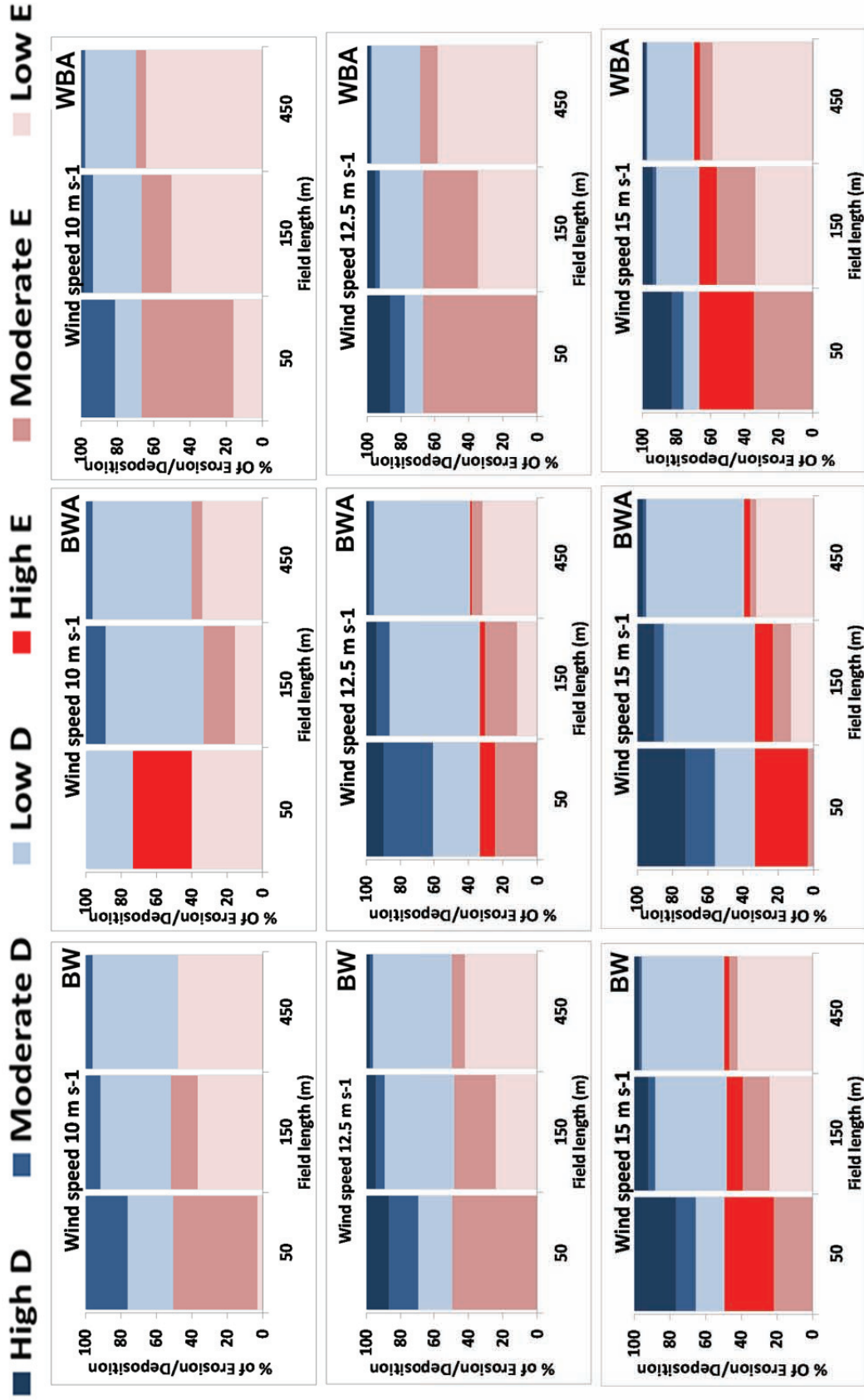
Figure 6.7. The percentage of the region falling in each of the severity classes of erosion and deposition for all scenarios and all wind speeds for the field lengths of 50 m, 150 m and 450 m. In the figure the red colour represents the erosion and the blue colour represents the deposition

RS-WEQ provides an estimation of the mean mass flux in a region. Results show that this value changes with wind speed and field length. Specifically, it is shown that a 2.5 m s^{-1}increase in wind speed (from 12.5 to 15 m s^{-1}) resulted in an increase in the mean flux of around 210%. Previous experimental studies showed that the increase in wind speed resulted in an increase in the damage of plants due to abrasion (Armbrust and Retta, 2000; Woodruff, 1956). RS-WEQ also showed that an increase in field length results in an increase in plant damage due to abrasion. Therefore, long fields may have a lower productivity compared to short fields. Some previous studies (Fryrear and Saleh, 1996; Skidmore, 1986; Skidmore and Hagen, 1977; Tibke, 1988) on the effect of field length on mass flux and abrasion reported results that are comparable with those found here. These studies focused mainly on the use of windbreaks (shrubs and trees) to shorten field lengths and they found that the reduction in flux and abrasion is due to the reduction in wind speed. The reduction of field length through "strip farming" in which cultivated (cropped) and fallow land covers are alternated has been found to be an effective method to decrease the mass flux and abrasion in regions vulnerable to wind erosion (Bravo and Silenzi, 2002; Chepil, 1957). Specifically, results of the current study show that the increase in field length from 50 m to 150 m results in a 100 – 140% increase in the proportion of the area with plant damage in the severe class, depending on wind speed and vegetation cover. Gregory et al. (1990) used field sampling to show that the increase in field length from 100 m to 500 m resulted in an increase in the mass flux from 100 kg m^{-1} to 225 kg m^{-1} (225% increase). The results of the two studies are comparable as both of them showed comparable numbers for the rates of the increase in mass flux due to the increase in field length. In addition to the effect of wind speed and field length, the current study showed that the land use pattern is another factor that affects the rate of mass flux and abrasion. However, its effect is relatively small (Figure 6.4). Thus, while the current study showed results that are in the agreement with some previous studies, it provided further details on the effect of field length on abrasion at a region that may have several neighbouring land covers.

The results of soil loss and deposition agree with the results of Gregory et al. (1990) who reported an increase in soil loss from approximately 200 t ha^{-1} to around 450 t ha^{-1} with a decrease in field length from 180 m to 60 m (Gregory et al., 1990). This increase of 225% is comparable to the increase in erosion between field lengths of 150 and 50 m observed here, which was between 90 and 265% depending on wind speed and vegetation cover, as calculated from Figure 6.7.

Our model considers the process of sediment transport in the wind direction (mainly by saltation), and ignores the process in which sediment transport perpendicular to the wind direction (mainly by suspension). It also ignores the creep process in which a small part of sediment is moving. By neglecting these two processes, we underestimate regional scale erosion, as 20-35% of total transport can be through creep or suspension (Sivakumar et al., 2005). It should be possible, however, to add model components for these transport modes in future studies. Furthermore, our model considers wind speed to be constant along the transect, not taking into account possible changes in wind speed as a function of land cover. Ley et al. (2009) provided a method to adjust wind speed according to each land cover in a region. In RS-WEQ we assume that the threshold velocity is a function of the percentage of vegetation cover as shown in Youssef et al. (2012a, chapter 4) and thus the model considers the change in wind factor with the change in land cover. However, adding the method of Ley et al. (2009) to the current model will improve the model prediction.

Finally, RS-WEQ uses the parameters of the calibrated and validated field scale model of RWEQ and proposed that these parameters are valid in the regional scale model and that opens a question about the validity of these parameters for the regional scale.

Future application of our model to regional scale modelling could be done along various lines. One is an approach where scenarios of land cover pattern are defined in a similar style as was done in this study. Since focus in this study was on showing general relationships between land use pattern and erosion, we defined scenarios that assumed many properties to be uniform in space, for instance field length, while

only three different land use types were considered. Any combination of land use types and field lengths can be defined however in RS-WEQ, which allows to model typical land use patterns occurring in a region in order to quantify wind erosion, or evaluation of different possible land use pattern scenarios, in order to design optimal land management strategies.

In addition, the modelling approach presented here could be used to map variation in wind erosion intensity at regional to continental scales, although this would need additional methodology. To keep the modelling computationally tractable, mapping at continental scales would require a resolution between 10-100 km^2, for instance using grid cells of this size. At this resolution, our model could be run for each grid cell independently, calculating mean soil loss and mass flux over the grid cell, using the typical land use pattern occurring within the grid cell, or a probability distribution of land use patterns occurring in the grid cell. This approach would require high-resolution land use maps to extract land use pattern data for different wind directions, which is nowadays possible using remotely sensed information, and distributed information on wind climate. Another approach for mapping is converting our model to a fully distributed two-dimensional simulation model, as was done for RWEQ (Fryrear et al., 1998). This would be possible without changing the model equations of the model, by simulating mass flux at transects positioned over the modelling area in the direction of the wind. To properly solve the model equations this would require a model resolution of 4 x 4 m^2 or less (grid size), which poses constraints on the extent of the area simulated. Given the simplicity of the model equations used, however, we expect it would be feasible to run such a model for areas of up to 200 km^2 with acceptable run times on a desktop computer.

Chapter 7

Synthesis

Synthesis

Wind erosion is a serious environmental problem in the (semi-) arid regions of the earth. Wind erosion reduces soil productivity due to nutrient losses, causes damage to crops, reduces agricultural production, and has negative effects on human health and society. Vegetation is one of the most important factors in the protection of the soil surface against erosive winds and it is the key element of any protection activity. Vegetation has the potential to decrease soil loss due to wind erosion through: the protection of the soil surface, the reduction of the wind speed and the trapping of saltation particles. In wind erosion regions, land use with a certain vegetation cover at one land unit may have a significant effect on the quantity and intensity of the wind erosion process at its neighbouring land units. Thus, the amount of incoming and outgoing sediment into or from a field is interrelated with the surrounding area. Insight in this interrelation is required for better understanding of wind erosion at the regional scale. Therefore the aim of this thesis is to improve our insight in the effect of vegetation and vegetation transitions on regional scale wind erosion.

In theory, wind erosion models can provide insights in the impact of wind erosion at a regional scale. But the current generation of wind erosion models cannot yet provide the required insights, because the models are either developed for application on a small spatial scale or have a relatively high level of uncertainty. Small scale models (e.g. the field scale) provide precise insight in the wind erosion process at a relatively small area that has a uniform land cover but do not show the process of wind erosion at different land covers, nor provide insight on the interaction between neighbouring fields in a region. This scale problem is the main problem for the models on scales such as field ($10-10^4$ m^2) or village (10^4-10^8 m^2).

For policy makers, information on wind erosion at the regional scale (> 20-25 km^2) is required to take steps through which they can reduce the negative socioeconomic effects of wind erosion in vulnerable regions. And this knowledge will be important for designing the land use for sustainable natural resources and environment. Uncertainty is the main problem with large scale models (>20-25 km^2). The relatively high uncertainty of these models can be partially linked to the fact that they mainly consider suspension, and no saltation, as a central transport process and that observations of dust storms from space (remote sensing technology) are used to calibrate and validate these models (Shao et al., 2002). These observations are not based on direct measurement of actual (saltation) fluxes. Consequently, although wind erosion is a serious environmental problem, a validated regional-scale model that takes into account the saltation mode of the transport process is not available. As the vegetation cover is one of the most important parameters in protecting the soil surface, a calibrated and validated model that takes into account the transitions in vegetation cover and can predict the effect of vegetation cover on wind erosion will be a useful tool to explore measures for more sustainable land use.

To provide data for calibration and validation of a regional scale wind erosion model measurement of saltation transport is needed over a large range of vegetation covers. Field measurements on saltation transport are performed with a wide range of saltation type catchers but the efficiency of sediment samplers (catchers) varies with texture and wind speeds. Current field scale measurements of saltation are time and money consuming and do not provide insights in the interrelations between the different neighbouring land units. Therefore a new measurement method, which provides data for the calibration and validation of regional scale wind erosion models considering saltation transport, is required. Consequently, the following research questions were defined:

- How efficient is the currently available equipment for measuring saltation?
- What is the best method to measure wind erosion at the regional scale?
- How can a field scale model be adapted for use at the regional scale?
- What is the effect of spatial vegetation transitions on saltation transport?

This synthesis describes the major findings of the Chapters 2 through 6 answering these questions. Gained scientific insights and their implications are presented in reflection with current knowledge.

7.1 Efficiency of currently available equipment

In this research saltation is considered the main process in regional-scale wind erosion. Several sediment traps were developed for use in field observations and wind tunnel experiments such as the Big Spring Number Eight (BSNE, Bagnold, 1954), the Vertical Rod Sand Trap (VRST, Leatherman, 1978), the Cake Pan Collector (CPC, De Ploey, 1980), the Modified Wilson And Cooke (MWAC, Wilson and Cooke, 1980) and the Vaseline Slide (VS) (Cornelis et al., 2008). For accurate calculation of the wind-driven mass flux and the soil loss, the efficiency of wind erosion equipment needs to be determined (Fryrear et al., 1991; Fryrear et al., 2008; Spaan and van den Abeele, 1991; Zobeck et al., 2003). Zobeck et al. (2003) emphasized that the selection of the type of catcher should be based upon the particle size of the sediment that is expected to be trapped, as the efficiency of the catchers depends on the particle size (Goossens and Offer, 2000).

In Chapter 2, the efficiency of the Vaseline Slide (VS) and the Modified Wilson and Cooke (MWAC) catchers was determined in wind-tunnel experiments. The efficiencies were determined for different soil textures and for a range of wind velocities (9 -13 m s^{-1}). The results show that the efficiencies of the tested sediment samplers vary significantly with particle size and wind speed (Figure 2.8).

Whereas the efficiency of the MWAC catcher increases with an increase in particle size, the efficiency of the VS catcher decreases with an increase in the particle size. The efficiency of the MWAC for particles smaller than 50 μm, is around 0 % and for the VS this is around 92 %. The results showed also, that with particles of 200–400 μm, the efficiency of MWAC is 25 % and 2 % for the VS. Thus, it can be concluded from our experiments, that the VS catcher is more suitable for trapping sediment that moves in suspension (2-63 μm) than the MWAC. The latter is more suitable than the VS for trapping sediment that is transported in saltation mode (63-500 μm). The efficiency of MWAC increases gradually with an increase of wind speed, which can be explained by the fact that with a higher wind speed coarser material will become airborne than is the case with lower wind speed. These results emphasized the need for a site-specific determination of the trapping efficiency.

Goosens et al. (2000) showed opposite results for the MWAC. They reported that the efficiency of MWAC increased with a decrease in particle sizes and they showed that the efficiency of MWAC ranged from 90-120% for wind speed in the range of 6.5-14.4 m s^{-1}. The disagreement between the two studies can be linked to the differences in the range of particle sizes used in the two studies and the wind speed applied. In our study the efficiency was tested for a wide range of particle sizes (from <50 μm to 400 μm), compared to the study of Goosens et al. (2000); from 132 μm to 287 μm. Given the sensitivity of the traps for variation in wind speed particle size, we conclude that the comparison between the two studies is quite difficult due to the different class range of particle sizes and wind speed.

This study emphasized the recommendation of Zobeck et al. (2003) who mentioned that the kind of sediment catcher to be used should be chosen upon the sediment to be trapped. On the basis of our results and the focus on saltation transport, we decided to use the MWAC for sampling wind-blown sediment in our further research.

7.2 Method to measure wind erosion at the regional scale

Measurements on wind erosion can be divided into two main groups: saltation-based methods and the suspension-based methods. The main interest of this thesis is on the wind erosion process and factors affecting it at regional scale (minimum of 20-25 Km^2). So far, observation of large scale wind erosion depends on the monitoring of dust storms with the use of remote sensing technology (Shao, 2008; Webb and McGowan, 2009; Webb et al., 2006; Zobeck et al., 2000). In this research however, we mainly consider transport by saltation, because with the absence of saltation, suspension is hardly started (Zhang and Lee, 2009), saltation is the most effective process on soil productivity (Sterk, 1997), and saltation can directly

destroy crops causing a huge decrease in production from agriculture in vulnerable regions (Sivakumar et al., 2005, Baker, 2007; Baker et al., 2009). In saltation-based measurements, saltating grains are directly trapped into the sediment catchers (Leenders, 2006; Sterk, 1997; Visser et al., 2005a). This type of measurements provides precise information on mass fluxes at the point scale over time and when multiple locations within a plot are sampled, spatial variation in mass transport can also be determined. However, to collect data on the saltation process at regional scale using this 'traditional' method in which the measurement continued for a relatively long time would be incredibly time and money consuming because an enormous number of catchers would be required. Therefore, a measurement method of portable plots was developed to obtain data from several land uses and vegetation covers in the region in a relatively short period of time.

Chapter 3 describes this method, which was applied on 16 plots with different land use and vegetation cover in the Khanasser Valley in Syria in 2009 and 2010. Results showed that for bare land uses, a positive and relatively strong relationship between the wind value and mass transport exists, however, the relation did not exist for the land uses that have vegetation cover. Furthermore, in this chapter, the wind value-standardized mass transport was suggested for the comparison of the mass transport at different land covers regardless the power of the event. Furthermore is shown that in an area, the land use at the neighbouring land units plays essential role in the spatial distribution of the mass transport within this area. This was also observed by Hupy (2004) and Leenders (2006).

As the portable plot method focuses on saltation, it gives more accurate knowledge on the process of sediment transport than the measurements that rely on the monitoring of dust storms by remote sensing technology. It is expected that data collected with the portable plot method are suitable for calibration and validation field scale models for different land covers in a region and thus the development of this method is an important step in the modelling of wind erosion at the regional scale.

7.3   An adapted field scale model for use at the regional scale

To develop a regional scale model that takes the saltation process into account and considers the interrelation between neighbouring land units, we started with the adaptation of the existing field scale model RWEQ (Revised Wind Erosion Equation). Model adaptations were, among others, using time steps of 6 hours, estimation of mass flux over the field boundaries and the routing of sediment. Originally, RWEQ was created and calibrated for application in the USA. Due to our adaptations to the original RWEQ and the different environmental conditions in Syria, an intensive calibration process was required before applying the model to estimate the net soil loss from the experimental fields. Data for the calibration and validation of the adapted RWEQ, that represents the entire region, were derived from the portable plot method for the main land uses in the region (see 7.2).

The adjusted RWEQ model provides an estimation of the spatial pattern of mass flux and soil loss taking into account the distance between the non-erodible border (in the upwind direction) and the edge of the simulated plot. The relationship between the simulated and measured spatial variation in mass flux within the plots was poor (Figure 4.6). The statistical analyses of model results for the relationship between average predicted and measured mass flux for the 20 wind events at the six tested plots gave an R^2=0.48 (d=0.85). Van Pelt et al. (2002) validated RWEQ for 41 wind erosion events in six states in the USA and the results of their test gave a relationship between measured and predicted mass flux of $R^2 = 0.49$ which is almost the same value found in this the current research. Buschiazzo and Zobeck (2008) tested the RWEQ model for Argentinean environment and the results of model test of 28 wind erosion events in the same field was $R^2 = 0.57$ and they reported results of $R^2 = 0.90$ for a single event. Thus, results of our test fall in the magnitude of previous tests of RWEQ.

Since the focus of this thesis is mainly on the regional scale, we conclude that the adapted RWEQ model provides acceptable predictions for the average mass flux at a plot taking into account previous tests of the model and the high number of different vegetation covers in the region. The obtained results show that the adjusted, calibrated and validated RWEQ model in a PCRaster GIS environment has the potential to be scaled up to a regional scale model.

7.4 Effects of spatial vegetation transitions on saltation transport

The portable plot method provided insight in the effect of climate (wind speed) on the quantity and intensity of wind erosion for several land use types in a region. However, as the size of each measurement plot is relatively small (60 x 60 m^2) the larger distance effect of the interrelation between neighbouring land units cannot fully be measured with this method. Insights on the effect of vegetation pattern (creating vegetation transitions) on sediment transport at regional scale are required for instance the development of re-vegetation plans for degraded land (Bowker et al., 2006; Leenders, 2006). To gain knowledge on the effect of the interrelation between neighbouring land units and on the influence of vegetation pattern on the process of sediment transport a set of wind-tunnel experiments were performed. Chapter 5 describes a wind-tunnel experiment designed to obtain a more profound insight in these border effects. In this experiment, sand was used as it is the most erodible material (Chandler et al., 2005) and a wind speed of 11 m s^{-1} was chosen because this speed enabled sediment movement without destroying the designed vegetation model. In previous wind tunnel experiments on the effect of vegetation on wind-blown sediment, vegetation was simulated using pieces of dead vegetation (Molina-Aiz et al., 2006), living vegetation (Burri et al., 2011), or artificial vegetation (Cornelis and Gabriels, 2005; Udo et al., 2008; (Wuyts et al., 2008) as surrogates for real-world vegetation. In our experiments a scale model for the "Atriplex halimus" was designed to represent the natural vegetation. We used artificial vegetation as it is not affected by the sand abrasion and thus, comparison between results from all scenarios was possible.

We simplified the experiment by considering two main land uses; vegetated and bare land. In the vegetated area different vegetation patterns (in which the vegetation elements were distributed in different style along the experimental tray, for example rows of the vegetation elements) were tested, each with a vegetation cover of 11%, but varying in the number of individual shrubs, and the positioning of these shrubs, either in a regular grid or in an offsetting grid. The results of the experiments showed that vegetation pattern has a clear influence on the intensity and quantity of the erosion and deposition of wind-blown sediment in a region (Figure 5.7). Our experiments showed the formation of "streets" of erosion in the pattern of rows for the simulated shrubs (Figure 5.4). Bowker et al. (2006) showed similar formation of "streets" of erosion in desert environments with the rows of shrubs parallel to the main wind direction. Our simulations also indicated that with some vegetation pattern and cover and under a certain wind speed the vegetation can accelerate the sediment-transport process. This was also found by (Raupach, 1990; Raupach, 1992 Raupach et al., 1993; Michels et al., 1995; Sterk et al., 1998; Maurer et al., 2009).

7. 5 A new process-based regional scale wind erosion model (RS-WEQ): the effect of land cover pattern on wind erosion

Chapter 6 describes extensions to the RWEQ model required to construct a model that can be run at regional scale. Although the RWEQ model was the starting point for developing this regional scale model, the current model is not restricted in its application to a single field. The new model considers the saltation process as the main transport mode and uses erodibility parameters for each land use. It predicts mass flux, soil loss and deposition for series of neighbouring fields and reflects the interrelation between

neighbouring land units by adjusting the mass flux equations to account for sediment transport across field borders. The model can simulate the effect of climate (mainly wind speed), field length and land use pattern (the sequences of land use in a region) on the quantity and severity of regional scale wind erosion. The model was tested on sequences of bare fields, wheat fields and Atriplex fields, with lengths of 50, 150 and 450 m and wind speeds of 10, 12.5 and 15 m. These scenarios were prepared to represent main land uses in dry regions in general and in Khanasser valley specifically as RWEQ was calibrated and validated under data collected from this region.

The model outputs showed that in a region, the quantity and severity of abrasion, soil loss and deposition were affected strongly by wind speed and field length and slightly by land use pattern. As expected, the abrasion risk due to the sediment flux increased with an increase in wind speed and field length. These results agree with previous studies on the effect of wind speed and field length of single fields on abrasion rate and mass flux (Fryrear and Saleh, 1996; Skidmore, 1986; Skidmore and Hagen, 1977; Tibke, 1988).

The model outputs also showed also that the soil loss decreases with an increase in field length, and that the severity of soil loss and deposition is higher for shorter fields than for longer fields. The results on soil loss agree with the results of Gregory et al. (1990) who reported a decrease in soil loss with the increase in field length (Gregory et al., 1990). Fryrear et al. (1998) also reported a decrease in soil loss with an increasing downwind distance from the non-erodible border. However, the previous studies did not provide an integrated model that accounts for the combined effect of field length, vegetation pattern, and climate as was developed here. As our regional scale model can be run with data that can in principle be collected over large regions, using remote sensing and global meteorological data sets, it has a high potential for mapping wind erosion over large areas.

7.6 Limitations of the study

In this thesis, the saltation process was considered as the key transport mode when measuring and modelling aeolian sediment transport at the regional scale. Therefore suspension and creep transport modes were not considered. Of course to consider the complete wind erosion process all transport processes should be included in a research. However, give the scale of the processes studied we believe that the focus on saltation transport is justified.

In the wind tunnel simulation, we used an artificial vegetation model to test the effect of vegetation on wind-blown sediment transport. This simulation is accepted from the physical view as the vegetation model represented relatively the physical characteristic of real vegetation. However, in the simulation the biological characteristic of the real vegetation was not simulated. For instance the negative effects of abrasion on the vegetation are not shown in our simulation. And these can be considered as a limitation of this simulation.

7.7 Recommendations for further research

Understanding wind erosion at the regional scale is significant for coping with this environmental problem and taking steps to reduce its hazard on humanity and environment. However, knowledge on this natural phenomenon is still limited and the gap between what is known and what is required is still wide. To reduce this gap some recommendations for future research are illustrated:

1. Improving methods that enable data collection to fully represent the region. Although in this thesis, we covered relatively a large number of land use areas in our field observations, we still think that the increase in the number of measurement plots will improve the understanding of the factors and conditions affecting the aeolian sediment transport. And thus, future research may focus on

developing a new measurement method that provides data that fully represent each land use in a region.

2. Improving methods for data analyses to drive knowledge on the wind erosion processes. Having data set on aeolian sediment transport in a large scale is rather complicated and difficult. Therefore, correct, intensive and precise analyses of obtained data are highly significant for insight on the wind erosion in vulnerable regions. Currently there are limited methods for analyses the data of aeolian sediment transport and, in so usually similar methods for data analyses are followed to derive conclusions. Searching for new methods or improving the current methods for data analyses may progress the current knowledge on wind erosion research and it is recommended for future researches.

3. Improving the current regional scale wind erosion models: the majority of these models ignore one or two of the transport modes (saltation, suspension or creep) in which important part of sediment is transported. Consequently, none of these models fully represents the real transport conditions. Therefore, developing or improving a regional scale wind erosion models that combines all of these transport modes together will be a large step towards the understanding of the regional scale wind erosion.

4. Combine data obtained throughout different methods to calibrate and validate regional scale wind erosion models: the models that represent all transport modes will require a large range of data. Obtaining the required data for calibration and validation will need the use of several methods for data collection. For instance, whereas, field observations generally provide data mainly on saltation mode and partially on suspension and creep, the RS technology provides data mainly on the suspension mode. Thus, the calibration and validation of regional scale models that include saltation and suspension will require data collected throughout field measurements (for saltation data) and RS technology (for suspension data).

7.7   Recommendations for mitigating policies for wind erosion in drylands

This thesis focuses on the improvement of our knowledge on the effect of vegetation cover and land use on regional scale wind erosion. The outputs of this study provided insight on the effect of land use application on the quantity and severity of wind erosion. Some recommendations for policy makers can be summarized under few themes:

Improving the knowledge of farmers about wind erosion

It is recommended for policy makers to teach the local inhabitants about the threat of wind erosion and the economic effects of this process on their lives and future. Once the farmers/inhabitants become aware about the negative effects of wind erosion on their fiscal conditions and on their health, they will respect the drawn policy more carefully. In this framework a simple educational program can be initiated, several methods can be followed to achieve this program, for example, arranging simple courses at local schools. Such these courses will allow to easy transfer ideas about the important of natural resources, negative effects of the soil erosion, sustainability of on environment to locals of these regions.

Direct applications

1. The study showed that there was no soil erosion at the rehabilitated rangeland areas while a large amount of soil erosion was observed in the non-rehabilitated rangeland areas. Furthermore, it was shown that all agricultural zones suffer from different degrees of erosion. Upon these results the planting of shrubs that survive dry conditions (i.e. Olives in Zone 4 and Atriplex in the stability zone 5) are strongly recommended. Relying on the result of the current study two points can be highlighted

for this application; (a) The combination of shrubs and other farming should be avoided. (b) The vegetation pattern should be selected after the careful analyses of long term wind directions.

2. The study concluded that the saltation and abrasion risk increases with the increase in field size and therefore, it can be recommended to use the strip farming in which cultivated (cropped) and fallow land covers are alternated to decrease these processes. The decrease of saltation will cause direct reduction in the suspension process too and thus this application will reduce the amount of soil loss due the saltation and suspension and also will reduce the general negative effects of abrasion.

Future planning and forecasting

As the control of wind erosion problem is much easier at the elementary stage than the advance stages, it is recommended to use wind erosion stations for forecasting the future of this problem in vulnerable regions. In these stations besides the recoding of wind rates, saltiphones can be used to observe the saltation process. Data collected from these stations can be analysed (i.e. in seasonal basis). The conclusions of these analyses may highlight vital knowledge that can help to take some decisions by policy makers and land managers. To improve the outcomes of this activity, the current study recommends the use of simple calibrated and validated wind erosion models to help for future planning of the land use.

References

Abdourhamane, T.A., Rajot, J.L., Garba, Z., Marticorena, B., Petit, C., Sebag, D., 2011. Impact of very low crop residues cover on wind erosion in the Sahel. Catena, 85(3), 205-214.

Alfaro, S.C., Gomes, L., 2001. Modeling mineral aerosol production by wind erosion: Emission intensities and aerosol size distributions in source areas. Journal of Geophysical Research D: Atmospheres, 106(D16), 18075-18084.

Almansa, C., Calatrava, J., Martínez-Paz, J.M., 2012. Extending the framework of the economic evaluation of erosion control actions in Mediterranean basins. Land Use Policy, 29(2), 294-308.

Andrew, W., 2007. Sustainability: A view from the wind-eroded field. Journal of Environmental Sciences, 19(4), 470-474.

Armbrust, D.V., Retta, A., 2000. Wind and Sandblast Damage to Growing Vegetation. Annals of Arid Zone, 39(3), 273-284.

Bagnold, R.A., 1941. The Physics of Blown Sand and Desert Dunes, Chapman and Hall, London.

Bagnold, R.A., 1954. Physical aspects of dry deserts, In Biology of Deserts, The Proceedings of a Symposium on the Biology of Hot and Cold Deserts Organized by the Institute of Biology, Cloudsley-Thompson JL (ed), London Institute of Biology, London, 7–12.

Baker, J.T., 2007. Cotton seedling abrasion and recovery from wind blown sand. Agronomy Journal, 99(2), 556-561.

Baker, J.T., McMichael, B., Burke, J.J., Gitz, D.C., Lascano, R.J., Ephrath, J.E., 2009. Sand abrasion injury and biomass partitioning in cotton seedlings. Agron. J., 101(6), 1297-1303.

Basaran, M., Erpul, G., Uzun, O., Gabriels, D., 2011. Comparative efficiency testing for a newly designed cyclone type sediment trap for wind erosion measurements. Geomorphology, 130(3-4), 343-351.

Baveye, P.C., Rangel, D., Jacobson, A.R., Laba, M., Darnault, C., Otten, W., Radulovich, R., Camargo, F.A.O., 2011. From dust bowl to dust bowl: Soils are still very much a frontier of science. Soil Science Society of America Journal, 75(6), 2037-2048.

Bielders, C.L., Michels, K., Rajot, J.L., 2000. On-farm evaluation of ridging and residue management practices to reduce wind erosion in Niger. Soil Science Society of America Journal, 64(5), 1776-1785.

Bierkens, M.F.P., Finke, P.A., De Willigen, P. (eds), 2000. Upscaling and Downscaling Methods for Environmental Research, Published 2000 as vol. 88 in the "Developments in Plant and Soil Sciences" Series by Kluwer Academic Publishers, 190pp.

Bilbro, J.D., Fryrear, D.W., 1985. Effectiveness of residues from six crops for reducing wind erosion in a semiarid region. Journal of Soil & Water Conservation, 40(4), 358-360.

Blöschl, G., Sivapalan, M., 1995. Scale issues in hydrological modelling: a review. Hydrological Processes 9, 251-290.

Blöschl, G., 1999. Scaling issues in snow hydrology. Hydrological Processes, 13(14-15), 2149-2175.

Bowker, G.E., Gillette, D.A., Bergametti, G., Marticorena, B., 2006. Modeling flow patterns in a small vegetated area in the northern Chihuahuan Desert using QUIC (Quick Urban & Industrial Complex). Environmental Fluid Mechanics, 6(4), 359-384.

Bowker, G.E., Gillette, D.A., Bergametti, G., Marticorena, B., Heist, D.K., 2008. Fine-scale simulations of aeolian sediment dispersion in a small area in the northern Chihuahuan Desert. Journal of Geophysical Research. field of Earth-Surface Processes, 113(2).

Bravo, O., Silenzi, J.C., 2002. Strip cropping in the semi-arid region of Argentina: Control of wind erosion and soil water accumulation. Soil Science, 167(5), 346-352.

Breshears, D.D., Whicker, J.J., Johansen, M.P., Pinder Iii, J.E., 2003. Wind and water erosion and transport in semi-arid shrubland, grassland and forest ecosystems: Quantifying dominance of horizontal wind-driven transport. Earth Surface Processes and Landforms, 28(11), 1189-1209.

Breshears, D.D., Whicker, J.J., Zou, C.B., Field, J.P., Allen, C.D., 2009. A conceptual framework for dryland aeolian sediment transport along the grassland-forest continuum: Effects of woody plant canopy cover and disturbance. Geomorphology, 105(1-2), 28-38.

Bruggeman, A., Rieser A, Asfahani J, Abou Zakhem, B., (eds.), L.E., 2010. Water Resources and Use of the Khanasser Valley, Chapter 2 ICARDA, Aleppo, Syria. International Center for Agricultural Research in the Dry Areas, Aleppo, Syria (in press, 2010).

Bunn, J.A., 1997. The implications of alternative beliefs about soil-erosion-productivity relationships and conservation treatments for the economic dynamics of soil erosion on the southern Texas High Plains. Journal of Soil and Water Conservation, 52(5), 368-375.

Burri, K., Gromke, C., Lehning, M., Graf, F., 2011. Aeolian sediment transport over vegetation canopies: A wind tunnel study with live plants. Aeolian Research, 3(2), 205-213.

Buschiazzo, D.E., Zobeck, T.M., 2008. Validation of WEQ, RWEQ and WEPS wind erosion for different arable land management systems in the Argentinean Pampas. Earth Surface Processes and Landforms, 33(12), 1839-1850.

Buschiazzo, D.E., Zobeck, T.M., Aimar, S.B., 1999. Wind erosion in loess soils of the Semiarid Argentinian Pampas. Soil Science, 164(2), 133-138.

Butler, H.J., Hogarth, W.L., McTainsh, G.H., 1996. A source-based model for describing dust concentrations during wind erosion events: An initial study. Environmental Software, 11(1-3), 45-52.

Cai, Y., Barry, S., 1996. Sensitivity and adaptation of chinese agriculture under global climate change. Acta Geographica Sinica, 51(3), X2-212.

Campbell, E.P., Palmer, M.J., 2010. Modeling and forecasting climate variables using a physical-statistical approach. Journal of Geophysical Research, 115(D10), D10114.

Chandler, D.G., Saxton, K.E., Busacca, A.J., 2005. Predicting wind erodibility of loessial soils in the pacific northwest by particle sizing. Arid Land Research and Management, 19(1), 13-27.

Chang, E.H., Chen, C.T., Chen, T.H., Chiu, C.Y., 2011. Soil microbial communities and activities in sand dunes of subtropical coastal forests. Applied Soil Ecology, 49(1), 256-262.

Chappell, A., Warren, A., 2003. Spatial scales of 137Cs-derived soil flux by wind in a 25 km2 arable area of eastern England. Catena, 52(3-4), 209-234.

Chappell, A., Zobeck, T.M., Brunner, G., 2006. Using bi-directional soil spectral reflectance to model soil surface changes induced by rainfall and wind-tunnel abrasion. Remote Sensing of Environment, 102(3-4), 328-343.

Chen, J., Franklin, J.F., Spies, T.A., 1995. Growing-season microclimatic gradients from clearcut edges into old-growth Douglas-fir forests. Ecological Applications, 5(1), 74-86.

Chepil, W.S., 1942. Measurement of wind erosiveness of soils by the dry sieving procedure. Sci Agric 23(3), 154–160.

Chepil, W.S., 1957. Width of Field Strip to Control Wind Erosion. Kansas Agricultural, Experimental Station Technical Bulletin, 92. p. 16 Dec.

Chepil, W.S., Woodruff, N.P., 1963. The Physics of Wind Erosion and its Control, Advances in Agronomy, pp. 211-302.

Cook, B.I., Miller, R.L., Seager, R., 2008. Dust and sea surface temperature forcing of the 1930's 'Dust Bowl' drought. Geophysical Research Letters, 35.

Copeland, N.S., Sharratt, B.S., Wu, J.Q., Foltz, R.B., Dooley, J.H., 2009. A wood-strand material for wind erosion control: Effects on total sediment loss, PM10 vertical flux, and PM10 loss. Journal of Environmental Quality, 38(1), 139-148.

Cornelis, W., Hartmann, R., Gabriels, D., 1998. Assessing and controlling dust pollution in the harbour of Ghent. In: Gabriels D, Cornelis WM (eds) Proceedings of the International Workshop on Technical aspects and use of wind tunnels for winderosion control, combined effect of wind and water on erosion processes. Ghent, Belgium, , pp 25–32.

Cornelis, W.M., Gabriels, D., 2004. A simple model for the prediction of the deflation threshold shear velocity of dry loose particles. Sedimentology, 51(1), 39-51.

Cornelis, W.M., Gabriels, D., 2005. Optimal windbreak design for wind-erosion control. Journal of Arid Environments, 61(2), 315-332.

Cornelis, W.M., 2006. Hydroclimatology of wind erosion in arid environments (Chapter 9) In: P. D'Odorico, A. Porporato (Eds.), Dryland ecohydrology. Springer, Dordrecht, The Netherlands. , p. 141-157.

Cornelis, W., Kerckhoven, S.v., Riksen, M.J.P.M., Gabriels, D., 2010. Assessment of wind erosion risk in Flanders, Belgium, Third conference on Desertification and Land Degradation; Workshop Action of Rain and Wind in Soil Degradation Processes, Ghent, Belgium, 16 - 17 June, 2010. Unesco Chair of Eremology; International Centre for Eremology (ICE), Ghent University, Belgium, pp. 18-19.

Csavina, J., Sáez, A.E., Betterton, E.A., Barbaris, B., Rine, K., Campillo, A., Rheinheimer, P., Landázuri, A., Wonaschutz, A., Conant, W., 2010. Modeling and characterization of aerosol emissions from mining operations, AIChE Annual Meeting, Conference Proceedings. Salt Lake City, UT;7 November 2010through12 November 2010;Code83459

Cuadros, J., Spiro, B., Dubbin, W., Jadubansa, P., 2010. Rapid microbial stabilization of unconsolidated sediment against wind erosion and dust generation. Journal of Soils and Sediments, 10(7), 1415-1426.

De Longueville, F., Henry, S., Ozer, P., 2009. Saharan dust pollution: Implications for the Sahal? Epidemiology, 20(5), 780.

De Ploey, J., 1980. Some field measurements and experimental data on wind-blown sands. Wiley, Chichester, pp 143–115 141.

Dierickx, W., Gabriels, D., Cornelis, W., 2001. A wind tunnel study on wind speed reduction of technical textiles used as windscreen. Geotextiles and Geomembranes, 19(1), 59-73.

Drenova, A.N., 2011. Ancient continental dunes in the upper volga basin: Their orientation, structure, granulometric composition. Geomorfologiya, 1. 37-48.

Drew, R.T., Lippmann, M., 1978 Calibration of air sampling instruments. In: Air sampling instruments for evaluation of atmospheric contaminants, 5th edn. American Conference of Governmental Industrial Hygienists, Cincinnati, pp 1–138.

Feng, G., Sharratt, B., 2007. Predicting wind erosion and windblown dust emissions at the regional scale to guide strategic conservation targeting. Journal of Soil and Water Conservation, 62(5).

Floyd, K.W., Gill, T.E., 2011. The association of land cover with aeolian sediment production at Jornada Basin, New Mexico, USA. Aeolian Research, 3(1), 55-66.

Fryrear, D.W., Stout, J.E., Hagen, L.J., Vories, E.D., 1991. Wind erosion: field measurement and analysis. Transactions of the American Society of Agricultural Engineers (Gen Ed), 34(1), 155-160.

Fryrear, D.W., Saleh, A., 1996. Wind erosion: Field length. Soil Science, 161(6), 398-404.

Fryrear, D.W., Saleh, A., Bilbro, J., Schomberg, H., Stout, J., Zobeck, T., 1998. Revised Wind Erosion Equation (RWEQ). Wind Erosion and Water Conservation Research Unit, Technical Bulletin 1,. Southern Plains Area Cropping Systems Research Laboratory,USDA-ARS.

Fryrear, D.W., Bilbro, J.D., Saleh, A., Schomberg, H., Stout, J.E., Zobeck, T.M., 2000. RWEQ: Improved wind erosion technology. Journal of Soil and Water Conservation, 55(2), 183-189.

Fryrear, D.W., Wassif, M.M., Tadrus, S.F., Ali, A.A., 2008. Dust measurements in the Egyptian Northwest Coastal Zone. Transactions of the ASABE, 51(4), 1255-1262.

Funk, R., Skidmore, E.L., Hagen, L.J., 2004. Comparison of wind erosion measurements in Germany with simulated soil losses by WEPS. Environmental Modelling and Software, 19(2), 177-183.

Gabriels, D., Cornelis, W., Pollet, I., Van Coillie, T., Ouessar, M., 1997. The I.C.E. wind tunnel for wind and water erosion studies. Soil Technology, 10(1), 1-8.

Gash, J.H.C., 1986. Observations of turbulence downwind of a forest-heath interface. Boundary-Layer Meteorology, 36(3), 227-237.

Gee, G.W., Bauder, J.W., 1986. Particle-size analysis by hydrometer: a simplified method for routine textural analysis and a sensitivity test of measurement parameters. Soil Science Society of America Journal 43 (5) , pp, Madison, pp 383–411.

Gillette, D.A., 1977. Fine particle emissions due to wind erosion. Transactions of the American Society of Agricultural Engineers (20),890-897.

Gomes, L., Rajot, J.L., Alfaro, S.C., Gaudichet, A., 2003. Validation of a dust production model from measurements performed in semi-arid agricultural areas of Spain and Niger. Catena, 52(3-4), 257-271.

Goossens, D., Offer, Z.Y., 2000. Wind tunnel and field calibration of six aeolian dust samplers. Atmospheric Environment, 34(7), 1043-1057.

Goossens, D., Gross, J., 2002. Similarities and dissimilarities between the dynamics of sand and dust during wind erosion of loamy sandy soil. Catena, 47(4), 269-289.

Gregory, J.M., Borrelli, J., Fedler, C.B., 1990. Windstorm erosion and soil deposition simulation. Journal of Wind Engineering and Industrial Aerodynamics, 36(1-3), 1415-1424.

Gregory, J.M., Wilson, G.R., Singh, U.B., Darwish, M.M., 2004. TEAM: integrated, process-revised wind erosion equation based wind-erosion model. Environmental Modelling and Software, 19(2), 205-215.

Guo, Z., Zobeck, T.M., Stout, J.E., Zhang, K., 2012. The effect of wind averaging time on wind erosivity estimation. Earth Surface Processes and Landforms, 37(7), 797-802

Gupta, J.P., Rama, P., 1996. Wind erosion and it control in hot arid areas of Rajasthan, India. In Buerkert, B. Allison, B. E. and M. V. Oppen (Ed). Proceedings of International. symposium. " Wind erosion" in West Africa. The problem and its control, University of Hohenheim, 5-7th December 1994. Margraf Verlag, Weikersheim, Germany.

Hagen, L.J., 1991. A wind erosion prediction system to meet user needs. Journal of Soil and Water Conservation, 46(2), 106-111.

Hagen, L.J., 1996. Crop residue effects on aerodynamic processes and wind erosion. Theoretical and Applied Climatology, 54(1-2), 39-46.

Hagen, L.J., 1999. Assessment of wind erosion parameters using wind tunnels. In: D.E. Stott, R.H. Mohtar, and G.A. Steinhardt (eds.) Sustaining the Global Farm; 1999 May 24-29; Purdue University, West Layfayette, IN. pp 742–746.

Hagen, L.J., 2004. Evaluation of the Wind Erosion Prediction System (WEPS) erosion submodel on cropland fields. Environmental Modelling and Software, 19(2), 171-176.

Hassine, A.B., Lutts, S., 2010. Differential responses of saltbush Atriplex halimus L. exposed to salinity and water stress in relation to senescing hormones abscisic acid and ethylene. Journal of Plant Physiology, 167(17), 1448-1456.

Heisler, G.M., Dewalle, D.R., 1988. 2. Effects of windbreak structure on wind flow. Agriculture, Ecosystems and Environment, 22-23(C), 41-69.

Herrmann, L., Stahr, K., Sivakumar, M.V.K., 1996. Dust deposition on soils of Southwest Niger. In A. Buerkert, B.E. Allison, M. Von Oppen (Eds.), Wind erosion in West Africa: The Problem and its Control: 35-47. Margraf Verlag, Weikersheim, Germany: Hohenheim, Germany.

Hesse, P.P., Magee, J.W., van der Kaars, S., 2004. Late Quaternary climates of the Australian arid zone: A review. Quaternary International, 118–119 87-102.

Hoogmoed, W.B., Stroosnijder, L., Posthumus, H., Tammes, H.B., 2000. Effect of decreasing soil organic matter content and tillage on physical properties of sandy Sahelian soils In: Soil Erosion and Dryland Farming, Laflen, JM, Junliang Tian, Chi-Hua Huang (eds). CRC press, Boca Raton, FL;. Soil erosion and dryland farming 191 – 201.

Humberto, B., Rattan, L., 2010. Principles of Soil Conservation and Management. Springer,ISBN-10: 140208708X

Hupy, J.P., 2004. Influence of vegetation cover and crust type on wind-blown sediment in a semi-arid climate. Journal of Arid Environments, 58(2), 167-179.

ICARDA, 2005. Sustainable Agricultural Development for Marginal Dry Areas Khanasser Valley Integrated Research Site. International Center for Agricultural Research in the Dry Areas: agriculture, research, training and publications (ICARDA, 2005).

Ikazaki, K., Shinjo, H., Tanaka, U., Tobita, S., Funakawa, S., Kosaki, T., 2011. Aeolian materials sampler for measuring surface flux of soil nitrogen and carbon during wind erosion events in the Sahel, West Africa. Transactions of the ASABE, 54(3), 983-990.

Irvine, M.R., Gardiner, B.A., Hill, M.K., 1997. The evolution of turbulence across a forest edge. Boundary-Layer Meteorology, 84(3), 467-496.

Jabbar, M.T., Zhou, X., 2011. Eco-environmental change detection by using remote sensing and GIS techniques: a case study Basrah province, south part of Iraq. Environmental Earth Sciences 64: 1397-1407. DOI: 10.1007/s12665-011-0964-5., 1-11.

Jackson, D.W.T., 1996. A new, instantaneous aeolian sand trap design for field use. Sedimentology, 43(5), 791-796.

Jason, P.F., 2009. Differential response of wind and water erosion under climatic extremes and alternate land management practices, Doctoral thesis, School Of Natural Resources and the Environment, the University of Arizona.

Karssenberg, D., De Jong, K., 2005. Dynamic environmental modelling in GIS: 2. Modelling error propagation. International Journal of Geographical Information Science, 19(6), 623-637.

Kind, R.J., 1992. One-dimensional aeolian suspension above beds of loose particles - A new concentration-profile equation. Atmospheric Environment - Part A General Topics, 26 A(5), 927-931.

King, J., Nickling, W.G., Gillies, J.A., 2005. Representation of vegetation and other nonerodible elements in aeolian shear stress partitioning models for predicting transport threshold. Journal of Geophysical Research F: Earth Surface, 110(4).

Kjelgaard, J.F., Chandler, D.G., Saxton, K.E., 2004. Evidence for direct suspension of loessial soils on the Columbia Plateau. Earth Surface Processes and Landforms, 29(2), 221-236.

Klik, A., 2004. Wind Erosion Assessment in Austria using Wind Erosion Equation and GIS", in OECD, Agricultural Impacts on Soil Erosion and Soil Biodiversity: Developing Indicators for Policy Analysis, Paris, France, www.oecd.org/tad/env/indicators.

Lal, R., 1990. Soil erosion in the tropics : Principles and management. McGrawInc., New York.

Lancaster, N., Baas, A., 1998. Influence of vegetation cover on sand transport by wind: Field studies at Owens Lake, California. Earth Surface Processes and Landforms, 23(1), 69-82.

Leatherman, S.P., 1978. A new aeolian sand trap design. Sedimentology, 25(2), 303-306.

Leenders, J.K., van Boxel, J.H., Sterk, G., 2005. Wind forces and related saltation transport. Geomorphology, 71(3-4), 357-372.

Leenders, J.K., 2006. Wind erosion control with scattered vegetation in the Sahelian zone of Burkina Faso. Doctoral thesis Wageningen University, Wageningen.

Leenders, J.K., van Boxel, J.H., Sterk, G., 2007. The effect of single vegetation elements on wind speed and sediment transport in the Sahelian zone of Burkina Faso. Earth Surface Processes and Landforms, 32(10), 1454-1474.

Leenders, J.K., Sterk, G., Van Boxel, J.H., 2011. Modelling wind-blown sediment transport around single vegetation elements. Earth Surface Processes and Landforms, 36(9), 1218-1229.

Leslie, L.M., Speer, M.S., 2006. Modelling dust transport over central eastern Australia. Meteorological Applications, 13(02), 141-167.

Letnic M. 2004. Cattle grazing in a hummock grassland regenerating after fire: The short-term effects of cattle exclusion on vegetation in south-western Queensland. Rangeland Journal 26(1):34-48.

Ley, T.W., Allen, R.G., Jensen, M.E., 2009. Adjusting wind speed measured over variable height Alfalfa for use in the ASCE standardized penman-monteith equation, Proceedings of World Environmental and Water Resources Congress 2009 - World Environmental and Water Resources Congress 2009: Great Rivers, pp. 4141-4157.

Leys, J., McTainsh, G., Shao, Y., 2001. Wind erosion monitoring and modeling techniques in Australia. In Sustaining the Global Farm, Selected Papers from the 10th International Soil Conservation Organization Meeting May 24-29, 1999, Stott, DE, Mohtar, RH, Steinhardt GC (eds). USDA-ARS National Soil Erosion Research Laboratory, Purdue University, Richmiond, IN; . 940-950.

Li, S.X., Wang, Z.H., Hu, T.T., Gao, Y.J., Stewart, B.A., 2009. Chapter 3 Nitrogen in Dryland Soils of China and Its Management, Advances in Agronomy, pp. 123-181.

Li, Z., Wu, S., Dale, J., Ge, L., He, M., Wang, X., Jin, J., Liu, J., Li, W., Ma, R., 2008. Wind tunnel experiments of air flow patterns over nabkhas modeled after those from the Hotan River basin, Xinjiang, China (II): Vegetated. Frontiers of Earth Science in China, 2(3), 340-345.

Liang, H., Shi, H., 2011. Liang H, Shi H. 2011. Assessment of wind erosion hazard in typical transect Erenhot-Zhangjiakou. In Proceedings 2011 International Conference on Remote Sensing, Environment and Transportation Engineering. IEEE, Piscataway, NJ, pp. 140-143.

Loosmore, G.A., Hunt, J.R., 2000. Dust resuspension without saltation. Journal of Geophysical Research D: Atmospheres, 105(D16), 20663-20671.

López, M.V., 1998. Wind erosion in agricultural soils: An example of limited supply of particles available for erosion. Catena, 33(1), 17-28.

Lopez, M.V., Sabre, M., Gracia, R., Arrue, J.L., Gomes, L., 1998. Tillage effects on soil surface conditions and dust emission by wind erosion in semiarid Aragon (NE Spain). Soil and Tillage Research, 45(1-2), 91-105.

Lu, H., Shao, Y., 2001. Toward quantitative prediction of dust storms: An integrated wind erosion modelling system and its applications. Environmental Modelling and Software, 16(3), 233-249.

Lyles, L., 1988. 4. Basic wind erosion processes. Agric. Ecosyst. Environ., 22-23(C), 91-101.

Martínez-Fernández, D., Walker, D.J., 2011. The Effects of Soil Amendments on the Growth of Atriplex halimus and Bituminaria bituminosa in Heavy Metal-Contaminated Soils. Water, Air and Soil Pollution, 223(1), 63-72.

Masri, Z., Zìôbisch, M., Bruggeman, A., Hayek, P., Kardous, M., 2003. Wind erosion in a marginal Mediterranean dryland area: a case study from the Khanasser Valley, Syria. Earth Surface Processes and Landforms, 28(11), 1211-1222.

Maurer, T., Herrmann, L., Stahr, K., 2009. The effect of surface variability factors on wind-erosion susceptibility: A field study in SW Niger. Journal of Plant Nutrition and Soil Science, 172(6), 798-807.

Maurer, T., Herrmann, L., Stahr, K., 2010. Wind erosion characteristics of Sahelian surface types. Earth Surface Processes and Landforms, 35(12), 1386-1401.

Mazzucato, V., Niemeijer, D., 2000. The cultural economy of soil and water conservation: Market principles and social networks in Eastern Burkina Faso. Development and Change, 31(4), 831-855.

McKie, R., 2001. Deadly dust 'brought foot and mouth here'. Guardian unlimited archive 9 September

McTainsh, G.H., Pitblado, J.R., 1987. Dust storms and related phenomena measured from meteorological records in Australia. Earth Surface Processes & Landforms, 12(4), 415-424.

McTainsh, G.H., Lynch, A.W., 1996. Quantitative estimates of the effect of climate change on dust storm activity in Australia during the last glacial maximum. Geomorphology, 17(1-3 SPEC. ISS.), 263-271.

McTainsh, G.H., Leys, J.F., Nickling, W.G., 1999. Wind erodibility of arid lands in the channel country of western Queensland, Australia. Zeitschrift fur Geomorphologie, Supplementband, 116, 113-130.

MEA, 2005. Ecosystem and Human Well-being: Desertification Synthesis. Millennium Ecosystem Assessment World Resources Institute, Washington. DC, USA.

Michels, K., Sivakumar, M.V., Allison, B.E., 1995. Wind erosion control using crop residue. II. Effects on millet establishment and yields. Field Crops Research, 40(2), 111-118.

Middleton, N.J., Goudie, A.S., Wells, G.L., 1986. The frequency and source areas of dust storms. 17th annual, In: Mickling, W.G. (ed.) Aeolian Geomorphology. Allen and Unwin, London , 237–259.

Molina-Aiz, F.D., Valera, D.L., Álvarez, A.J., Madueño, A., 2006. A Wind Tunnel Study of Airflow through Horticultural Crops: Determination of the Drag Coefficient. Biosystems Engineering., 93(4), 447-457.

Morgan, R.P.C. (2005). Soil Erosion and Conservation (3rd ed.). Malden, MA: Blackwell Publishing, Oxford, 2005. x + 304 pp, paperback. ISBN 1-4051-1781-8.

Munson, S.M., Belnap, J., Okin, G.S., 2011. Responses of wind erosion to climate-induced vegetation changes on the Colorado Plateau. Proceedings of the National Academy of Sciences of the United States of America, 108(10), 3854-3859.

Musick, H.B., Trujillo, S.M., Truman, C.R., 1996. Wind-tunnel modelling of the influence of vegetation structure on saltation threshold. Earth Surface Processes and Landforms, 21(7), 589-605.

Nanney, R.D., Fryrear, D.W., Zobeck, T.M., 1993. Wind erosion prediction and control. Water Science and Technology, 28(3-5), 519-527.

Nishimura, K., Hunt, J.C.R., 2000. Saltation and incipient suspension above a flat particle bed below a turbulent boundary layer. J. Fluid Mech., 417, 77-102.

Nicholson, S., 2000. Land surface processes and Sahel climate. Reviews of Geophysics, 38(1), 117-139.

Nickling, W.G., Neuman, C.M., 1997. Wind tunnel evaluation of a wedge-shaped aeolian sediment trap. Geomorphology, 18(3-4), 333-345.

Nickling, W.G., McTainsh, G.H., Leys, J.F., 1999. Dust emissions from the Channel Country of western Queensland, Australia. Zeitschrift fur Geomorphologie, Supplementband, 116, 1-17.

Niemeijer, D., Mazzucato, V., 2002. Soil degradation in the West African Sahel: How serious is it? Environment, 44(2), 20-31.

Nordstrom, K.F., Hotta, S., 2004. Wind erosion from cropland in the USA: A review of problems, solutions and prospects. Geoderma, 121(3-4), 157-167.

NRCS, 2010. Soil Texture Calculator, The Natural Resources Conservation Service (NRCS), United States Department of Agriculture, http://soils.usda.gov/technical/aids/investigations/texture/.

Okoba, B.O., Sterk, G., 2006. Quantification of visual soil erosion indicators in Gikuuri catchment in the central highlands of Kenya. Geoderma, 134(1-2), 34-47.

Pacheco, A.M., McNairn, H., Merzouki, A., 2010. Evaluating TerraSAR-X for the identification of tillage occurrence over an agricultural area in Canada, Proceedings of SPIE - The International Society for Optical Engineering.

Papadimitriou, F., Mairota, P., 1996. Spatial scale-dependent policy planning for land management in Southern Europe. Environmental Monitoring and Assessment, 39(1-3), 47-57.

Pietersma, D., Stetler, L.D., Saxton, K.E., 1996. Design and aerodynamics of a portable wind tunnel for soil erosion and fugitive dust research. Transactions of the American Society of Agricultural Engineers (Gen Ed), 39(6), 2075-2083.

Qi, L., Wang, T., Li, Q., 2011. Investigation on dust suppressant for the ash field of coal-fired power plant, 2011 International Conference on Remote Sensing, Environment and Transportation Engineering, RSETE 2011 - Proceedings, pp. 4129-4132.

Rajot, J.L., 2001. Wind blown sediment mass budget of Sahelian village land units in Niger. Bilan de masse de l'érosion et des dépôts éoliens à l'échelle de terroirs villageois au Niger. Bulletin de la Société Géologique de France172(5):523-531. doi: 10.2113/172.5.523., 523-531.

Rajot, J.L., Ribolzi, O., Thiebaux, J.P., .2002. Wind erosion in a small catchment of grazing area in Northern Burkina Faso: influence of surface features. In Proceeding of the ICAR5/GCTE-SEN Joint Meeting, Lee JA, Zobeck TM (eds). Lubbock, Texas; 185–190.

Raupach, M.R., 1990. Turbulent transfer in plant canopies. In: Russel, G., Marshall, B., and Jarvies P.G. (eds.) Plant canopies, their growth and function. Cambridge University Press, 178 pp.

Raupach, M.R., 1992. Drag and drag partition on rough surfaces. Boundary-Layer Meteorology, 60(4), 375-395.

Raupach, M.R., Gillette, D.A., Leys, J.F., 1993. The effect of roughness elements on wind erosion threshold. Journal of Geophysical Research, 98(D2), 3023-3029.

Riksen, M., Brouwer, F., De Graaff, J., 2003. Soil conservation policy measures to control wind erosion in northwestern Europe. Catena, 52(3-4), 309-326.

Romm, J., 2011. Desertification: The next dust bowl. Nature, 478(7370), 450-451.

Ruiz-Mirazo, J., Robles, A.B., 2011. Short- and medium-term response of Atriplex halimus L. to repeated seasonal grazing in south-eastern Spain. Journal of Arid Environments, 75(6), 586-595.

Saleh, A., 1993. Soil Roughness Measurement - Chain Method. Journal of Soil and Water Conservation, 48(6), 527-529.

Seyfried, M.S., Wilcox, B.P., 1995. Scale and the nature of spatial variability: field examples having implications for hydrologic modeling. Water Resources Research, 31(1), 173-184.

Shao, Y., Leslie, L.M., 1997. Wind erosion prediction over the Australian continent. Journal of Geophysical Research D: Atmospheres, 102(25), 30091-30105.

Shao, Y., Raupach, M.R., Findlater, P.A., 1993. Effect of saltation bombardment on the entrainment of dust by wind. Journal of Geophysical Research, 98(D7), 12,719-712,726.

Shao Y, Raupach MR, Leys JF. 1996. A model for predicting aeolian sand drift and dust entrainment on scales from paddock to region. Australian Journal of Soil Research 34(3):309-342.

Shao, Y., Zhao, S., 2001. Wind Erosion and Wind Erosion Research in China: A Review. Annals of Arid Zone, 40(3), 317-336.

Shao, Y., Jung, E., Leslie, L.M., 2002. Numerical prediction of northeast Asian dust storms using an integrated wind erosion modeling system. Journal of Geophysical Research D: Atmospheres, 107(24).

Shao, Y., 2008. Physics and Modelling of Wind Erosion. Springer, Berlin, Heidelberg, New York.

Sharratt, B., Wendling, L., Feng, G., 2012. Surface characteristics of a windblown soil altered by tillage intensity during summer fallow. Aeolian Research, 5, 1-7.

Sivakumar, M.V.K., Motha, R.P., Das, H.P., 2005. Impacts of sandstorms/dust storms on agriculutre. In Natural Disasters and Extreme Events in Agriculture: Impacts and Mitigation. Sivakumar MVK, Motha RP, Das HP (eds). Springer Berlin, Heidelberg, New York; 159-178.

Skidmore, E.L., Hagen, L.J., 1977. Reducing wind erosion with barriers. Transactions of the American Society of Agricultural Engineers (Gen Ed), 20(5), 911-915.

Skidmore, E.L., 1986. Wind erosion control. Climatic Change, 9(1-2), 209-218.

Spaan, W.P., van den Abeele, G.D., 1991. Wind borne particle measurements with acoustic sensors. Soil Technology, 4(1), 51-63.

Sterk, G., 1993. Sahehan wind erosion research project, Report III. Description and calibration of sediment samplers. Department of Irrigation and Soil & Water Conservation, Wageningen University, Wageningen.

Sterk, G., Herrmann, L., Bationo, A., 1996. Wind-blown nutrient transport and soil productivity changes in Southwest Niger. Land Degradation and Development, 7(4), 325-335.

Sterk, G., Raats, P.A.C., 1996. Comparison of models describing the vertical distribution of wind-eroded sediment. Soil Science Society of America Journal, 60(6), 1914-1919.

Sterk, G., 1997. Wind Erosion In The Sahelian Zone Of Niger: Processes, Models, and Control Techniques. Doctorate thesis, Wageningen University Wageningen.

Sterk, G., Jacobs, A.F.G., Van Boxel, J.H., 1998. The effect of turbulent flow structures on saltation sand transport in the atmospheric boundary layer. Earth Surface Processes and Landforms, 23(10), 877-887.

Sterk, G., López, M.V., Arrúe, J.L., 1999. Saltation transport on silt loam soil in Northeast Spain. Land Degradation and Development, 10(6), 545-554.

Sterk, G., Spaan, W.P., 1997. Wind erosion control with crop residues in the Sahel. Soil Science Society of America Journal, 61(3), 911-917.

Sterk, G., Stein, A., 1997. Mapping wind-blown mass transport by modeling variability in space and time. Soil Science Society of America Journal, 61(1), 232-239.

Stetler, L.D., Saxton, K.E., 1996. Wind erosion and PM10 emissions from agricultural fields on the Columbia Plateau. Earth Surface Processes and Landforms, 21(7), 673-685.

Stout, J.E., Zobeck, T.M., 1996. The Wolfforth field experiment: A wind erosion study. Soil Science, 161(9), 616-632.

Stroosnijder, L., 2005. Measurement of erosion: is it possible? Catena, 64(2-3), 162-173.

Stroosnijder, L., 2007. Rainfall and land degradation. In Sivakumar, MVK and N Ndiang'ui (Eds) Climate and land degradation Springer, Berlin, 167-195

Tegen, I., Fung, I., 1995. Contribution to the atmospheric mineral aerosol load from land surface modification. Journal of Geophysical Research, 100(D9), 18,707-718,726.

Tenge, A.J., De Graaff, J., Hella, J.P., 2005. Financial efficiency of major soil and water conservation measures in West Usambara highlands, Tanzania. Applied Geography, 25(4), 348-366.

Thomas, R.J., Turkelboom, F., 2008. An Integrated Livelihoods-based Approach to Combat Desertification in Marginal Drylands. In: C. Lee, T. Schaaf (Eds.), Future of Drylands. Springer, Dordrecht, pp. 631-646.

Tibke, G., 1988. 5. Basic principles of wind erosion control. Agriculture, Ecosystems & Environment, 22–23(0), 103-122.

Todd, R.W., Guo, W., Stewart, B.A., Robinson, C., 2004. Vegetation, phosphorus, and dust gradients downwind from a cattle feedyard. Journal of Range Management., 57(3), 291-299.

Udo, K., Takewaka, S., 2007. Experimental study of blown sand in a vegetated area. J. Coast. Res., 23(5), 1175-1182.

Udo, K., Kuriyama, Y., Jackson, D.W.T., 2008. Observations of wind-blown sand under various meteorological conditions at a beach. Journal of Geophysical Research F: Earth Surface , field of Earth Surf., 113(4).

Van De Ven, T.A.M., Fryrear, D.W., Spaan, W.P., 1989. Vegetation characteristics and soil loss by wind. Journal of Soil & Water Conservation, 44(4), 347-349.

Van Pelt, R.S., Zobeck, T.M., Potter, K.N., Stout, J.E., Popham, T.W., 2004. Validation of the wind erosion stochastic simulator (WESS) and the revised wind erosion equation (RWEQ) for single events. Environmental Modelling and Software, 19(2), 191-198.

Visser, S.M., Sterk, G., Karssenberg, D., 2005a. Modelling water erosion in the Sahel: Application of a physically based soil erosion model in a gentle sloping environment. Earth Surface Processes and Landforms, 30(12), 1547-1566.

Visser, S.M., Sterk, G., Karssenberg, D., 2005b. Wind erosion modelling in a Sahelian environment. Environmental Modelling and Software, 20(1), 69-84.

Visser, S.M., Stroosnijder, L., Chardon, W.J., 2005c. Nutrient losses by wind and water, measurements and modelling. Catena, 63(1), 1-22.

Visser, S.M., Palma, J., 2004. Upscaling wind and water erosion models, Far from reality?. Chapter in the book of Wind and rain Interaction in erosion. In: Wind and rain interaction in erosion / Visser, S.M., Cornelis, W.,Wageningen: Erosion & Soil and Water Conservation Group, 2004 (Tropical Resource Management Papers (TRMP) 50) - ISBN 906754843X.

Visser, S.M., Sterk, G., 2007. Nutrient dynamics - Wind and water erosion at the village scale in the Sahel. Land Degradation and Development, 18(5), 578-588.

Vories, E.D., Fryrear, D.W., 1991. Vertical distribution of wind-eroded soil over a smooth, bare field. Transactions of the American Society of Agricultural Engineers (Gen Ed), 34(4), 1763-1768.

Walkley, A., Black., I.A., 1934. An examination of the Degtjareff method for determining organic carbon in soils: Effect of variations in digestion conditions and of inorganic soil constituents. Soil Science 29:602-608., 63, 251-263.

Wang, S., Zhao, X., Qu, H., Zuo, X., Lian, J., Tang, X., Powers, R., 2011. Effects of shrub litter addition on dune soil microbial community in horqin sandy land, Northern China. Arid Land Research and Management, 25(3), 203-216.

Warren, A., 2010. Sustainability in aeolian systems. Aeolian Research, 1(3-4), 95-99.

Washington, R., Todd, M., Middleton, N.J., Goudie, A.S., 2003. Dust-storm source areas determined by the total ozone monitoring spectrometer and surface observations. Annals of the Association of American Geographers, 93(2), 297-313.

Wassif, M.M., 1998. Some observations on wind erosion in Egypt. International Center for Agricultural Research in the Dry Areas (ICARDA), Aleppo, pp 59–80.

Webb, N.P., McGowan, H.A., Phinn, S.R., McTainsh, G.H., 2006. AUSLEM (AUStralian Land Erodibility Model): a tool for identifying wind erosion hazard in Australia. Geomorphology, 78(3-4), 179-200.

Webb, N.P., McGowan, H.A., 2009. Approaches to modelling Land erodibility by wind. Progress in Physical Geography, 33(5), 587-613.

White, B.R., 1996. Laboratory simulation of aeolian sand transport and physical modeling of flow around dunes. Annals of Arid Zone, 35(3), 187-213.

White, B.R., 1997. A Wind Tunnel Study to Determine Vegetation Cover Required to Suppress Sand Dust Transport at Owens (dry) Lake, California, Univ. of Cal, Davis, Dept. of Mechanical and Aeronautical Engineering, Interagency Agreement no.9464, Final Report, pp. 1-168. Prepared for: Cal. State Lands Commission, Sacramento, CA 95814-7187.

Williams, G., 1964. SOME ASPECTS OF THE EOLIAN SALTATION LOAD. Sedimentology, 3(4), 257-287.

Willmott, C.J., 1981. On the validation of models. Phys. Geogr., 2(2), 184-194.

Wilson, S.J., Cooke, R.U., 1980. Wind erosion. In Soil Erosion, Kirkby, M.J., Morgan, R.P.C. (eds). John Wiley & Sons, Chichester, UK; 217-251.

Wilson, T.M., Cole, J.W., Stewart, C., Cronin, S.J., Johnston, D.M., 2011. Ash storms: Impacts of wind-remobilised volcanic ash on rural communities and agriculture following the 1991 Hudson eruption, southern Patagonia, Chile. Bulletin of Volcanology, 73(3), 223-239.

WMO., 1983. Meteorological aspects of certain processes affecting soil degradation-especially erosion. WMO no. 591. WMO, Geneva, Technical note no 178,.

Woodruff, N.P., Siddoway, F.H., 1965. A wind erosion equation. *Soil Science Society of America Journal*. Proc. 29:602-608.

Woodruff, N.P., 1956. Wind-blown soil abrasive injuries to winter wheat plants, Agronomy Journal, Vol 48:499-504.

Wuyts, K., Verheyen, K., De Schrijver, A., Cornelis, W.M., Gabriels, D., 2008. The impact of forest edge structure on longitudinal patterns of deposition, wind speed, and turbulence. Atmospheric Environment, 42(37), 8651-8660.

Xue, M., Song, D., Zhang, J., 2008. Compaction and testing method of wind-blown-sand subgrade, Proceedings of the 7th International Conference of Chinese Transportation Professionals Congress 2007: Plan, Build, and Manage Transportation Infrastructures in China, pp. 858-866.

Yan, C., Wang, T., Han, Z., 2005. Using MODIS data to assess land desertification in Ordos Plateau - Mu us sandy land case study, International Geoscience and Remote Sensing Symposium (IGARSS), pp. 2373-2375.

Young, D.L., Schillinger, W.F., 2012. Wheat farmers adopt the undercutter fallow method to reduce wind erosion and sustain profitability. Soil and Tillage Research, 124, 240-244.

Youssef, F., Visser, S., Karssenberg, D., Bruggeman, A., Erpul, G., 2012a. Calibration of RWEQ in a patchy landscape; a first step towards a regional scale wind erosion model. Aeolian Research, 3(4), 467-476.

Youssef, F., Visser, S., Karssenberg, D., Erpul, G., Cornelis, W.M., Gabriels, D., Poortinga, A., 2012b. The effect of vegetation patterns on wind-blown mass transport at the regional scale: A wind tunnel experiment. Geomorphology. 159-160, 178-188.

Zealand, E.M.N., 2001. Soil conservation technical The Ministry for the Environment hand book. Wellington, New Zealand.

Zhao, F., Liu, H., Yin, Y., Hu, G., Wu, X., 2011. Vegetation succession prevents dry lake beds from becoming dust sources in the semi-arid steppe region of China. Earth Surf. Processes Landf., 36(7), 864-871.

Zhang, D., Zhou, Z., Zhang, B., Du, S., Liu, G., 2012. The effects of agricultural management on selected soil properties of the arable soils in Tibet, China. Catena, 93, 1-8.

Zhang, W., Lee, S.J., 2009. Recent experimental studies on the saltating sand particle transport and wind-sand interaction in saltation. Chapter in the book of Arid Environments and Wind Erosion, Nova Science Pub Inc.

Zobeck, T.M., Fryrear, D.W., 1986. Chemical and physical characteristics of windblown sediment I. Quantities and physical characteristics. Transactions of the American Society of Agricultural Engineers (Gen Ed), 29(4), 1032-1036.

Zobeck, T.M., Parker, N.C., Haskell, S., Guoding, K., 2000. Scaling up from field to region for wind erosion prediction using a field-scale wind erosion model and GIS. Agriculture, Ecosystems and Environment, 82(1-3), 247-259.

Zobeck, T.M., 2002. Field measurement of erosion by wind. Encyclopedia of Soil Science. Marcel Dekker, New York,503–507

Zobeck, T.M., Sterk, G., Funk, R., Rajot, J.L., Stout, J.E., Van Pelt, R.S., 2003. Measurement and data analysis methods for field-scale wind erosion studies and model validation. Earth Surface Processes and Landforms, 28(11), 1163-1188.

Zou, X.Y., Cheng, H., Zhang, C.L., Zhao, Y.Z., 2007. Effects of the Magnus and Saffman forces on the saltation trajectories of sand grain. Geomorphology, 90(1-2), 11-22.

Summary

Wind erosion is a critical environmental problem that threatens mainly the arid and semi-arid regions of our planet. Usually this problem is associated with desertification, poverty and other environmental and socioeconomic problems. Wind erosion causes the loss of fertile topsoil, and has a negative effect on agricultural production and on human health. When conditions favorable for wind erosion are present, the process can cause large scale environmental disasters like the Dust Bowl in the USA in the 1930s. This event is considered one of the worst environmental disasters of the 20th century, and was caused by a reduction in vegetation cover due to a change in land use combined with an increased dryness in the region. Wind erosion involves the detachment, transport and deposition of soil particles. Depending on their size, particles can move in three different types of transport: creep, saltation and suspension.

Vegetation is one of the key factors in the protection of the soil against erosive winds. Although research on wind erosion has started a few decades ago there is still a big gap between the available knowledge provided by current measurement and modeling tools and the knowledge which is required by policy makers and land managers. This thesis focuses on improving the knowledge of the effects of vegetation cover and land use on regional scale wind erosion. The thesis covers improvement of wind erosion measurement techniques (Chapters 2, 3 and 5) and wind erosion modeling on the regional scale (Chapter 4 and 6).

In Chapter 2, the efficiencies of the Vaseline Slide (VS) and Modified Wilson and Cooke (MWAC) catchers were determined with different sand particle sizes (<50, <75, 50–75, 200–400, and 400– 500 μm) at a fixed wind speed (13.3 m s^{-1}) and with different soil textures at different wind velocities (10.3, 12.3, and 14.3 m s^{-1}). The study showed that whereas the VS trap is better for catching fine particles, the MWAC trap is better for trapping coarse particles. In the experiments with different soil textures, the efficiency of each catcher considerably changed with the with wind speed. This also varies importantly between catchers: for instance, for sand the MWAC efficiency was relatively high, whereas the efficiency of VS catcher was relatively low. Results concluded that the efficiency of each catcher varies critically with particle size, soil texture and wind speed.

Equipment or measurement techniques for the observation of saltation at the regional scale does not exist although these are essential for improving the understanding of wind erosion problem at that scale. In Chapter 3, the portable plot method for measuring regional scale wind erosion with a specific focus on the saltation process was developed. With this strategy the number of measurement locations is increased with limited budget and time. The portable plot method was applied at agricultural stability zones 4 and 5 in the Khanasser Valley in Syria in 2009 and 2010. During the measurement period, a meteorological station was installed at each plot together with MWAC sediment catchers. Results showed that, with this method, information on the effect of wind regime on the aeolian mass transport for different land uses in the region can be obtained. Also, insights into the interrelation between neighboring land units can be gained and the data for scaling-up a field scale model to the regional scale are obtainable. We concluded that this method provides insight into the wind erosion at regional scale and data collected through it are important for progressing the modeling of wind erosion at a regional scale.

The new measurement method enabled the calibration and validation of the field scale model of RWEQ (Revised Wind Erosion Equation) at several land use areas in the Khanasser valley in Syria (Chapter 4). In this chapter, the RWEQ model was modified to estimate mass flux and soil loss at a field scale for different types of land use. We implemented this modified version of RWEQ that represents wind erosion as a transient process, using time steps of 6 hours. Beside this, a number of adaptations including the estimation of mass flux over the field boundaries and the routing of sediment have been added. The results showed that this modified version of RWEQ provided acceptable predictions for the average mass flux from our measurement plots compared with the results of previous tests of the model.

While the portable plot method provided insights on the effect of land use and climate on the quantity and intensity of wind erosion in a region, more knowledge was required on the border effect between different land uses as the portable plot method provided only limited knowledge on the effect of vegetation pattern and border effect. To get sufficient knowledge on this subject a simulation of sediment transport in a regional scale environment was designed and tested in wind-tunnel experiments (Chapter 5). This simulation showed the effect of vegetation pattern on sediment transport within a land unit and at the border between land units. Wind tunnel experiments were conducted with artificial shrubs representing *Atriplex halimus*, a native shrub in Khanassar valley. In the experiments, a wind speed of 11 m s^{-1} was applied and after each 200-230 second wind run the sediment redistribution was measured using a graph paper. Results showed that: 1) the transport within a land unit is affected by the vegetation density and pattern for the land unit itself and for the neighboring units; 2) plans for re-vegetation of degraded land need to take into account the 'streets' effect; 3) the effect of neighboring land units includes a sheltering effect and the regulation of sediment passing from one land unit to the neighboring land units and 4) re-vegetation projects in regions vulnerable to wind erosion not only need to investigate the effect of vegetation pattern on erosion and deposition within the region in general, but also should consider the redistribution of sediment at smaller scales.

In Chapter 6, The Regional Scale Wind Erosion Equation (RS-WEQ) was developed. This model takes the different land uses in a region into account, considers the interrelation between neighboring land units and considers saltation as the main transport mode. Although the RWEQ was the starting point for the development of RS-WEQ, the new model is not restricted in its application to a single field. RS-WEQ predicts mass flux, soil loss and deposition for all land uses in a region. The model considers the erodibility parameters for each land use independently and takes the effect of the borders into account. Its output provides a clear insight on wind erosion processes at the regional scale. RS-WEQ was run using scenarios that represent main land uses in dry regions in general and in Khanasser valley specifically. The model outputs showed that the wind speed, field length and land use patterns affect the quantity and severity of mass flux, soil loss and deposition in a region. Specifically, the results showed that the mean mass flux and its related abrasion risk increased with the increase in wind speed and field length. The model provides further details on the effect of field length and land use patterns on the severity of soil loss and deposition at the regional scale. Therefore the developed model can be considered as a useful tool for land managers and policy makers in regions that are vulnerable to wind erosion.

This thesis showed that for comprehensive understanding of the aeolian sediment transport at regional scale a combination of measuring and modeling of wind-blown sediment transport is required. And the intensively calibrated and validated wind erosion models can be used in the framework of wind erosion mitigation.

Samenvatting

Winderosie is een serieus milieuprobleem dat vooral de droge en semi-aride gebieden van onze planeet bedreigt. Meestal wordt dit probleem geassocieerd met woestijnvorming, armoede en andere milieu- en sociaal-economische problemen. Wind erosie veroorzaakt verlies van vruchtbare bovengrond en heeft een negatief effect op de landbouwproductie en op de gezondheid van mensen. Als de omstandigheden gunstig zijn voor winderosie, kan het proces leiden tot grootschalige ecologische rampen zoals de 'Dust Bowl' in de Verenigde Staten in de jaren 30. Deze gebeurtenis wordt beschouwd als één van de ergste milieurampen van de 20st eeuw, en werd veroorzaakt door een vermindering van de vegetatiebedekking als gevolg van een verandering in landgebruik in combinatie met een toegenomen droogte in de regio. Winderosie omvat het losmaken, transporteren en afzetten van bodemdeeltjes. Afhankelijk van hun grootte, kunnen deeltjes op drie verschillende manieren in beweging zijn: rollen (creep), saltatie (saltation) en suspensie (suspension).

De vegetatie is één van de belangrijkste factoren die bescherming van de bodem bieden tegen erosieve wind. Hoewel het onderzoek naar winderosie al een paar decennia geleden begon, bestaat er nog steeds een grote kloof tussen de beschikbare kennis die door onze huidige meet- en modelleer technieken is verkregen en de kennis die vereist is voor beleidsmakers en terreinbeheerders. Dit proefschrift richt zich op het verbeteren van de kennis van de effecten van de vegetatie en landgebruik op winderosie in een regio. Het proefschrift heeft betrekking op verbetering van meettechnieken voor winderosie (hoofdstukken 2, 3 en 5) en van winderosie modellering op regionale schaal (hoofdstukken 4 en 6).

In hoofdstuk 2 wordt de efficiëntie van de Vaseline Slide (VS) en Modified Wilson en Cooke (MWAC) vangers (catchers) bepaald voor verschillende deeltjesgroottes (<50, <75, 50-75, 200-400, en 400 - 500 µm) bij een vaste windsnelheid (13,3 m s^{-1}), maar ook voor verschillende bodemtypen bij verschillende windsnelheden (10,3, 12,3 en 14,3 m s^{-1}). Dit onderdeel van het onderzoek toonde aan dat terwijl de VS catcher beter is voor het invangen van fijn materiaal (omdat zijn vang efficiency voor fijne deeltjes groot is), de MWAC catcher beter is voor het invangen van grover materiaal (omdat zijn vang efficiency voor grotere deeltjes hoog is). In de experimenten met verschillende texturen varieerde de doelmatigheid van de vangers aanzienlijk als gevolg van een veranderde windsnelheid. De efficiency van de MWAC nam toe met de windsnelheid terwijl de efficiency van de VS afnam met toenemende windsnelheid. Concluderend kunnen we stellen dat de efficiëntie van elke catcher afhankelijk is van de deeltjesgrootte en de windsnelheid.

Apparatuur en meettechnieken voor het waarnemen van 'saltation' transport op regionale schaal bestaan niet, hoewel die essentieel zijn voor het verbeteren van de kennis van het winderosie probleem op die schaal. In hoofdstuk 3 is een strategie ('portable plot strategy') ontwikkeld voor het meten van winderosie op regionale schaal met een specifieke focus op het 'saltation' proces. Met deze strategie wordt met een beperkt beschikbaar budget en binnen gelimiteerde tijd het aantal meetpunten verhoogd. Deze 'portable plot strategy' werd toegepast in (landbouw) stabiliteit zones 4 en 5 in de Khanasser vallei in Syrië in 2009 en 2010. Tijdens de meetperiode werd een meteorologisch station geïnstalleerd bij elk perceel samen met de MWAC sediment vangers. De resultaten tonen aan dat met deze meetstrategie, belangrijke informatie over het effect van het wind-regime op het eolische massa transport kan worden verkregen voor verschillende vormen van landgebruik in de regio. Ook werd inzicht in de onderlinge relatie tussen naburige landgebruikseenheden verkregen en werden gegevens verzameld voor de opschaling van een veld schaalmodel naar een regionale schaal niveau. Concluderend; deze meetstrategie geeft inzicht in het winderosie proces op regionale schaal en biedt tevens de gelegenheid gegevens te verzamelen voor de kalibratie en validatie van regionale winderosie modellen.

Met de nieuwe meetstrategie kon het veld schaalmodel RWEQ (Revised Wind Erosion Equation) worden gekalibreerd en gevalideerd voor verschillende vormen van landgebruik in de Khanasser vallei in Syrië (hoofdstuk 4). In dit hoofdstuk wordt beschreven hoe RWEQ is aangepast om de massa flux en het bodemverlies op veldschaal te schatten voor verschillende vormen van landgebruik. We gebruikten deze gewijzigde versie van RWEQ voor een dynamische beschrijving van het winderosie proces met behulp van tijdstappen van 6 uur. Daarnaast zijn een aantal aanpassingen, inclusief de schatting van de massa flux over veldgrenzen en de stroming van het sediment binnen het simulatie grid toegevoegd. De resultaten tonen aan dat deze gewijzigde versie van RWEQ aanvaardbare voorspellingen voor de gemiddelde massa flux op onze meet percelen voorspelt, zeker als we dit vergelijken met de resultaten van vroeger onderzoek met het originele RWEQ model.

Terwijl de 'portable plot strategy' inzicht geeft over de invloed van het (wind)klimaat op de hoeveelheid en intensiteit van winderosie voor verschillende vormen van landgebruik in een regio, is meer kennis nodig over het grens-effect tussen verschillende landgebruikseenheden. Om voldoende kennis te krijgen over dit onderwerp is een simulatie van het sedimenttransport in een regionale schaal omgeving ontworpen en getest in windtunnel experimenten (hoofdstuk 5). Deze simulatie toonde het effect van het vegetatie patroon op sedimenttransport binnen een landgebruikseenheid aan en het grenseffect tussen landgebruikseenheden. Windtunnel experimenten werden uitgevoerd met kunstmatige struiken die Atriplex halimus, een inheemse struik in de Khanassar vallei, vertegenwoordigden. In de experimenten is een windsnelheid van 11 m s^{-1} toegepast en na elke 200-230 seconden 'windrun' is de sediment herverdeling gemeten met behulp van een grafiekpapier. De resultaten toonden aan dat: 1) het transport binnen een landgebruikseenheid beïnvloedt wordt door de vegetatiedichtheid en het patroon van de landgebruikseenheid zelf en die van de aangrenzende units, 2) bij plannen voor her-vegetatie van gedegradeerd land moet rekening worden houden met het 'straat' effect, 3) naburige landgebruiks- eenheden voorzien in een beschermend effect en in de regulering van sedimenttransport van de ene naar de andere landgebruikseenheid en 4) re-vegetatie projecten in regio's welke kwetsbaar zijn voor winderosie dienen niet alleen het effect te onderzoeken van vegetatiepatronen op erosie en afzetting, maar ook van de herverdeling van het sediment op kleinere schaal.

In hoofdstuk 6, is een regionale schaal winderosie vergelijking (RS-WEQ) ontwikkeld. Dit model neemt de verschillende vormen van landgebruik in een gebied in aanmerking, de onderlinge relatie tussen naburige landgebruikseenheden en beschouwt saltatie als belangrijkste transport proces. Hoewel de RWEQ het uitgangspunt was voor de ontwikkeling van RS-WEQ, wordt het nieuwe model niet beperkt tot de toepassing ervan op één veld. RS-WEQ voorspelt massa-flux, bodemverlies en depositie voor al het landgebruik in een regio. Het model gebruikt de erodibility parameters voor elke ruimtelijke eenheid en neemt het effect van de grenzen in beschouwing. Model output levert een helder inzicht van winderosie processen op regionale schaal. RS-WEQ werd gebruikt voor scenario's voor droge gebieden in het algemeen en voor de Khanasser vallei in het bijzonder. Model output laat zien dat de windsnelheid, veldlengte en bodemgebruikspatronen de hoeveelheid en de ernst van de massa flux, bodemverlies en depositie in een regio beïnvloeden. In het bijzonder bleek dat de gemiddelde massa flux en het bijbehorende 'abrasion' risico toeneemt met een toename van de windsnelheid en veldlengte. Het model biedt nog meer informatie over het effect van de veldlengte en landgebruik patronen op de ernst van bodemverlies en depositie op regionale schaal. Daarom kan het ontwikkelde model worden beschouwd als een nuttig instrument voor land-managers en beleidsmakers in de regio's die kwetsbaar zijn voor winderosie.

Dit proefschrift laat zien dat voor een beter begrip van het eolische sedimenttransport op regionale schaal een combinatie van meten en modelleren van sedimenttransport is vereist. Verder toont het proefschrift aan dat intensief gekalibreerde en gevalideerde winderosie modellen gebruikt kunnen worden in het kader van het bestrijden van winderosie. Tot slot markeert dit proefschrift punten die belangrijk zijn om ons begrip van winderosie op regionale schaal te verbeteren.

PE&RC PhD Education Certificate

With the educational activities listed below the PhD candidate has complied with the educational requirements set by the C.T. de Wit Graduate School for Production Ecology and Resource Conservation (PE&RC) which comprises of a minimum total of 32 ECTS (= 22 weeks of activities)

Review of literature (3 ECTS)
- Measurement methods for wind erosion; presented in Ankara University (2008)

Writing of project proposal (4.5 ECTS)
- Effect of changing vegetation cover in dryland on regional wind erosion: upscaling a process-based wind erosion modelling at regional scale

Post-graduate courses (7 ECTS)
- Coping with climate change in integrated watershed management; Wageningen University (2008)
- Postgraduate courses PCR: dynamic modelling; Utrecht University (2008)
- Postgraduate courses PCR: Python; Utrecht University (2008)

Laboratory training and working visits (6 ECTS)
- Visiting to Gent University, Soil Care Department; Gent University (2008)
- Visit wind erosion site in Karapinar, Turkey; Ankara University (2009)
- PEST, model calibration; Utrecht University (2010)

Invited review of (unpublished) journal manuscript (2 ECTS)
- Soil Science Society of America Journal: wind erosion measurements (2009)
- Environmental Monitoring and Assessment journal: water erosion and land degradation (2010)

Deficiency, refresh, brush-up courses (4.4 ECTS)
- Spatial modelling and statistics (2008)
- Postgraduate courses PCR: map algebra and cartographic modelling; Utrecht University (2008)
- Modelling wind erosion, WEPS (2008)
- Land management; Ankara University (2008)

Competence strengthening / skills courses (1.2 ECTS)
- Techniques for writing and presenting a scientific paper; Wageningen University (2008)
- Endnote; Wageningen University (2008)

PE&RC Annual meetings, seminars and the PE&RC weekend (1.5 ECTS)
- PE&RC Introduction weekend (2008)
- Environmental policy and biodiversity; PE&RC (2008)
- Innovation for sustainability; PE&RC (2011)

Discussion groups / local seminars / other scientific meetings (5 ECTS)
- Discussion groups: Modelling Group (2008)
- Erosion group meeting: TUBITAT; Ankara University (2009)
- The national meeting on desertification; Konya , Turkey (2009)
- Management of natural resources to sustain soil health and quality; international congress; Samsun, Turkey (2010)
- Discussion groups: Modelling Group (2010)

International symposia, workshops and conferences (9 ECTS)
- The 7th International Conference on Aeolian Research (ICAR-VII); poster (2010)
- Third Conference on Desertification and Land Degradation; presentation; Gent, Belgium (2010)
- The Annual DESIRE Meeting; presentation (2009)

Curriculum vitae and author's publication

Feras Ibrahim Youssef was born on 10 June 1974 in Jableh, Latakia, Syria where he completed his secondary school. In 1994, he started his study at the Environmental and Forest Department, Tishreen University, Latakia and in 1998 he obtained his BSc in Forest and Environment. In 1999, he started studying at Aleppo University and obtained in 2000 a high education diploma (comparable to MSc degree) in the subject of forest and environment. From 2000 to 2002, Feras worked at the Environmental Ministry in Syria and during that period he gained some work experience on dealing with Mediterranean environmental problems. Due to his high score in the high education program, he got a scholarship from the Syrian High Education Ministry to complete a Master degree in Ankara, Turkey. In the period of 2003 and 2006, besides learning Turkish language, Feras obtained a MSc degree from the Soil Science and Plant Nutrition Department, Ankara University, Turkey. To get more work experience and to improve his English Language, Feras travelled to the United Kingdom (UK) in 2007 where he worked with an agricultural company. In September 2007, he was selected among few candidates to do his PhD at Wageningen University. In January 2008, he started his PhD program in the framework of the European-funded EU project of Desire at the Land Degradation and Development Group, Wageningen University, the Netherlands. In 2010, Feras got a scholarship from the Turkish research council (TUBITAK), Turkey to carry out some field research in Konya, Turkey and in 2011, he got an ERASMUS scholarship from Wageningen University to do wind-tunnel experiments in Gent, Belgium. During his PhD, he gained experience in developing GIS-physically-based models and he managed to develop a physically-based regional scale wind erosion model and to calibrate and validate the Revised Wind Erosion Equation model (RWEQ). Moreover, Feras developed a new method for measuring wind erosion at the regional scale and to simulate regional scale environments in wind-tunnel experiments. Feras built a wide network in several countries and institutions in EU, Syria and Turkey. He participated in several international meetings and he is a member in the International Society for the Aeolian Research and in the European Geosciences Union (EGU). Feras will work at the Syrian environmental ministry and can be contacted via: y1061974@gmail.com; ferasyoussef5@hotmail.com

Journal papers:

Youssef, F., Visser, S., Karssenberg, D., Erpul, G., Cornelis, W., Gabriels, D., Poortinga, A., 2012. The effect of vegetation patterns on wind-blown mass transport at the regional scale: A wind tunnel experiment, Geomorphology 158-159: 178-188.

Youssef, F., Visser, S., Karssenberg, D., Bruggeman, A., Erpul, G., 2012. Calibration of RWEQ in a Patchy Landscape; a First Step towards a Regional Scale Wind Erosion Model. Aeolian Research 3(4): 467-476.

Youssef, F., Erpul, G., Cornelis, W., Gabriels, D., Pogman, P., 2008. Determination of Efficiency of Vaseline Slide and Wilson and Cooke Sediment Traps by Wind Tunnel Experiments, Environmental Geology 55: 741-750.

Conference abstracts:

Youssef, F., Visser, M.S., Karssenberg, D., Erpul, G., Cornelis, M.W., Gabriels, D., Poortinga, A., De Boever, M., 2012. The effect of vegetation patterns on wind-blown mass transport at the regional-scale: A wind tunnel experiment, 1 - 4 May, Wageningen, the **Netherlands.**

Youssef, F., Erpul, G., Basaran, M., Gharahassanlou, A., Deviren, S.S., Ozcan, A.U., Uzun., O., 2012. Approach towards assessing wind erosion vulnerability at a regional scale in semi-arid environment in Turkey. Fourth Conference on Desertification and Land Degradation, 19 June 2012, Ghent, **Belgium**.

Youssef, F., Visser, S., Karssenberg, D., Slingerland, E., Ziadat, F., Stroosnijder, L., Erpul, G., 2012. Strategies for Measuring Wind Erosion for Regional Scale Modelling. GM5.1 EGU2012-278, European Geosciences Union (EGU) 22 - 28 April 2012, Vienna, **Austria**

Youssef, F. Visser, S. Karssenberg, D. Bruggeman, A. Erpul, G. 2012. Calibration of RWEQ in a Patchy Landscape; a First Step towards a Regional Scale Wind Erosion Model. 7th International Conference on Aeolian Research (ICAR-VII), July 5 – 9, 2010. **Argentina**.

Youssef, F., Visser, S., Karssenberg, D., Bruggeman, A., Erpul, G., 2010, Calibration of RWEQ in a patchy landscape; a first step towards a regional scale wind erosion model, Third Conference on Desertification and Land Degradation, Ghent, **Belgium**. 16 - 17 July 2010.

Youssef, F., Visser, S., Karssenberg, D., Erpul, G., 2010. The Spatial Variation in Wind-Blown

Sediment Transport in Small Scales in Karapınar, Turkey. International Soil Science Congres, Department of Soil Science, Faculty of Agriculture, Ondokuz Mayıs University, 55139 Samsun, **Turkey**.

Papers under review or to be submitted

Youssef, F., Visser, S., Karssenberg, D., 2012. A new process-based regional scale wind erosion model (RS-WEQ): the effect of land cover pattern on wind erosion (under review at Environmental Modelling and Software).

Youssef, F., Visser, S., Karssenberg, D., Slingerland, E., Ziadat, F., Stroosnijder, L., Erpul, G., 2012. A new method for measuring wind erosion at the regional scale: Observing aeolian sediment transport at different land covers.